Doctoral Program in Neuroscience

Sensory innervation of the ocular surface: from peripheral nerves to brain cortex

Enrique Velasco Serna

Director: Dr. Juana Gallar Martínez

Codirector: Dr. Víctor Manuel Meseguer Vigueras

University Miguel Hernández de Elche

Neuroscience Institute, San Juan de Alicante

-2022-

This PhD thesis, entitled "**Sensory innervation of the ocular surface: from peripheral nerves to brain cortex"** is presented is presented as a compendium of the following publications:

"Membrane potential instabilities in sensory neurons: mechanisms and pathophysiological relevance"

Enrique Velasco, Julio L. Alvarez, Victor M. Meseguer, Juana Gallar, Karel Talavera

Pain (2022) Jan 1;163(1):64-74. doi: 10.1097/j.pain.0000000000002289.

Sant Joan d'Alacant

Dr. Juana Gallar Martínez, director, and Dr. Victor Manuel Meseguer Vigueras, codirector of the doctoral thesis entitled "**Sensory innervation of the ocular surface: from peripheral nerves to brain cortex"**

INFORM:

That Mr. Enrique Velasco Serna has performed, under our supervision, the work entitled "**Sensory innervation of the ocular surface: from peripheral nerves to brain cortex",** accomplishing the terms and conditions defined in his Research plan and agreeing with the Código de Buenas Prácticas of the Miguel Hernández University of Elche, satisfactorily fulfilling the planned objectives for its public defense as a PhD thesis.

Which we sign for the appropriate purposes.

Director	Codirector
Dr. Juana Gallar Martínez	Dr. Víctor Manuel Meseguer Vigueras

Sant Joan d'Alacant

Dr. Elvira de la Peña García, coordinator of the Neuroscience PhD program of the Instituto de Neurociencias de Alicante, mixed institution of the Miguel Hernández University (UMH) and the Estate Agency Superior Council for Scientifical Research (CSIC)

INFORMS:

That Mr. Enrique Velasco Serna has performed, under the supervision of our PhD program, the work entitled "**Sensory innervation of the ocular surface: from peripheral nerves to brain cortex"**, accomplishing the terms and conditions defined in his Research plan and agreeing with the Código de Buenas Prácticas of the Miguel Hernández University of Elche, satisfactorily fulfilling the planned objectives for its public defense as a PhD thesis.

Which I sign for the appropriate purposes

Dr. Elvira de la Peña García

Coordinator of the PhD program in Neurosciences

E-mail : elvirap@umh.es
www.in.umh.es

Tel: +34 965 919533
Fax: +34 965 919549

Av Ramón y Cajal s/n
CAMPUS DE SANT JOAN
03550 SANT JOAN D'ALACANT– ESPAÑA

Sant Joan d'Alacant

To whom it may concern, the doctoral thesis entitled "**Sensory innervation of the ocular surface: from peripheral nerves to brain cortex"** has been developed by myself, Enrique Velasco Serna. This work has been financially supported by: ayudas para la Formación del Profesorado Universitario (FPU) fellowship with reference FPU16/00283 awarded by the Ministerio de Universidades. It has been also supported by Ministerio de Ciencia e Innovación-AEI and FEDER funds "Una manera de hacer Europa".

Yours sincerely,

Enrique Velasco Serna

“Gracias a quien me quiso y quien me quiere, a quien quise y a quien amo:

habéis sido la dinamo que encendió el motor.

Descubrí la primavera compartiendo ramo,

porque en el fondo somos todas la misma flor

Con temblor, con duda, de espinas desnuda,

creyéndonos la luna que refleja al sol.

Invocamos la tormenta lenta porque es oportuna

cuando se seca la laguna de nuestro interior. “

“Flor del Inca” David Rebollo (Vito)

A los que vinieron antes, por enseñarme

A los que vendrán después, por hacerlo mejor

INDEX

Abbreviations

A1	Primary Auditory Cortex	Corteza Auditiva Primargia
AP	AnteroPosterior axis / Action Potential	Eje anteroposterior / Potencial de Acción
C1 spinal level	First cervical spinal level	Primer nivel medular cervical
CaCl2	Calcium Chloride	Cloruro de Calcio
CGRP	Calcitonin gene-related peptide	Péptido relacionado con el gen de la calcitonina
CI	Confidence Interval	Intervalo de Confianza
CNS	Central Nervous System	Sistema Nervioso Central
CV	Conduction Velocity	Velocidad de Conducción
DC mode	Direct Current Mode	Modo de Corriente Continua o Directa
DRG	Dorsal Root Ganglion	Ganglio de la Raíz Dorsal
DSF	Depolarizing Spontaneous Fluctuation	Fluctuación Despolarizante Espontánea
DV	DorsoVentral axis	Eje DorsoVentral
EEG	Electroencephalograpy	Electroencefalografía
EGTA	Egtazic acid	Ácido egtázico
fMRI	functional Magnetic Resonance Imaging	Análisis de imágenes de Resonancia Magnética Funcional
GC	Gustatory Cortex	Corteza Gustativa
GDNF	Glial cell-derived neurotrophic factor	Factor neurotrófico derivado de células gliales
HCN	Hyperpolarization-activated Cyclic Nucleotide–gated channels	Canales iónicos activados por la hiperpolarización y modulados por nucleótidos cíclicos
HEPES	4-(2-hydroxyethyl)-1-piperazineethanesulfonic acid	ácido 2(4(2hidroxietil)1piperazinil)etanosulfónico
HT-LB cold receptor	High-Threshold Low-Background cold receptor	Receptor de frío de alto umbral y poca actividad basal
IAht, IAs and IAf	Transient voltage-gated potassium currents	Corrientes de potasio dependientes de voltaje transitorias
IDP	Initial Depolarization Phase of the action potential	Fase de despolarización inicial del potencial de acción
KCl	Potassium Chloride	Cloruro de Potasio
KOH	Potassium Hydroxide	Hidróxido de Potasio
KVs	Voltage-gated Potassium channels	Canales de Potasio dependientes de Voltaje
LT-HB cold receptor	Low-Threshold High-Background cold receptor	Receptor de frío de bajo umbral y elevada actividad basal

Mes-V	Mesencephalic Nucleus of the Trigeminus	Núcleo mesencefálico del Trigémino
MgCl2	Magnessium Chloride	Cloruro de Magnesio
ML	MedioLateral axis	Eje MedioLateral
MPI	Membrane Potential Instabilities	Inestabilidades del Potencial de Membrana
MPT	Membrane Potential Transients	Transientes del Potencial de Membrana
MUA	Multiunit Activity	Actividad Multiunitaria
Na2ATP	Disodium Adenosine 5'-Triphosphate	Adenosín 5'-Trifosfato disódico
NaGTP	Sodium Guanosine 5'-Triphosphate	Guanosín 5'-Trifosfato sódico
NaVs	Voltage-gated Sodium channels	Canales de Sodio dependientes de Voltaje
NMDA	N-methyl-D-aspartate	N-metil-D-aspártico
NT4	Neurotrophin-4	Neurotrofina-4
OS	Ocular Surface	Superficie Ocular
PNS	Peripheral Nervous System	Sistema Nervioso Periférico
POm	Posteromedial thalamic nucleus	Núcleo talámico posteromedial
PrV / Pr5	Principal nucleus of the trigeminal	Núcleo principal del trigémino
PSD	Power Spectral Density	Densidad Espectral de Potencia
PSN	Peripheral Sensory Neuron	Neurona sensorial primaria o periférica
Ptfa1	Alfa subunit of pancreas associated transcription factor	Subunidad alfa del factor de transcripción del páncreas 1
S1	Primary Somatosensory Cortex	Corteza Somatosensorial Primaria
S2	Secondary Somatosensory Cortex	Corteza Somatosensorial Secundaria
SD	Standard Deviation	Desviación Estándar
SEM	Standard Error of the Mean	Error Estándar de la Media
SMPO	Subthreshold Membrane Potential Oscillation	Oscilación Subumbral del Potencial de Membrana
SpV / Sp5	Spinal nucleus of the trigeminal	Núcleo espinal del trigémino
STI	Spatial Tunning Index	Índice de sintonización espacial
TEA	Tetraethylammonium	Tetraetilamonio
TG	Trigeminal Ganglion	Ganglio Trigémino
Th	Thalamus	Tálamo
TRPs	Transient Receptor Potential ion channels	Canales iónicos Receptores de Potencial Transitorio
TTX-S / TTX-R	Tetrodotoxin sensitive / resistant voltage-gated sodium channels	Canales de Sodio dependientes de Voltaje sensibles / resistentes a tetrodotoxina
V1	Primary Visual Cortex / First branch of the trigeminal ganglion	Corteza Visual Primaria / Primera rama del ganglio trigémino
V2	Secondary Visual Cortex / Second branch of the trigeminal ganglion	Corteza Visual Secundaria / Segunda rama del ganglio trigémino

V3	Third branch of the trigeminal ganglion	Tercera rama del ganglio trigémino
Vm	Membrane potential	Potencial de Membrana
VPL	Ventral posterolateral thalamic nucleus	Núcleo ventral posterolateral del tálamo
VPM	Ventral posteromedial thalamic nucleus	Núcleo ventral posteromedial del tálamo

Resumen

Los receptores sensoriales que inervan la superficie ocular (SO) transforman los estímulos físicoquímicos en señales eléctricas que son transmitidas al sistema nervioso central (SNC), donde evocan sensaciones usualmente percibidas como molestas o dolorosas. Las neuronas somatosensoriales primarias se clasifican en mecanorreceptoras, termorreceptoras de frío y nociceptoras en función de su capacidad para detectar y codificar estímulos de diferentes modalidades. Existe un escaso conocimiento sobre cómo la actividad neural evocada por los distintos estímulos aplicados sobre la SO se integra en el SNC. Las distintas clases de neuronas sensoriales primarias muestran diferentes niveles de actividad basal, cuyos mecanismos de generación son muy poco conocidos. En este trabajo, registramos extracelularmente la actividad basal y evocada por estímulos mecánicos y térmicos de neuronas que procesan la información somatosensorial originada en la SO, en el ganglio trigémino (GT), el tálamo somatosensorial (TS) y la corteza somatosensorial primaria (S1). Nuestros objetivos han sido describir la representación somatotópica talámica y cortical de la SO, así como la actividad neural evocada por estímulos de diferente modalidad (enfriamiento suave, enfriamiento intenso, estímulo mecánico, calentamiento suave y calentamiento nocivo) en el GT, el TS y la S1. Además, mediante registro intracelular en neuronas trigeminales disociadas, hemos estudiado las fluctuaciones del potencial de membrana, implicadas en la generación del disparo repetitivo de potenciales de acción.

Los resultados indican que la intensidad y la modalidad del estímulo están codificadas como la magnitud y los componentes temporales de la respuesta poblacional de las neuronas en TS y S1. Las neuronas sensoriales primarias del GT que inervan la SO responden solamente a una o unas pocas modalidades de estímulo. Las aferencias somatosensoriales de la SO parecen divergir y converger a diferentes niveles del SNC, existiendo neuronas corticales y talámicas que responden a múltiples combinaciones de estímulos de distinta modalidad. Las neuronas que procesan información de la SO se organizan espacialmente en TS y S1, estando agrupadas

aquellas neuronas que responden a una misma combinación de estímulos. El patrón de actividad basal de las neuronas de TS y S1 que inervan la SO es distinto en función de la modalidad de estímulo al que responden, lo que podría ser consecuencia de los diferentes niveles de actividad de las neuronas sensoriales primarias y/o del procesamiento realizado a lo largo de la vía somatosensorial. El disparo espontáneo de potenciales de acción (actividad basal) se asocia a fluctuaciones espontáneas en el potencial de membrana de las neuronas somatosensoriales primarias, denominadas inestabilidades del potencial de membrana (IPM). Las IPM son variaciones del potencial de membrana subumbrales y dependientes de voltaje, generadas por una interacción de corrientes de Na+ y K+, y se ven modificadas en numerosas condiciones patológicas que cursan con síntomas sensoriales, como el dolor. Nuestros resultados muestran que las IPM, cuya forma y dinámica es diferente en cada clase de neurona sensorial primaria, están presentes en la mayor parte de neuronas del GT con actividad basal, bien produciéndose espontáneamente o tras estimulación térmica, química o eléctrica. Asimismo, nos han permitido proponer un modelo en el que las IPM guardan una relación causal con la generación de los potenciales de acción en la actividad neuronal basal.

En conjunto, los resultados contribuyen a establecer relaciones entre la actividad de las neuronas sensoriales primarias y los circuitos del SNC que procesan la información originada en la superficie ocular, así como a describir la localización estereotáxica de su representación somatotópica en el tálamo y la corteza somatosensorial primaria. Además, los resultados aportan nueva información sobre cómo el sistema somatosensorial que inerva la superficie ocular procesa la modalidad de los estímulos, lo que podría explicar las sensaciones tan características que se perciben en la superficie ocular, como la sequedad y la sensación de arenilla o de cuerpo extraño evocadas por la estimulación mecánica o térmica de la superficie del ojo.

Abstract

Sensory receptors innervating the ocular surface (OS) convert physicochemical stimuli into electrical signals that are conveyed to the CNS, where sensations usually perceived as discomfort or pain are generated. Primary somatosensory neurons are classified as mechanoreceptor, cold receptor, and nociceptor neurons depending on their ability to detect and encode different stimulus modalities. Little is known on how the sensory activity evoked by the different stimuli applied to the OS is integrated at the CNS. The different classes of primary sensory neurons innervating the eye display different levels of ongoing activity, whose molecular mechanisms remain elusive unlike those of the stimulus-evoked activity. Here, we recorded extracellularly the ongoing and stimulus-evoked activity of neurons processing OS information at the trigeminal ganglion (TG), the somatosensory thalamus (Th) and the primary somatosensory cortex (S1). Our aims was describing the thalamic and cortical somatotopic representation of the OS, as well as the neural activity of TG, Th and S1 neurons evoked by stimuli of different modalities (mild cooling, intense cooling, mechanical, mild warming, noxious heating) applied to the OS. Also, we performed patch-clamp experiments on dissociated trigeminal neurons to characterize the presence of membrane potential instabilities (MPIs), involved in the action potential generation in primary sensory neurons.

The results pinpointed that OS neurons recorded at Th and S1 encode both the modality and intensity of the stimulus in the magnitude and the temporal course of their firing response. TG primary sensory neurons innervating the OS were responsive to only one or few stimulus modalities. Their input seemed to diverge and converge at higher levels of the CNS, generating Th and S1 OS neurons responding to multiple combinations of stimulus modalities. These functionally different OS neurons are spatially organized in the Th and S1, being clustered the neurons responding to the same combination of stimulus modalities.

The pattern of ongoing activity of Th and S1 neurons innervating the OS depends on the stimulus modalities to which they are sensitive, which may result from the different levels of ongoing activity of the primary sensory neurons and/or to the processing along the OS sensory pathway. The presence of ongoing activity generation is based on the presence of spontaneous changes of membrane potential in primary somatosensory neurons. Membrane potential instabilities (MPIs) are subthreshold voltage-dependent variations of the membrane potential generated by an interplay between Na^+ and K^+ currents that are modified in several pathological conditions coursing with sensory alterations such as pain. Our experiments revealed that MPIs, which display different shape and dynamics in each class of primary sensory neuron, are present in most TG neurons with ongoing activity, either spontaneously or upon electrical, chemical or thermal stimulation. Also, we propose a model in which MPIs are causally related to the action potential generation during ongoing activity.

Altogether, the results contribute to establishing relationships between primary sensory neurons and CNS circuits carrying somatosensory information arising from the ocular surface, and describe the stereotaxic location of the eye surface thalamic and cortical representation. Moreover, the results have provided new insights about how the somatosensory system innervating the OS processes the stimulus modality, which may explain the distinctive perceptions like dryness, gritty eyes, or discomfort experienced after mechanical and thermal stimulation of the eye surface.

Introduction

1. The somatosensory system

The somatosensory system is defined as “the sensory system that mediates the sensation of touch, pressure, vibration, limb position, heat, cold, itch and pain, transduced by receptors within the skin, muscles or joints and conveyed to a variety of CNS target” (Purves et al., 2001). While most senses are spatially constricted to a particular organ, generally located in the face (i.e., eyes for vision, ears for hearing) the somatosensory system is present in almost all the organs in our body. The somatosensory system innervates those organs and detects external and internal stimulation produced over them, in a multimodal fashion. Unlike other sensory systems, the somatosensory system detection capability is not restricted to a single form of energy or stimulus, as in case of vision, in which photoreceptors are only sensitive to the electromagnetic radiation so-called “visible light”. Instead, the somatosensory system detects mechanical forces, temperature changes and chemicals (Emery et al., 2016). As it innervates tissues exposed to the external environment like the skin, their sensory receptors are classified as exteroceptive, while sensory receptors at inner organs, like the guts or the musculoskeletal system, generating proprioception, are considered interoceptive (Herman et al., 2021).

The skin is one of the most studied organs of the somatosensory system (Laverdet et al., 2015; Lumpkin and Caterina, 2007), being densely innervated and covering almost the entire body (Corniani and Saal, 2020). Nevertheless, other tissues are relevant in terms of somatosensory innervation, such as the nasal mucosa, the tongue, or the ocular surface (OS) (Corniani and Saal, 2020), as a dense and fine-tuned innervation is fundamental for the maintenance and protective behaviors of these highly exposed orofacial tissues (Basso et al., 2019; Pagella et al., 2014).

The somatosensory neural pathway is initiated by primary sensory neurons at the peripheral nervous system that detect the distinct physiochemical stimuli, afterwards conveying the

sensory information to the central nervous system, where it is processed by nuclei located at the spinal cord (for the body) and brainstem (for the face). Then, the information ascends segregated in modality-specific pathways towards different thalamic nuclei, which are integrated in specific circuits contributing to distinct functions. From the thalamus, the information is then relayed to different cortical areas of the cortex, each of which will compute different parameters of the external stimuli. Thalamocortical representations of the stimulus are intimately correlated with our conscious perception, and direct electrical stimulation of these areas could generate artificial perceptions (Kandel et al., 2000).

1.1. Primary somatosensory neurons

Primary sensory neurons are responsible of sensing for the somatosensory innervation of all the tissues in our body, and they have their cell bodies located in peripheral ganglia (Kandel et al., 2000; Vermeiren et al., 2020). Primary sensory neurons innervating the skin, limbs, trunk, and the majority of the body, except for the face, are located in the dorsal root ganglia (DRGs) inside the vertebral column. There is a pair (left and right) of DRGs at each spinal cord level, providing innervation to a determined portion of the body, which is known as dermatome for the skin, myotome for the muscles or sclerotome for the bones. In total, there are 31 DRGs (Vermeiren et al., 2020). Primary sensory neurons of the DRGs are typically pseudo-unipolar, meaning that a single axon is originated from their soma, that in turn is divided into two branches: one going to the periphery (ultimately producing the sensory terminals) and the other one going to the spinal cord (Devor, 1999; Kandel et al., 2000) (Figure 1). Otherwise, the face is innervated by a differentiated structure, the trigeminal ganglion (TG), also known as V par cranealis (Vermeiren et al., 2020). The TG is the biggest sensory ganglion in mammals and their neurons show some differences respect to DRG cells (Megat et al., 2019). It is divided in three branches, each with its own innervated territory: the ophthalmic branch innervates the supraorbital region and the ocular surface, the maxillary branch innervates the infraorbital region and the mandibular

branch innervates the lower jaw (Vermeiren et al., 2020). This latter branch also innervates some muscles of the jaw, being the only one with a mixed functional profile, sensory and motor. There are other sensory ganglia in the body, such as the mesencephalic nucleus of the trigeminus (Mes-V), which contains jaw and eye proprioceptors, and although being hosted in the brainstem inside the central nervous system, contains primary sensory neurons (Lazarov, 2000).

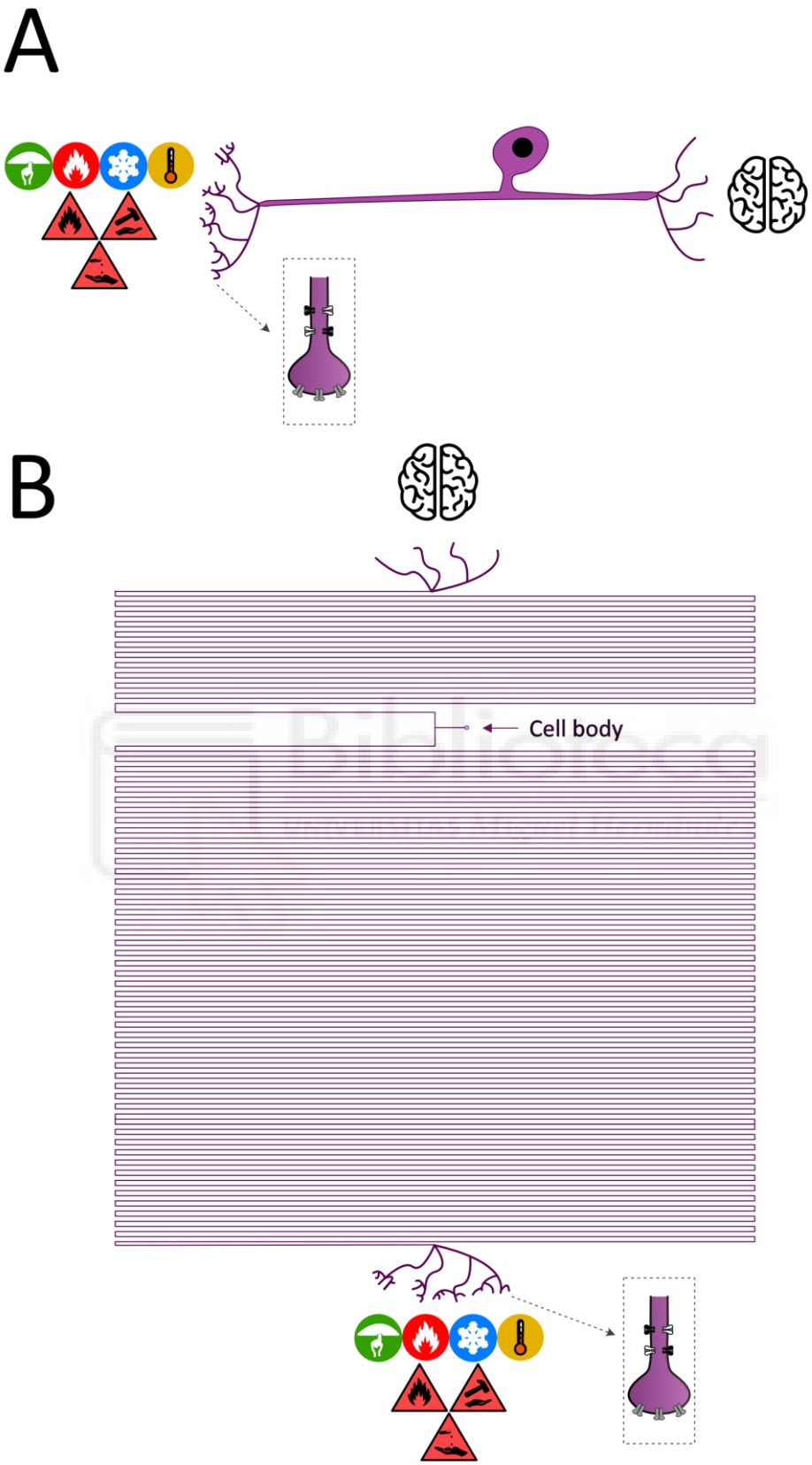

Figure 1. Primary somatosensory neuron. A. *Conceptual image of a primary sensory neuron, with a pseudounipolar axon dividing in two endings: one at the periphery, forming the sensory nerve terminals*

(peripheral nerve axon) and other at the central nervous system, forming presynaptic terminals (central axon). ***B.*** *More realistic drawing of a primary sensory neuron of the DRG innervating the leg of a human. Proportions between parts are conserved, representing the following typical dimensions: soma diameter 50 µm, axon diameter 5 µm, stem axon length 500 µm, dorsal root axon 30 cm and peripheral nerve axon 120 cm (Based on Devor 1999).*

Aside from their localization, another characteristic of primary sensory neurons is their functional variety, required to produce specialized responses to different kind of stimuli. Primary sensory neurons are divided into different functional subtypes, which have specific properties that make them able to preferentially detect one or other type of stimuli (Figure 2) (Lumpkin and Caterina, 2007; Kandel et al., 2000).

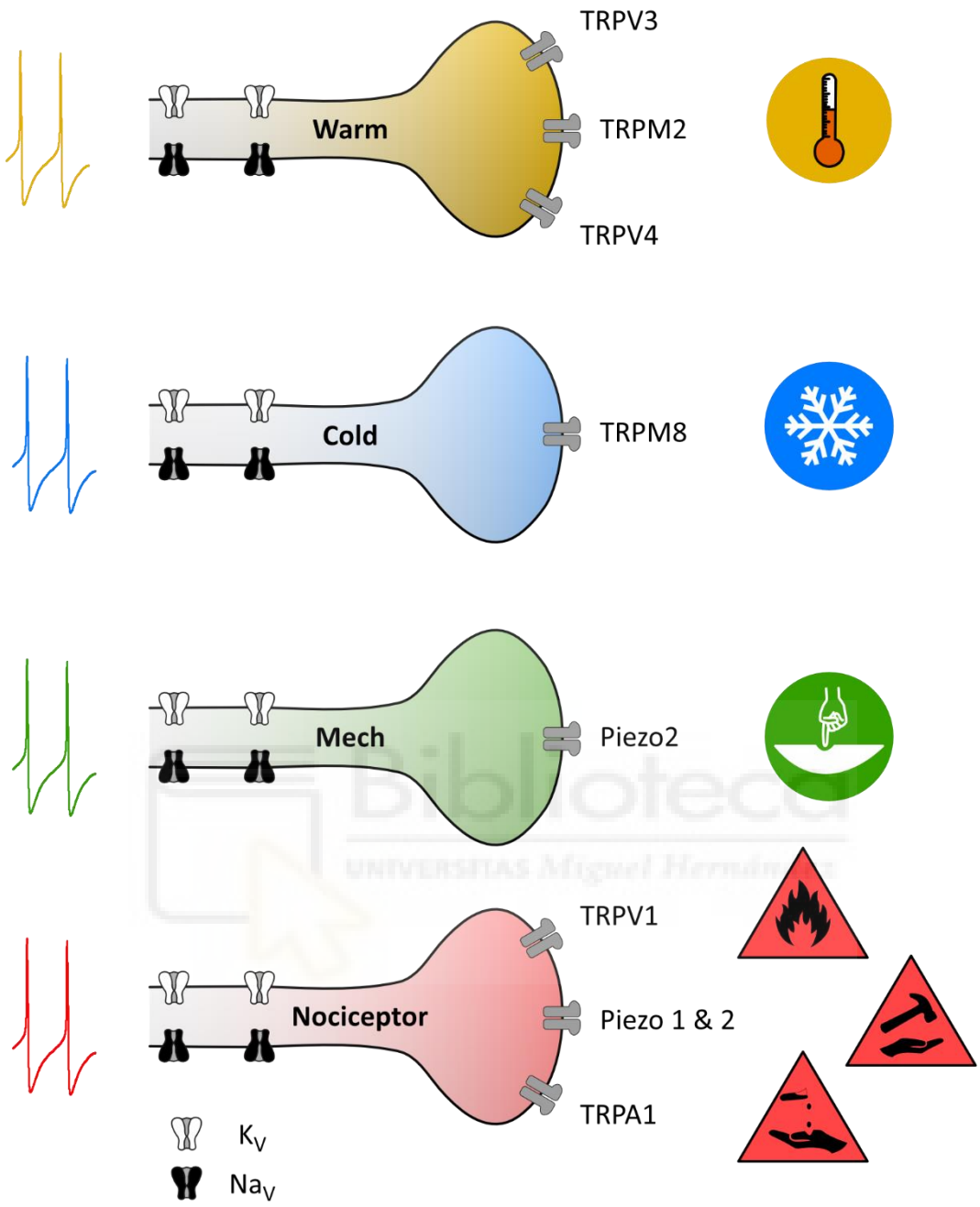

Figure 2. Molecular basis of sensory transduction at somatosensory receptors. *Scheme depicting different subpopulations of modality specific primary sensory neurons, and some of the putative transducing molecules that might provide each receptor subtype with its stimulus affinities. The stimuli refer to the preferred stimulus for each sort of sensory receptor but does not rule out the activation by other types. Adapted from Belmonte and Viana, 2008.*

Somatosensory nerve terminals are either enveloped by a specialized sensory organ, or the nerve is otherwise freely exposed to the stimulus (free nerve endings). The majority of low threshold mechanoreceptors, the sensory terminals detecting skin deformation produced by mechanical forces, are enveloped (Iggo and Andres, 1982; Johnson, 2001; Li et al., 2011; Zimmerman et al., 2014). On the other hand, cold thermoreceptors detecting the cold temperature are free nerve endings (Iggo and Andres, 1982; McKemy, 2013). Terminals detecting potentially noxious stimuli (nociceptors), heat and chemicals also fall into this category (Dubin and Patapoutian, 2010). This latter case presents special interest, as a group of nociceptors is specialized in the detection of a single modality of stimulation (like cold thermoreceptors or mechanoreceptors) but are rather polymodal, responding to different modalities and forms of energy, the so-called polymodal nociceptors (Lawson et al., 2019).

Primary somatosensory neurons carry out two main functions, which are transduction and encoding of the stimuli into electrical signals, which are ultimately relayed to the CNS (Kandel et al., 2000).

Sensory Transduction and encoding at somatosensory receptors.

Sensory transduction is defined as the conversion of one type of energy into another one (Purves et al., 2001). In the case of somatosensory terminals, mechanical forces, temperature variations and chemical energy is transduced into electrical signals, which the nervous system is able to propagate and process (Torre et al., 1995). Primary somatosensory receptors are able to detect stimuli due to the expression of transducing molecules, which are activated by external forms of energy and convert them into changes in the electrical potential of the sensory terminal. This electric potential change is known as receptor or generator potential. The receptor potential contains the information about the intensity and duration of the stimulus in its amplitude and duration (Purves et al., 2001). Subsequently, voltage-gated channels are activated by the receptor potential, generating action potentials. This process is referred to as “encoding” and

comprises the integration of the properties of the stimulus in the frequency of trains of action potentials (Purves et al., 2001). Therefore, while amplitude and duration of the receptor potential contain information about the stimulus, action potential coding is based in the number, frequency and temporal distribution of action potentials being produced (Figure 3) (Azarfar et al., 2018; Panzeri et al., 2010). Mechanistically, encoding happens when the receptor potential reaches the action potential threshold, i.e. the point in which voltage-gated channel starts to open, generating action potentials (Purves et al., 2001).

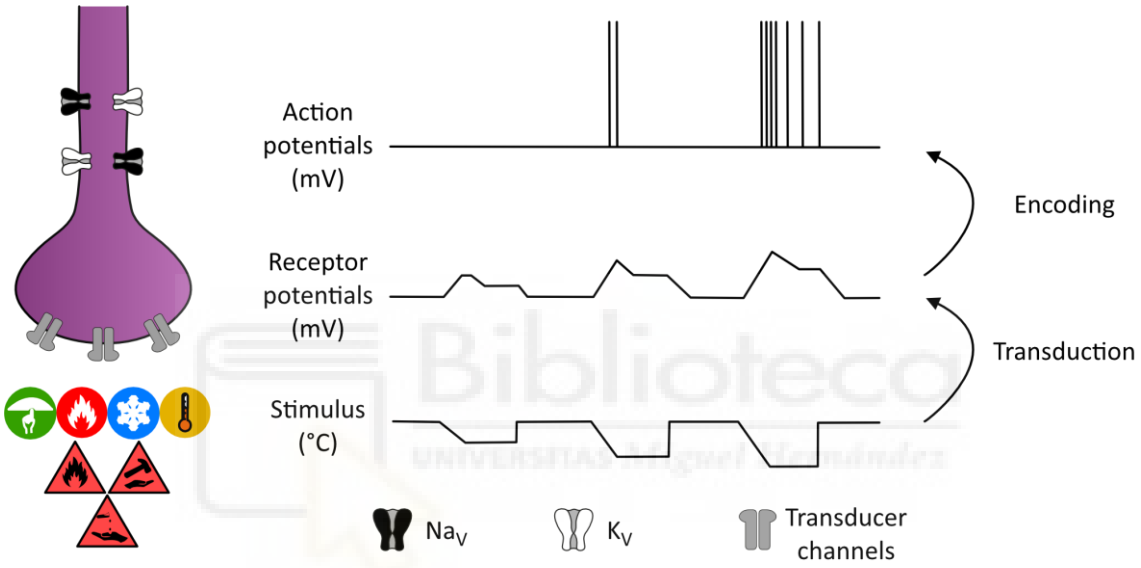

Figure 3. Sensory transduction and encoding at the somatosensory nerve terminal. *Transducer ion channels convert the stimulus energy into a local depolarization known as receptor potential (transduction) which activates voltage-gated channels, triggering action potentials trains (encoding) which are then propagated towards the central nervous system. While the properties of the stimulus are determining the duration and amplitude of the receptor potential, action potentials train codify them in their number and instantaneous frequency.*

Molecular basis of sensory transduction at somatosensory receptors

Several transducing molecules have been identified in primary somatosensory neurons. Among them, some members of the Transient Receptor Potential (TRPs) channel subfamilies TRPV, TRPA and TRPM have been demonstrated to play a key role in the sensory transduction of

somatosensory receptors and are subsequently classified as sensory TRPs (Julius, 2013; Venkatachalam and Montell, 2007; McKemy et al., 2002).

TRPV1 was the first described TRP channel implied in somatosensory detection (Caterina et al., 2000). This channel is sensitive to noxious heating (>43 °C), protons, and irritating chemical compounds like capsaicin or animal toxins. Furthermore, it is able to integrate different stimulus modalities already at the molecular level (Chung and Wang, 2011; Tominaga et al., 1998). In primary sensory neurons, TRPV1 is expressed in medium and small nociceptive neurons of the DRG as well as in C and Aδ-fibers (Hwang et al., 2005; Kobayashi et al., 2005)

TRPM8 is a cold-sensitive channel further activated by chemicals that produce "fresh" or "cooling" perceptions in humans, as menthol (McKemy et al., 2002; Peier et al., 2002) or icilin (Yin et al., 2019). Regarding TRPM8 expression in primary sensory neurons, it has been identified in small and medium diameter TG and DRG neurons (Kobayashi et al., 2005; McKemy et al., 2002). It has been demonstrated that TRPM8 is heavily contributing to cooling perception (Bautista et al., 2007; Colburn et al., 2007; Dhaka et al., 2007; McKemy, 2013; Milenkovic et al., 2014) and that is required for cooling-mediated activation of the primary sensory cortex (Milenkovic et al., 2014).

TRPA1 is a polymodal receptor which integrates at the molecular level different types of stimuli (Story et al., 2003). Among others, TRPA1 is activated by stimuli as diverse as intense cold and heat (Sawada et al., 2007; Sinica et al., 2019), chemical irritants as mustard oil or allyl isothiocyanate (Bandell et al., 2004), inflammatory molecules such as bradykinin (Bandell et al., 2004) or bacterial endotoxins (Meseguer et al., 2014). Due to the irritant or harmful properties of the stimuli that activate TRPA1, it is considered a molecular sensor of tissue stress and damage (Viana, 2016). It is expressed in small neurons in the DRG and TG, which co-express

molecular markers related with peptidergic nociceptors (Story et al., 2003). Understanding of TRPA1 contribution to temperature perception remains elusive, as there are works providing evidence that demonstrates a TRPA1 role in cold-sensing related behaviors (Karashima et al., 2009) and there are works denying it (Bautista et al., 2006; Knowlton et al., 2010).

TRPM3 is activated by intense noxious heat (Vriens et al., 2011) and the neurosteroid pregnenolone sulfate (Thiel et al., 2017). Although mice lacking TRPV1, TRPM3 or both display diminished heat avoidance, it is required to delete both channels together with TRPA1 to abolish behavioral responses against noxious heating (Vandewauw et al., 2018). TRPM3 is expressed in a subpopulation of nociceptors both in DRG and TG, both in mice (Vriens et al., 2011) and in humans (Vangeel et al., 2020).

Aside sensory TRPs, Piezo channels have been postulated as meaningful contributors to mechanical transduction. Piezo 1 and 2 are sensitive to mechanical forces, detecting cell membrane deformations (Coste et al., 2010; Syeda et al., 2016). Additionally, Piezo 1 is activated by the agonist Yoda 1 (Syeda et al., 2015). Regarding their expression pattern, Piezo 2 has been pan-neurally identified in DRG neurons (Shin et al., 2021), while Piezo 1 expression is restricted to small and medium diameter neurons, overlapping with TRPV1, thereby suggesting a nociceptive role for this channel in somatosensory receptors (Wang et al., 2019). In TG, Piezo 2 is mainly expressed in medium to large sized neurons (Bron et al., 2014). Indeed, Piezo 2 is required for sensory transduction in low threshold mechanoreceptors responsible for touch (Woo et al., 2014). More recently, Piezo channels are proposed as the molecular basis for mechanical transduction mediating blood pressure sensing (Zeng et al., 2018) or mechanically evoked pain (Fernández-Trillo et al., 2020).

Regarding warmth transduction in primary sensory neurons, the identification of the molecular mechanisms responsible for it remain elusive. TRPM2 is sensitive to warming (Tan and McNaughton, 2016), as well as TRPV3 and V4 (Huang et al., 2011; Vriens et al., 2014). However, their genetic deletions produce modest deficits in behavioral tests related with warmth detection (Huang et al., 2011). Remarkably, recent experiments suggest that warmth detection could be produced through ongoing activity inhibition in TRPM8-positive cold sensitive neurons (Paricio-Montesinos et al., 2020).

Molecular basis of the action potential at somatosensory receptors

Action potentials in somatosensory receptors are generated as follows: the receptor potential generated by transducing molecules activates voltage-gated sodium channels (Na_Vs) that start to open, allowing Na^+ to flow into the intracellular compartment, depolarizing the membrane, that in turn activates more Na_Vs and goes into a positive feedback loop, called Hodgkin cycle. This produces a large depolarization phase of the action potential that is shut down afterwards by the late opening of voltage-gated potassium channels (K_Vs) that conduct K^+ outside of the cell, repolarizing the membrane voltage again. After action potential generation in a compartment of the axon, it depolarizes the segment adjacent to it, triggering a new action potential and making possible the signal propagation across long distances (Kandel et al., 2000; Raghavan et al., 2019). Moreover, most Na_Vs channels go into inactivation state after opening, preventing them from opening again until repolarization happens, and rendering the neuron unable to fire for a period. This period is known as refractory period, and prevents backpropagation, monotonical depolarization or constant, saturating firing, enabling the neurons to generate a coherent frequency code (Berry and Meister, 1998). Subsequently, voltage-gated sodium and potassium channels constitute the molecular basis of encoding of the receptor potential in somatosensory receptors, and therefore determine the excitability of the

receptor and its capability to conduct action potentials towards the CNS (Hodgkin and Huxley, 1952).

Na_Vs α-subtypes channels expressed by primary sensory neurons are Na_Vs 1.1, 1.6-1.9 (Bennett et al., 2019; Goodwin and McMahon, 2021). While Nav 1.8 and Nav 1.9 are resistant to blockade by the antagonist tetrodotoxin (TTX-R), the others are sensitive to the drug (TTX-S). Each of these channels' isoform present differential functional features at their voltage-current curves or their activation/inactivation time constants (Rush et al., 2007). Expression of TTX-S channels is ubiquitous to all sensory neurons, while Na_Vs 1.7-1.9 are specifically related to small neurons, such as cold receptors and nociceptors (Blair and Bean, 2002; Fukuoka et al., 2008). Interestingly, Na_V 1.3 is expressed during development in sensory neurons and re-expressed in the adulthood after neuropathic damage (Waxman et al., 1994). Alterations in the function of these channels produce pathologies that could present positive symptoms in the case of gain of function mutations, such as spontaneous intense pain, or negative symptom for loss of function mutation, implying partial or total insensitivity to pain, touch or other stimulation modalities (Baker and Nassar, 2020; Bennett and Woods, 2014; George, 2005; Huang et al., 2017; Kanellopoulos and Matsuyama, 2016).

K_Vs channels are a superfamily of molecules with many known isoforms presenting diverse properties. In primary sensory neurons, six voltage-gated K^+ currents have been identified, three of them being transient and the other three, sustained (Gold et al., 1996). Both transient currents IAht and IAs are expressed in small-diameter, capsaicin-sensitive neurons, likely nociceptors, while the other transient current (IAf) is characteristic of large-diameter neurons (Gold et al., 1996). More recent works have focused on revealing the function of many K_Vs isoforms in low threshold mechanoreceptors, and reported that K_V1 governs firing pattern in distinct subtypes of these receptors, while K_V 4.3 specifically enables C-type low threshold

mechanoreceptors to present a delayed firing pattern (Zheng et al., 2019). In cold sensory neurons, K_Vs 1.1 and 1.2 regulate cooling threshold, and their expression altered in neuropathic pain conditions presenting cold hypersensitivity (Madrid et al., 2009; González et al., 2017). K_Vs 1.4, 3.4 and the whole 4 family have been identified in DRG nociceptors (Zemel et al., 2018).

Aside from voltage-gated sodium and potassium channels, voltage-gated calcium channels play a crucial role in action potential encoding, by contributing to the depolarization of primary sensory cells (Baccei and Kocsis, 2000), with a prominent role in nociceptors action potential enlargement (Blair and Bean, 2002; McGivern and McDonough, 2004). Besides, hyperpolarization-activated cyclic nucleotide–gated (HCN) channels regulate the firing rate by influencing repolarization and refractory period, , thereby allowing characteristic firing patterns to each sensory neuron subtype (Doan et al., 2004; Liu et al., 2020).

2. The ocular surface somatosensory system

2.1 The ocular surface

The ocular surface (OS) is the part of the eye directly exposed to the environment, not being covered by the orbital bones nor eyelids while opened (Gipson, 2007) (Figure 4).

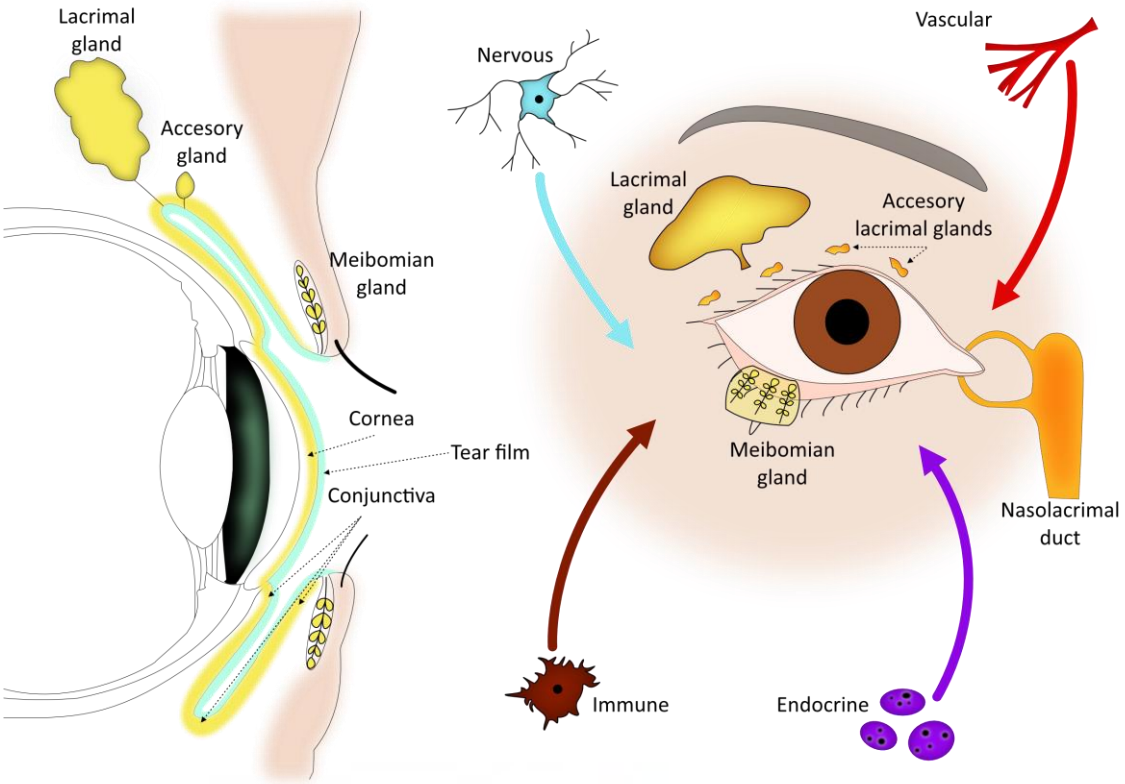

Figure 4. The ocular surface unit. *Sagittal and frontal view of the ocular surface and their associated structures. Only those components of the OS system have been colored, with the exception of the crystalline (colored as a reference). Of note, Meibomian glands produce the lipid layer of the tear film, while principal and accessory lacrimal glands produce the aqueous layer. The mucin layer is produced by goblet cells and the epithelium of the conjunctiva. Additionally, immune, endocrine, vascular and nervous system also contribute to assure the OS maintenance.*

The main tissues composing the OS are the cornea and the sclera, being this latter enfolded by the conjunctiva. Cornea and conjunctiva are soft connective tissues covered by mucosae and designed to provide protection to the inner components of the eye, ensuring the arrival of light to the retina. The cornea is transparent and avascular, covering one sixth of the eye globe in humans, and being the rest occupied by the opaque sclera. The corneal curvature displays a major role in vision, not only allowing the light to reach the inner eye due to its transparency, but also being the more important refractive tissue of the eye, by providing about 44 out of the about 60 diopters of its refractive power (DelMonte and Kim, 2011). Its transparency relies on

the absence of blood vessels and the homogeneity of stromal collagen fibril diameter, located at a fixed distance from each other. The cornea is divided in five layers, three of them considered cellular (epithelium, stroma, and endothelium) and two considered interfaces (Bowman's and Decemet's membranes). From outside to inside, the epithelium is the first layer encountered and the one directly in contact with the external environment and the tears. It is a highly uniform non-keratinized stratified structure with a thickness of around 4 to 6 cell layers (DelMonte and Kim, 2011). The tear film and the epithelium are closely related, in terms of light refractivity in the interfaces air-tear and tear-epithelium from an optical point of view. Indeed, tear protects the OS from microbial invasion, carrying immunological and growth factors, and nurturing the cornea through oxygen diffusion. In fact, the mucinous/mucous layer of the tear film, the most inner one, is produced directly by the goblet cells of the corneal epithelium, much like the mucus in the airways (Pflugfelder and Stern, 2020). Interestingly, epithelial cells are completely renovated in 7 to 10 days through controlled apoptosis. This continuous renewal gives an idea of the dynamicity of this epithelium and the high maintenance of its integrity while being exposed to the external environment (DelMonte and Kim, 2011). The OS somatosensory innervation plays a key role in this process (Eguchi et al., 2017). Bowman's layer is an acellular condensate of the anterior part of the stroma (DelMonte and Kim, 2011), allocated immediately below the epithelium. The stroma occupies around ~80% of the corneal thickness and is mainly composed of collagen, that are organized in parallel and embedded in bigger lamellae, which are subsequently parallel respect to each other. Due to the heterodimeric composition of its collagen (type I combined with type V), the fibers of the stroma are exceptionally narrow. Corneal transparency is generated through both the organization of collagen bundles and the narrow fibers. The main type of cells in the stroma are keratocytes, which maintain the extracellular matrix producing the collagen (DelMonte and Kim, 2011). Descemet membrane is directly located under the stroma, and is produced by the endothelium, being partially formed *in utero* and after birth. The endothelium is a monolayer of continuous thickness composed by

flattened cells which display tight junctions between them. The endothelium maintains a deturgescent state of the cornea by means of a pump-leak mechanism which dehydrates the stroma continuously.(DelMonte and Kim, 2011).

Unlike the cornea, the sclera is a vascular tissue with larger collagen fibrils of different diameters and inter-fibrillar spaces, thus refracting differently the light at each point and being opaque (Levin and Adler, 2011). The sclera is covered by the bulbar conjunctiva, a mucous membrane composed by loose connective tissue covered by 2-5 columnar or cuboidal epithelium layers. Conjunctiva covers the inner part of the eyelids (tarsal conjunctiva), the exposed episclera (bulbar conjunctiva), and the junction between tarsal and bulbar conjunctiva (fornix conjunctiva) (Figure 4). Bulbar conjunctiva has a thickness of approximately 30 microns and is richly vascularized by thin blood vessels, supported by the ophthalmic artery (Efron et al., 2009). The conjunctiva includes goblet cells secreting mucus that contributes to the mucin layer of the tear and lubricates the eye surface.

Together with the above-mentioned structures, the Ocular Surface System includes the main and accessory lacrimal glands (producing the aqueous layer of the tear), the Meibomian glands (producing the lipid layer of the tear), the eyelashes with their associated glands (Moll and Zeiss glands), the nasolacrimal duct, and the eyelid including the muscle fibers responsible for the blink (Figure 4) (Gipson, 2007). All components of the system are linked functionally, being the afferent and the efferent arms of a closed regulation loop, mediated by the somatosensory and autonomous nervous system, and the endocrine, the vascular and the immune systems (Gipson, 2007). Altogether, these structures contribute to the maintenance of the ocular surface integrity by lacrimal production, conjunctival and scleral blood flow regulation, and blinking.

2.2 Ocular surface innervation

The ocular surface innervation allows the detection of environmental and local cellular conditions, encoding and relaying such information to actuators that assure the maintenance of OS integrity (Eguchi et al., 2017; Labetoulle et al., 2019). This general scheme produces from protective reflex behaviors, like increasing tear production (Parra et al., 2014) and blinking in dry conditions (Hirata et al., 2018; Quallo et al., 2015), to conscious perceptions (Acosta et al., 2001b; Belmonte et al., 2004a, 2015).

The neurons innervating the OS are located in the ophthalmic branch of the trigeminal ganglion (TG, par cranealis V). These primary sensory neurons innervate the OS through distinct nerves, from which the ciliary nerves form a plexus between the cornea and the sclera, a zone called limbus (Labetoulle et al., 2019). From there, small nerve bundles penetrate the cornea in a symmetrical disposition (figure 5). Nerves are mainly non-myelinated from this point, which allows a correct corneal transparency. Nerve fibers decouple from the main trunks and penetrate into the epithelium, forming the sensory nerve terminals of the cornea and the conjunctiva (Labetoulle et al., 2019; Launay et al., 2015; Marfurt, 1981; Marfurt et al., 2010). Attending to the stimulus they are responsive to, OS-innervating sensory nerve terminals could be classified in different groups: cold thermoreceptors, mechanonociceptors, and polymodal nociceptors (González-González et al., 2017). This division has been described in mice (González-González et al., 2017), guinea pigs (Acosta et al., 2014), cats (Gallar et al., 1993), and its perceptual and behavioral correlates have been investigated in humans (Acosta et al., 2001a; Kovács et al., 2016; Parra et al., 2010).

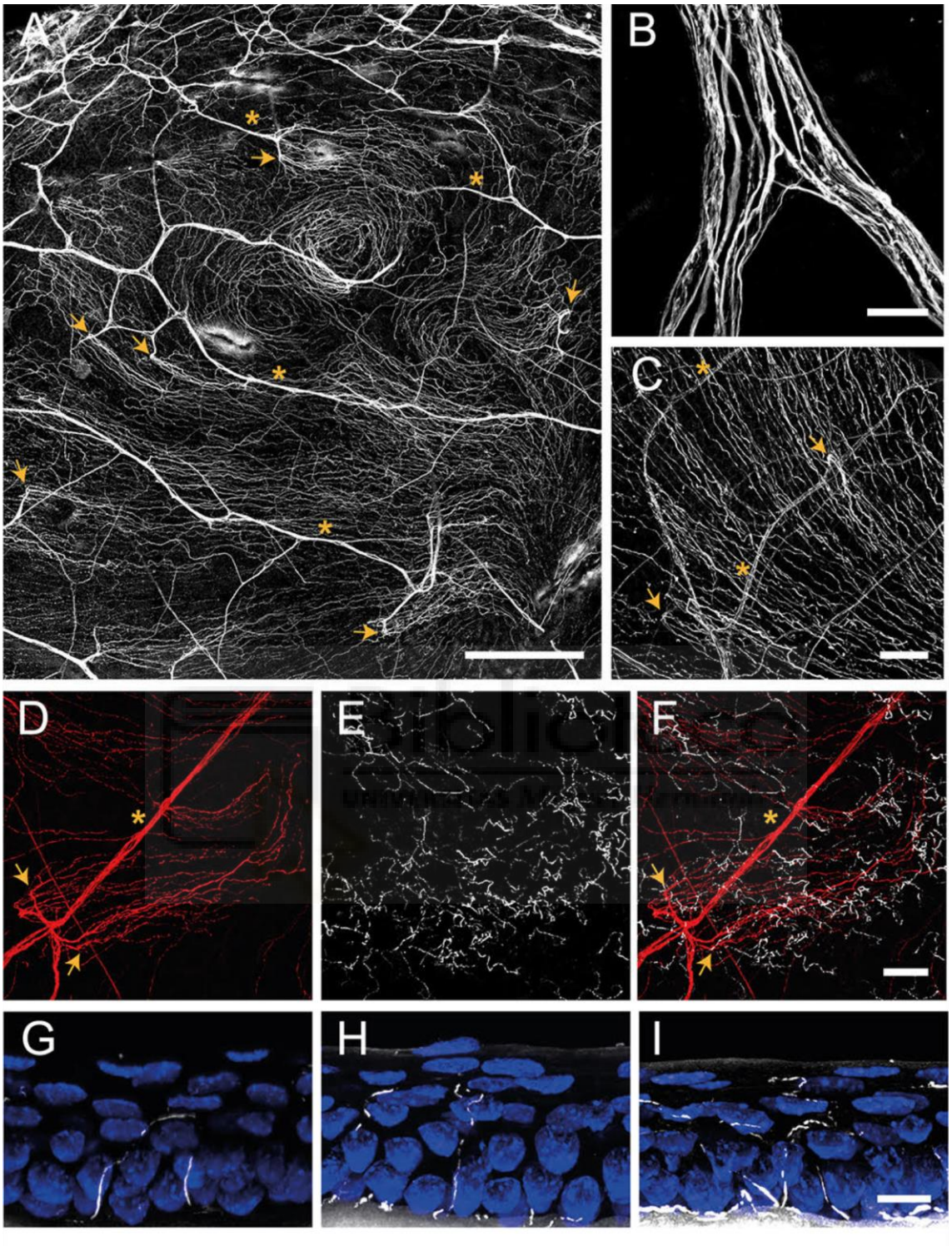

Figure 5. Confocal images of sensory nerves immunostained with anti–β tubulin III antibody in mouse cornea*. (A) Sensory nerve trunks enter from the limbus into the stroma of the cornea where they ramify, giving rise to a dense subepithelial plexus (asterisks). (B) Detail of a stromal nerve trunk branching. (C, D) From the stroma, nerve fibers penetrate through the basal lamina (arrowheads) and form the subbasal plexus. Subbasal nerve fibers run parallel for a long distance within the epithelium basal cell layer. (E–I)*

Subbasal nerves give rise to terminal branches that ascend along their trajectory through the epithelial cells. According to the number of branches, three morphological types of corneal nerve terminals are identified: simple (G), ramified (H), and complex (I) nerve terminals. Scale bars: (A) 250 µm; (B) 25 µm; (C–F) 50 µm; (G–I) 10 µm. From Frutos-Rincón et al., 2022)

Research in OS innervation is relevant both to achieve a deeper understanding of how our body interacts with the environment and preserves its integrity, and to characterize the pathophysiology of many worrying ophthalmological conditions, as information sensed in the OS is crucial to maintain corneal integrity, blinking and tearing (Belmonte et al., 2004b, 2017; Gallar et al., 1993; González-González et al., 2017; Parra et al., 2010; Quallo et al., 2015). OS innervation functionally differs from that of other tissues in some features; cold-thermosensitive nerves are sensitive to cooling, dryness and hyperosmolarity, being silenced by warmth stimulation (Gallar et al., 1993; Parra et al., 2014); heat is only positively detected by polymodal nociceptors (Belmonte and Giraldez, 1981; Belmonte et al., 1991; Gallar et al., 1993); mechanoreceptors are only found in the eyelid (Munger and Halata, 1984); while corneal mechanosensitive terminals are all mechanonociceptors (Acosta et al., 2001a; Belmonte et al., 1991). Cold thermoreceptors can be divided attending to their cold threshold and basal ongoing activity (background activity) in high threshold-low background (HT-LB) and low-threshold-high background (LT-HB) subtypes (Bech et al., 2018; González-González et al., 2017). Remarkably, perceptions originated in the OS are mainly irritation, pain, cooling and dryness, not producing a clear and localizable "touch" perception when mechanically stimulated (Acosta et al., 2001b, 2001a). Of note, the classification of somatosensory receptors in the OS and the skin is different.

Previously, many authors have extensively characterized the physiology of OS innervation in different species, giving a solid background for its study and comprehension. This is why OS is established as a good, readily accessible model to study sensory innervation (Aleixandre-Carrera et al., 2021; Belmonte et al., 2009). Disturbances of OS innervation modify its function (Bech et al., 2018; Kovács et al., 2016; Luna et al., 2021; Piña et al., 2019) and could result in neuropathies

such as dry eye or trigeminal neuralgia (Gallar et al., 2004; Golan and Randleman, 2018; Kasetsuwan et al., 2013; Kato et al., 2019; Toda, 2018). Apart from these pathological conditions, such disturbances can be produced by common medical procedures like cataract or photorefractive surgery, which result in iatrogenic consequences, (Chao et al., 2014; Lum et al., 2019). In fact, functional alterations of OS peripheral innervation could ultimately modify the activity of the central nervous system (CNS) neurons that receive and process OS-related information. This process is known by the term central sensitization, which was proposed by C.J. Woolf (Guerrero-Moreno et al., 2020; Woolf, 1983). It refers to a condition in which a peripheral damage produces an alteration of the nociceptive processing of the CNS, ultimately leading to chronicity of the symptoms independently of the resolution of the original peripheral damage. The process is sustained by plastic changes in the CNS circuits, and, particularly, plasticity of thalamocortical networks has been proved to be a key contributor to chronic pain and/or altered somatosensory function in other body parts (Meacham et al., 2017; Sanzarello et al., 2016). In this regard, it remains elusive whether central sensitization of thalamocortical networks could play a role in OS-related pathologies symptoms and chronicity. Indeed, this question is extremely relevant, as pathologies producing OS aberrant sensory perceptions represent an epidemiological burden to our society. For example, dry eye disease is a chronic disease which shows an high prevalence worldwide: Spain (18.4%), USA (14.5%) or South-East Asia (20-50%) (Stapleton et al., 2017).

3. Central somatosensory nervous system

The central axonal terminal of the primary sensory neurons enters the central nervous system and forms the presynaptic button of the first synapse in the somatosensory system, classically considered as the first point of information processing and integration. However, the location of this synapse varies depending on the ganglia and the type of primary sensory neuron. DRG

neuron projections enter the dorsal horn of the spinal cord, with low threshold mechanoreceptors and proprioceptors dividing in two branches. The first branch stays in the ipsilateral side and gives input to the deeper layers of the dorsal horn, thereby regulating automatic reflexes. The other branch directly crosses the midline and ascends through the dorsal column tracts, reaching *gracilis* and *cunneatus* nuclei in the brainstem (also known as Goll and Burdach nuclei) (Purves et al., 2001). Here, the first classical synapse of the pathway is formed. The length of a mechanoreceptor neuron, extending from the feet to the central terminal in the brainstem is very long, as is the energy required to maintain the infrastructure and functionality needed for the transduction and encoding of stimuli and the function of the synapses (Devor, 1999). From *gracilis* and *cunneatus*, this pathway projects into the ventroposterolateral nucleus of the thalamus (VPL) (Francis et al., 2008). Thalamic neurons then project to layer 4 of the primary somatosensory cortex (S1), finishing the so-called lemniscal pathway (El-Boustani et al., 2020; Mo et al., 2017).

On the other hand, DRG noci- and thermo-receptors have their first synapse at the superficial layers of the dorsal horn (Koch et al., 2018; Todd, 2010). This pathway crosses the midline and ascends through the lateral spinothalamic tract towards the brain, arriving to both the VPL and the postero-medial nuclei of the thalamus (POm) (Boivie, 1979; Gauriau and Bernard, 2004). POm gives projections mainly to layer 4 of the secondary somatosensory cortex (S2) and, although it also gives monosynaptic input to all layers of S1, the strongest input arrives to layers 2 and 5 (Buchan et al., 2021; El-Boustani et al., 2020). This is frequently referred to as the paralemniscal pathway (Frangeul et al., 2014; Mo et al., 2017). Recently, some authors have proposed a third pathway to add to the classical lemniscal and paralemniscal pathways: a division of neurons in medial VPL projects to S2 and S1 septa, forming a third pathway, known as extralemniscal (Haidarliu et al., 2008; Yu et al., 2006). A representation of these three pathways can be found in figure 6.

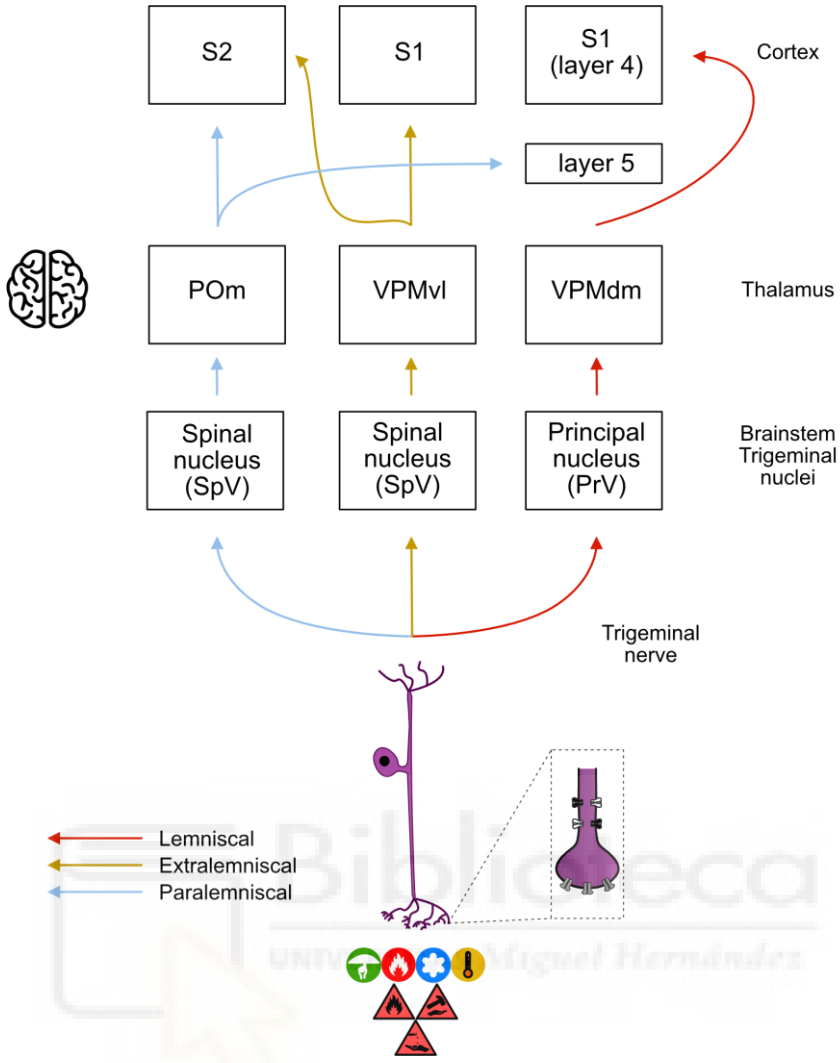

Figure 6. Classical trigeminal pathways in the CNS. *The three main somatosensory pathways described for the trigeminal information in the CNS. Brainstem nuclei are ipsilateral respect to trigeminal ganglion, whereas the thalamus and cortex ones are contralateral (Based on Diamond et al., 2008). POm: Posteromedial nucleus; VPM: ventral posteromedial nucleus; VPMvl: VPM ventrolateral; VPMdm: VPM dorsomedial; S1: primary somatosensory cortex; S2: secondary somatosensory cortex.*

The trigeminal system is also organized in lemniscal, paralemniscal and extralemniscal pathways, but its anatomical substrate differs from the somatic pathway previously described. Namely, the trigeminal ganglion projects into the trigeminal nuclei of the brainstem, which are traditionally divided in two: the principal nucleus (PrV) and the spinal nuclei (SpV). The latter is further divided in three subnuclei, from rostral to caudal: oralis, interpolaris and caudalis (Jacquin et al.,

1986; Olszewski, 1950). PrV receives inputs from fine touch and proprioception and sends projections to ventroposteromedial nucleus (VPM) that further projects to S1, much like the dorsal columns lemniscal pathway of the DRG (Diamond et al., 2008; Mo et al., 2017). SpV, like the spinothalamic tract, receives nociceptive and thermal information (Lu et al., 1993; Martinez and Belmonte, 1996; Meng and Bereiter, 1996) that projects to the POm, among many others, which then projects to S2 layer 4 and S1 layer 5, forming the paralemniscal pathway (Mo et al., 2017). The extralemniscal pathway, with VPM projecting to S2 and S1 septa is also present in the trigeminal system (Haidarliu et al., 2008; Yu et al., 2006; Zhang et al., 2021).

The peripheral information arrives to a first order nucleus in the thalamus (Guillery and Sherman, 2002). This first order nucleus in the thalamus project to layer 4 of the primary sensory cortex(S1) (Guillery and Sherman, 2002). The neurons in layer 4 project to layers 2-3, which in turn project to layer 5, the main output layer from the cortex, which sends corticofugal projections to subcortical structures, including the thalamus (Figure 7) (Grillner et al., 2005). The thalamic nuclei for which the main receiving input comes from layer 5 of a cortex are called “higher order nuclei”.

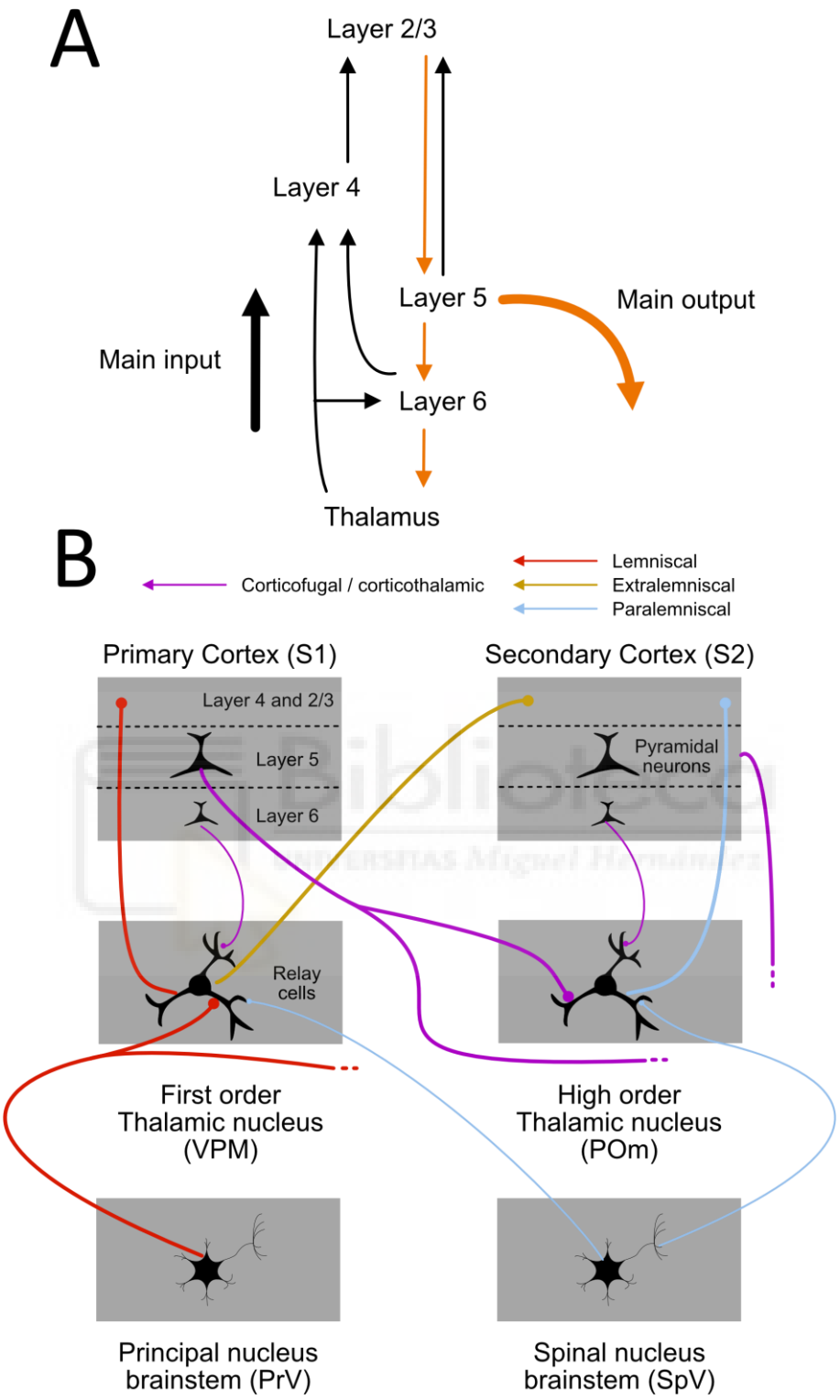

Figure 7. Somatosensory thalamocortical circuits. A. *Scheme representing the columnar circuit. The cortex is divided in columns in the vertical axis, which are heavily interconnected through layers. This scheme represents the interconnection between such layers in a single column. Modified from Grillner et al., 2005.* ***B.*** *Representation of the updated CNS trigeminal circuit. Note that the main input to POm does*

not come from SpV, but from the corticothalamic projection coming from layer 5 of S1. Furthermore, SpV projects to VPM, so information in these pathways is intermingled early in the circuit. The thick lines represent main, driver projection and the thin lines account for modulatory projections (Based on Guillery and Sherman 2002, with information from Mo et al., 2017; Friedberg et al., 2004; Zhang et al., 2021).

VPM main input comes from the peripheral dorsal columns carrying tactile information, and it projects to layer 4 of S1 (Mo et al., 2017). Conversely, A afferences to POm come from layer 5 of S1 (Mo et al., 2017) and its main output arrives to layer 4 of the secondary somatosensory cortex, S2, (Mo et al., 2017). . This suggests POm as an integrative high order nucleus, that puts into communication the precise spatial and temporal information conducted by the lemniscal pathway, that is coming from layer IV of S1, with other inputs, initiating the so-called cortico-thalamo-cortical loop, one of the circuit mechanisms proposed to be underlying integration of information from different modalities into a single multimodal perception (Guillery and Sherman, 2002; Murray Sherman and Guillery, 2011; Sherman, 2017). Furthermore, they are heavily interconnected, as S1 and S2 are wired directly through cortico-cortical projections and through POm, and their afferences from brainstem are also mixed, as some SpV neurons project directly to VPM (Friedberg et al., 2004). An actualized description of these two systems proposed by Mo et al., can be seen in figure 7B.

Apart from the canonical lemniscal, paralemniscal and extralemniscal pathways, the ascending somatosensory tracts give many collateral projections to other systems implied in sensation and perception processing. Some of the most relevant and studied ones are the parabrachial pathway, the solitary nucleus projection, and the descending modulatory system. The parabrachial nucleus received projections from the dorsal horn of the spinal cord and the trigeminal complex of the brainstem (Cechetto et al., 1985; Li et al., 2021), and it is considered an entry gate to polymodal sensory information, receiving not only nociceptive afferents, but also taste, thermoregulation, blood pressure and many other inputs. This nucleus is highly

relevant for the processing of the affective/emotional responses to stimulus, a crucial aspect for pain perception (Chiang et al., 2019). The nucleus of the solitary tract receives polymodal ascending afferences from the sensorial spinal cord and projects ascending efferences to the parabrachial, hypothalamic, periventricular nuclei and the amygdala. Moreover, it sends descending projections to the cervical and thoracic ventral and intermediate horns of the spinal cord. This allows the nucleus of the solitary tract to regulate autonomic processes such as blood pressure and sweating in response to sensory inputs, thereby contributing to flee or fight responses to threatening stimuli (Menétrey and Basbaum, 1987). Finally, the descending modulatory system is a spino-bulbo-spinal circuit that allows a complex of brainstem nuclei to integrate ascending sensory information coming from the spinal cord and descending central nervous system inputs, which ultimately facilitates or inhibits nociceptive transmission in the dorsal horn of the spinal cord (Chen and Heinricher, 2019; Ossipov et al., 2014). Its main neurotransmitters are serotonin and noradrenaline, and the most studied nuclei composing it are the rostral ventromedial medulla and the periaqueductal gray. The descending modulatory system is heavily implied in pain modulation, chronic pain development, and the pain relieving effects of opioids and other drugs (Millan, 2002) and exercise (Sluka et al., 2018).

4. Representation of the ocular surface in the CNS

The representation of the OS in the central nervous system has been scarcely explored. Some works studied OS representation in brainstem structures such as the principal (Pr5) and spinal nuclei (Sp5) of the trigeminal complex (Marfurt, 1981; Pozo and Cervero, 1993). These nuclei are the first station of the OS pathway in the CNS, directly receiving projections from the TG primary sensory neurons. Specifically, it has been demonstrated that corneal afferents project mainly to Sp5, pars interpolaris and caudalis, which is consistent with this nucleus receiving mainly thermal and nociceptive information, as the cornea is specialized in detecting this kind of stimuli. Corneal

projections arrive mainly to the outer half of lamina II of the pars interpolaris and caudalis, to the transition zone between the pars caudalis and C1 spinal level, and slightly to C1 to C3 spinal levels (Marfurt et al., 2010; McEchron et al., 1996). The fact that the majority of projections end on the superficial dorsal horn enforces the notion of the thermal and nociceptive nature of these afferents, as this is where nociceptors and thermoreceptors of the body project in the spinal cord. However, modality pathways are not as separated as previously thought. In this regard, Pozo & Cervero demonstrated already in 1993 that 68% of neurons responding to corneal stimulation in the Sp5 are also receiving input from the periorbital skin. Moreover, from these latter group, a 22% were activated both by noxious and innocuous mechanical stimulation of the skin (Pozo and Cervero, 1993). These early results have two severe implications: the first one is that the small receptive fields corresponding to single afferents are converging in Sp5, even when innervating different tissues. The second one is that central nervous system neurons receive inputs from different modality afferents, consequently increasing the possible combinations of modalities that a single neuron can display. Reinforcing this latter concept, Kurose & Meng demonstrated in 2013 that there are second order neurons in Sp5 receiving information both from cold thermoreceptor and polymodal nociceptor afferents (Kurose and Meng, 2013). Those phenomena are to be expected if many primary sensory neurons project to the same second order neuron, forming a system that is structurally divergent (one primary sensory neuron projects to many second order neurons), but produces modality and spatial information convergence (more than one primary neuron project to the same second order neuron). This configuration has been demonstrated for other sensory systems and has been proposed as a mechanism for pattern separation of the information and resolution refinement (Martinez et al., 2014). In fact, this organization of the system favors discrimination. An experimental example of this was provided by Meng & Bereiter in 1996, who demonstrated that mustard oil, a noxious chemical, activated mainly the superficial lamina of the pars interpolaris/caudalis in Sp5, while noxious heat activated pars caudalis/cervical spinal cord

transition zone (Meng and Bereiter, 1996). This suggests that information coming from different stimulus modalities detected by the same primary afferents of the OS (polymodal nociceptors) is discriminated and separated in the CNS. Intriguingly, other sensory systems, such as vision, convey and interact with the somatosensory system in Sp5, as blocking it with lidocaine reduces electromyographic responses of the blink muscles towards bright light (Rahman et al., 2014). Furthermore, Sp5 projects to the auditory medial nucleus of the medial geniculate in the thalamus, projections that are supposed to mediate conditioned learning between somatosensory stimulation and auditory cues (McEchron et al., 1996).

As mentioned above, CNS somatosensory representations display plasticity in pathological situations. For instance, a dry eye disease animal model presents functional changes in Sp5 OS representation (Rahman et al., 2015). These changes have been characterized as an increase in Sp5 neurons response against hypertonic saline, which is a type of noxious stimulation that imitates dryness conditions in the OS, and increased electromyographic response of the muscles producing blinking. Therefore, both central sensory and motor neurons responsiveness against noxious stimuli are increased in this pathological situation (Rahman et al., 2015). As a mechanistic explanation for these results, it has been demonstrated that GABAergic inhibition is diminished in the interpolaris/caudalis transition, while NMDA-dependent excitatory transmission is enhanced both in this region and in the transition zone between pars caudalis and the cervical spinal cord (Rahman et al., 2017). Other groups have demonstrated an increase in the expression of Piccolo protein in the presynaptic terminals of primary sensory neurons (Fakih et al., 2019), which is intimately related with vesicle retrieval and presynaptic plasticity (Cen et al., 2008). An extensive, updated review about the modifications produced by pathological conditions in the known OS pathway has been recently published (Guerrero-Moreno et al., 2020).

Strikingly, the OS representation has been poorly studied beyond this point of the somatosensory pathway. From Sp5, projections have been characterized to the commissural subnucleus of the solitary tract, superior salivatory nucleus, lateral periaqueductal gray matter, inferior colliculus, parabrachial nuclei and VPM/Pom thalamic nuclei (Hirata et al., 2000; Noseda et al., 2008). When tracing further projections from these nuclei into the CNS, two main pathways have been characterized for OS information, which are similar to previously identified somatosensory pathways for other body structures. The first one is the parabrachial pathway, in which Sp5 projections, mainly from the interpolaris/caudalis transition area, reach the contralateral parabrachial nucleus in the brainstem. Quantitatively, most corneal-receiving neurons in Sp5 project to this pathway (Aicher et al., 2013; Meng et al., 1997). Classically, after the parabrachial nucleus, somatosensory information is relayed in the amygdala and hypothalamus, being heavily implied in the affective-emotional aspects of pain processing (Chiang et al., 2019; Garcia-Larrea and Bastuji, 2018) although these further projections, and/or involvement in pain processing of this circuit have not been probed specifically for the OS somatosensory system. The other documented projection from Sp5 is the one that arrives to the contralateral thalamus, namely to VPM and POm (Aicher et al., 2013). Consistently, functional studies have identified neuronal responses to periorbital tissue stimulation in the VPM/POm complex in squirrel monkey (Kaas et al., 1984) and cats (Yokota et al., 1985). In rats, Diamond et al. found representation of the eyebrow's guard hair in the dorsal area of the PoM/VPM thalamic complex (Diamond et al., 1992b). VPM receives afferent projections both from Sp5 and Pr5, and sends efferences towards S1, which arrive mainly to its layer IV, the main input layer of the primary sensory cortices, and to layers I/II, which are mainly receptors of modulatory inputs (Rausell and Jones, 1991). Accordingly, functional studies in macaque S1 demonstrate representation of periocular tissues in the postcentral gyrus (Dreyer et al., 1975; Nelson et al., 1980). Strikingly, the OS representation of S1 is only referred to a case study of a human patient suffering from corneal pain. Functional brain imaging revealed that S1 was the

main region involved in corneal pain processing (Moulton et al., 2012). No deeper functional characterization of the OS thalamo-cortical circuit has been made beyond a raw characterization of "reponding/not responding", usually using only mechanical or electrical stimulation.

Stimulus modality integration at the somatosensory CNS.

While corneal primary sensory neurons are clearly separated in different functional groups (cold receptors, polymodal nociceptors and mechanonociceptors) (Gallar et al., 1993; González-González et al., 2017), perceptions arising from OS stimulation seem to be more complex than the expected sensation evoked by the stimulation of the distinct corneal sensory neurons subtypes separately. This way, the activation of cold thermoreceptors can produce cold perception, but also irritation or dryness. Otherwise, activation of mechanosensitive receptors does not produce touch perception, but pricking pain (Acosta et al., 2001a). This complex perceptions might result from the integration of the information carried by different peripheral populations (Ma, 2010, 2012). Therefore, it is assumed that at higher levels in the CNS, the information coming from separated peripheral pathways should be integrated to produce perceptions, but no studies aiming to answer how or where this is achieved have been performed until now.

Another unaddressed point regarding modality integration is how the input from different primary sensory neurons could shape the function of the CNS. There are numerous examples about how peripheral afferences shape and mold CNS circuit's function. For instance, when afferences from the periphery are disconnected from the thalamocortical networks by means of a spinal cord section, cortical response of the deafferentiated representation area to supralesion levels stimulation is immediately increased, while spontaneous activity decreases and the oscillatory EEG rhythm becomes slower (Aguilar et al., 2010; Yagüe et al., 2014). Rather than affecting only the deafferentiated cortex, peripheral disconnection also modifies the function of

the intact cortex adjacent to it, which exhibits these same changes, suggesting a full switch in the local circuit functioning (Humanes-Valera et al., 2013). Further extending this idea, the deafferentiated sensory thalamus exhibits similar changes, with increased responsiveness and reduced spontaneous activity (Alonso-Calviño et al., 2016). But disconnection from peripheral inputs not only produces acute, immediate changes. In fact, it chronically modifies thalamocortical functioning, and this phenomenon has been extensively studied both in humans and rodents. Basically, intact areas become enlarged and invade deafferentiated areas in S1. Even 3 months after the injury, the cortex is still reorganizing (Humanes-Valera et al., 2017). This process is quite similar to what happens in a full sense deprivation during development, for example eye enucleation, in which adjacent cortices invade the deafferentiated cortical area, a phenomenon referred to as cross-modal plasticity (Mezzera and López-Bendito, 2016). Further proving that spontaneous activity is crucial for cortex organization, even during development, recent works from the group of López-Bendito demonstrate that prenatal activity of thalamic networks is determining the formation of cortical maps in mice (Antón-Bolaños et al., 2018, 2019; Martini et al., 2021).

Ongoing activity of the primary sensory neurons innervating the OS.

Based on the aforementioned evidences showing the crucial role that somatosensory afferent activity plays in the central sensory processing it is noteworthy to hypothesize that afferent activity from one or another primary sensory neuron might affect the function of the circuit, as primary sensory neurons greatly differ in their ongoing activity. Indeed, LT-HB cold receptors display high levels of ongoing activity, between 2 and 12 Hz (González-González et al., 2017) while polymodal nociceptors have low ongoing activity (<1 Hz) and most mechanoreceptors and mechanonociceptors completely lack of it. However, unlike stimulus -evoked activity, very little is known on how spontaneous activity is generated at primary somatosensory neurons.

Therefore, a better understanding of the mechanisms underlying the spontaneous activity at the OS primary sensory neuron is needed as a first step to further exploring its contribution to central sensory processing.

Membrane potential instabilities at the primary somatosensory neuron

While ongoing activity at the CNS mainly arises from synaptic interplay between groups of neurons (Buzsáki et al., 2012; Colgin, 2016; Timofeev, 2013), primary sensory neurons lack synaptic communication almost completely (Lieberman, 1976). Thus, ongoing activity in primary neurons should be a cell-autonomous phenomenon, regulated by the excitability of the neuron itself, and by inputs or environmental conditions that are tonically encoded. The most robust candidate for this role is an electrophysiological event called Membrane Potential Instabilities (MPIs), which is defined as sustained variations of the membrane potential that occur either spontaneously or as a response towards a tonic depolarization (Figure 8). MPIs have been electrophysiologically recorded in DRG (Amir et al., 1999, 2002b, 2002a), TG (Puil et al., 1988, 1989; Puil and Spigelman, 1988) and Mes-V (Pedroarena et al., 1999; Wu et al., 2001), both *in vitro* (Dong et al., 2008; Ke et al., 2012; Wang et al., 2011) and *in vivo* (Amir et al., 2002b; Djouhri et al., 2018; Li et al., 2007), in human (North et al., 2019), rats (Amir et al., 1999; Verdier et al., 2004), and mice (Liu et al., 2002; Mathers and Barker, 1984).

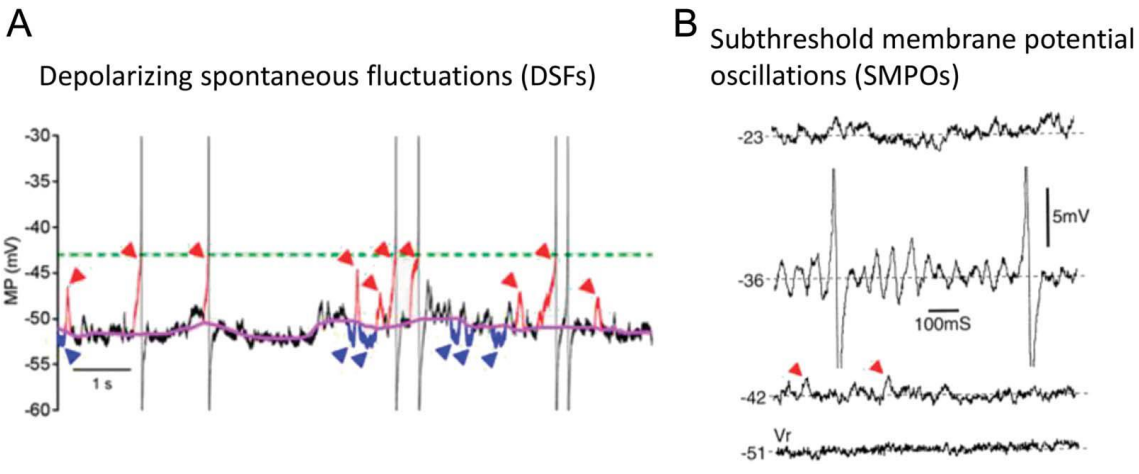

Figure 8. Two distinct types of membrane potential instabilities (MPIs) recorded in C-type DRG neurons. *(A) Voltage trace showing MPIs in the shape of depolarizing spontaneous fluctuations (DSFs). The purple line represents the median level determined with a sliding window. Note that the voltage deflections occur more prominently in the positive direction (red arrows) than in the negative direction (blue arrows). The green dash line represents the threshold of action potential firing. Taken from Odem et al., 2018, reproduced with permission of the copyright holders. (B) Voltage traces showing MPIs as subthreshold membrane potential oscillations (SMPOs) occurring around a membrane potential of -36 mV. Subthreshold membrane potential oscillations do not appear at more negative or more positive potentials. Interestingly, DSFs seem to occur at -42 mV (red arrows). Modified from Amir et al. 1999, reproduced with permission of the copyright holders. DRG, dorsal root ganglia. Complete figure extracted from Velasco et al., 2022.*

In the scientific literature, MPIs have been divided in subthreshold membrane potential oscillations (SMPOs) and depolarizing subthreshold fluctuations (DSFs). SMPOs are constant, compensated, sinusoidal oscillations of the membrane voltage, whereas DSFs are individual or short trains of voltage deflections skewed in the positive direction. Interestingly, SMPOs have been primarily described in large primary sensory neurons, typically identified with mechanoreceptors and proprioceptors, whereas DSFs are typical of small neurons, which comprises nociceptors, thermoreceptors, pruriceptors, and some small low-threshold mechanoreceptors (Lawson et al., 2019). As previously stated, these types of neurons display well-differentiated ongoing firing patterns, matching the notion that MPIs indeed shape them (Xing et al., 2001a). Moreover, nearly all neurons capable of generating spontaneous or ongoing activity display MPIs (Amir and Devor, 1997; Odem et al., 2018; Pedroarena et al., 1999; Verdier et al., 2004). MPIs are enhanced in pathophysiological conditions featuring increased excitability and ongoing activity, such as bone cancer (Ke et al., 2012) and neuropathic injury (Amir et al., 2005; Kapoor et al., 1997; Liu et al., 2000). Moreover, upon a demyelinating lesion, local MPIs are generated at the injury site, suggesting that they are intimately related with ectopic firing

(Kapoor et al., 1997). Other functions attributed to MPIs are cell-to-cell communication (Amir et al., 1996) and response to tonic or slow ramp-like stimulation.

Mechanistically, MPIs are hypothesized to be generated by an interplay between voltage-gated Na^+ channels (NaVs) and K^+ channels (Kvs), which enable the membrane to enter a stable resonance state spontaneously or upon depolarization (Kovalsky et al., 2009). However, the nature of the currents underlying MPIs seems to differ across nuclei and cell types. This leads to the hypothesis that somatosensory circuits at the CNS are shaped by the interplay between different modality afferences, and the latter are modulated by MPIs, in such a way that subtle differences in expression of voltage-gated channels at the peripheral receptor could determine the central sensory processing output.

Although MPIs have been investigated for 30 years, studies using trigeminal sensory neurons are the oldest ones and a thorough characterization of its MPIs is still lacking. Moreover, rough correlations between the capability of generating ongoing activity and MPIs have been reported in individual neurons, but a specific analysis and modelling of how MPIs may generate action potentials in actual experiments remains to be done. This situation impedes answering why different primary sensory neurons display distinct levels of ongoing activity and how such ongoing activity shapes the function of the CNS circuitry representing the OS.

Objectives

This thesis aimed at clarifying several of the questions proposed above, and its specific objectives are summarized as:

1) To determine the stereotaxic coordinates to record neurons receiving information from the ocular surface, in the primary somatosensory cortex and somatosensory thalamus.
2) To characterize the population and single unit responses of trigeminal ganglion, thalamus and primary somatosensory cortex neurons to stimuli of different modalities delivered to the ocular surface, and to investigate how modality is processed along the somatosensory pathway.
3) To analyze the spontaneous activity of cortical, thalamic and trigeminal neurons responding to ocular surface stimulation with different modalities of stimulus.
4) To characterize the membrane potential instabilities of trigeminal ganglion neurons, and their role in action potential generation.

To achieve objectives 1 to 3, we performed multi- and single-unit electrophysiological recordings in anesthetized rats while stimulating the OS. To accomplish objective number 4, we performed whole-cell patch-clamp recordings in primary sensory neurons using primary cultures of mouse TG neurons.

Methods

In vivo electrophysiological recordings

Animals

The experiments implying animals adhered to the International Council for Laboratory Animal Science, European Union 2010/63/EU regulation, and were authorized by the Ethical Committees for Animal Research of Hospital Nacional de Parapléjicos (Toledo, Spain) 177CEEA/2019 and Universidad Miguel Hernandez UMH.IN.JGM.03.20. Furthermore, we followed the ARVO (Association for Research in Vision and Ophthalmology) statement for animal experimenting. The final sample was composed by 17 male Wistar rats (between 2 and 4 months old, and weight between 250–400 g), housed in groups of maximum three individuals, with water and food *ad libitum*.

Surgical procedures

For anesthesia, we used urethane (i.p. 1.5 g/kg). Anesthesia level was kept constant at stage III-3 (Friedberg et al., 1999) during the entire experiment with additional doses of 1/10 of the original injection, if needed. Once anesthetized, we placed the animal in a stereotaxic frame (SR-6R; Narishige Scientific Instruments, Tokyo, Japan), keeping corporal temperature regulated at 36.5 °C by a closed-system heating blanket. To access the brain and the TG, we performed craniotomies in both sides of the skull (Paxinos and Watson, 2007). In this way, we studied both eyes of each animal, minimizing animal use for ethical reasons.

In vivo extracellular recordings

Tungsten electrodes were used to extracellularly record from neurons (2-5MΩ impedance) (TM33B20KT and TM31C40KT, WPI, Inc., Sarasota, FL, USA). Afterwards, the signal was amplified (x500) and filtered in DC mode (0 to 3 kHz), through a preamplifier, filter, and amplifier set up (Neurolog, Digitimer Ltd., Welwyn, UK). Signal was digitized at 20-50 kHz with 64-bit quantization using a CED Power 1401 (Cambridge Electronic Design, Cambridge, UK), equipped with Spike2 software (v7.12; Cambridge Electronic Design).

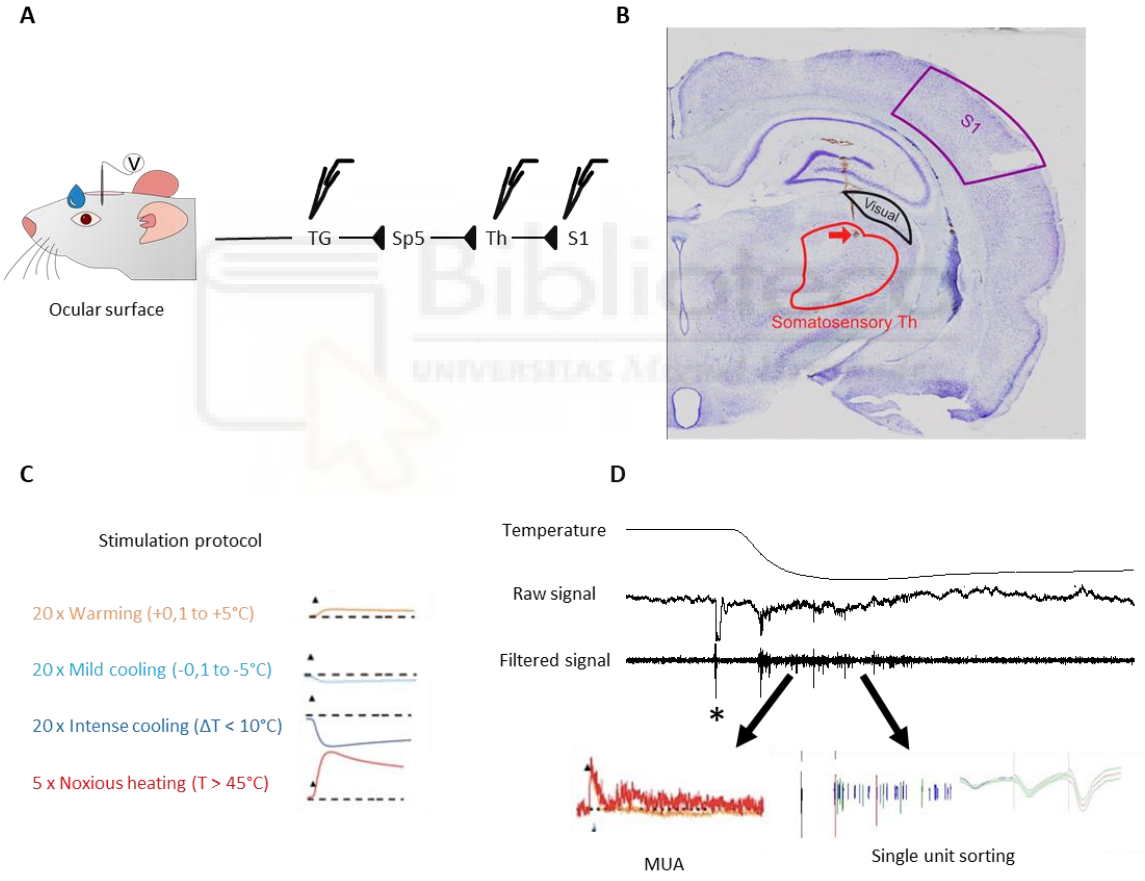

Figure 9. Recording experimental methods and protocol. A. *Scheme representing the stimulation method and recording sites distributed along the somatosensory pathway.* ***B.*** *Brain slice (coronal) showing electrode's track (brown mark), which finishes at the edge separating thalamic VPM and POm thalamic nuclei.* ***C.*** *Depiction of the stimulus applied in each characterization and the OS temperature change produced by them, with dotted line representing basal temperature (around 30ºC).* ***D.*** *S1 recording*

processing, showing an intense cold evoked response. Temperature is depicted in the upper line, with the raw recording immediately below, from which single action potentials were extracted after filtering and event detection (MUA). After a sorting protocol, single unit activity was constructed from MUA. (*) marks the electrical artifact that the drop produced when contacting OS, which was used as the onset of the stimulus to calculate latencies.

We have previously defined the coordinates to record neurons innervating the OS in the TG: AP= -1.5, L=2, DV=1 (Santiago et al., 2017). Regarding OS representation coordinates in S1 and Th, they have not been described before. As an starting point, we used the coordinates of periocular areas proposed by (Chapin and Lin, 1984) for S1, and by (Diamond et al., 1992a) for the Th (Figure 9). Using those references as starting point, we scanned close areas in search of neurons responsive to OS stimulation. S1 and Th recordings were contralateral respect to the stimulated eye, while TG was ipsilaterally recorded. We performed 38 recordings (S1: 17, Th: 13, TG: 8).

Receptive field location

We located the receptive field of active neurons to test if they were innervating the OS. For this purpose, we used a fine brush to gently swipe the cornea, eyelid borders, alpha whisker, and eyebrows. As a global and not exclusively mechanical stimulus, we applied a drop of ice cooled saline over the complete OS.

Ocular surface thermal stimulation

We topically applied 20 µL drops of saline at different temperatures (range 10-60°C), to induce temperature changes between -20 and +30ºC respect to OS basal temperature (29-31°C). An interval of at least 30s was kept between stimuli. To control the change of temperature

produced by each drop, OS temperature was monitored constantly with a thermal micro-probe carefully placed over the corneal surface (IT-24P, Physitemp, Clifton, NJ, USA) and connected to a digital thermometer (Physitemp Bat-12). Drop instillation produced fast temperature changes, followed by a slow recovery of basal temperature (Figure 9C-D).

Thermal stimuli were divided into five categories according to the maximal temperature change induced from the basal temperature around 30 °C as follows: intense cooling (ΔT greater than -10°C), mild cooling (ΔT between -0.1 and -5°C), warming (ΔT between +0.1 and +5°C) and noxious heating (ΔT +11°C) . For noxious heating, we used a single temperature that is sufficient to activate ocular nociceptive TG neurons.

At least, 20 stimuli of each category were applied, with the only exception for noxious heat, of which only 5 drops were applied, with 5 minutes between them, to avoid severe OS burn damage. Stimulation was applied in a fixed order, going from the most innocuous to most harmful stimulus: mild cool->mild warmth->intense cold->noxious heat (Figure 9C).

Analysis of the electrical activity

To analyze the impulse response of the recorded neurons raw recordings were first digitally filtered (0,3-3kHz). Then, event detection was performed using an amplitude threshold for spike detection (>2,576*SD [99% CI] away from background). The total of spikes detected in a recording location were considered as multiunit activity (MUA) (Figure 9D). Often, MUA responses were biphasic and, in these cases, both components of the response were separately analyzed.

A spike-sorting protocol based on templates formed by spike shape coincidences was used to extract single unit action potentials. This protocol was applied by semi-automated homemade

scripts in Spike 2 software and Python Anaconda (Spyder) (Rossum and Drake, 2009) (Figure 9D). 218 single units were extracted: 49 from TG recordings, 69 from Th and 101 from S1. To analyze the response of single units, peristimulus histograms were constructed using the time stamps generated by stimulus application over the OS. Units were categorized as responsive or not responsive to a given category of stimulus based on the increased firing frequency over the basal ongoing activity. Peristimulus histograms were constructed to define the response of single neurons to defined categories of thermal stimulus applied to the ocular surface.

Statistical analysis

For statistics, we used SPSS v25 (IBM Corporation) and Excel (Microsoft Corporation). Normality was tested for quantitative variables and, in the cases that it was confirmed, comparison between two groups was performed with independent t-Test. For comparisons between the same unit or recording site, paired t-Test was used. To compare more than one group, one-way ANOVA with Bonferroni post-hoc correction was used. If normality was not accomplished, non-parametric tests were used (Mann-Whitney's U test, Wilcoxon, and Kruskal-Wallis with Bonferroni post-hoc corrections over Mann-Whitney's U, respectively).

In vitro electrophysiological recordings

Experimental model

C57BL/6J strain mice were housed under controlled conditions, with a maximum of four animals per cage on a 12-h light cycle and with food and water ad libitum. Ten- to twelve-week-old mice were used in all experiments. All animal experiments were carried out in accordance with the

European Union Community Council guidelines and were approved by the local ethics committee (P021/ 2012).

Primary culture of trigeminal neurons

On the day of the culture, mice were killed using 100% CO_2 and ganglia were extracted immediately and cultured using a subtle variant of a method already described (Descoeur et al., 2011). After extraction, TG were placed in Neurobasal A medium (Invitrogen) + 10% fetal calf serum (FCS) + collagenase 1 mg/ml (Gibco) + dispase 2.5 mg/ml (Gibco) for 45-60 minutes at 37ºC. After enzymatic dissociation, the product was carefully washed two times using Neurobasal A+FCS and put into Neurobasal A medium containing glutamine, penicillin/streptomycin, NT4 (Peprotech), B27 and GDNF (Invitrogen). Once in this medium, the enzymatically digested TGs were mechanically dissociated using progressively smaller needles and the resultant product was centrifuged at 1500 rpm for 5 minutes and resuspended in the culture medium after removing the supernatant. The final product was seeded on poly-L-ornithine/laminin-coated glass bottom chambers (Fluorodish WPI) and cultured for 12–24 h at 37 °C before recordings.

Whole-cell patch-clamp recordings

Whole-cell patch-clamp recordings were made using standard borosilicate patch pipettes (3-5 MOhms) pulled with a DMZ-Universal puller (Zeitz Instruments). Pipettes were filled with intracellular solution containing (in mM): 115 K-methanosulfonate, 25 KCl, 11 EGTA, 10 HEPES, 2.5 $MgCl_2$, 2 Na_2ATP, 1 NaGTP, 1 $CaCl_2$ adjusted to pH 7.2 with KOH and 310 mOsm. For acquisition an EPC7 patch-clamp amplifier (LIST Electronics), a TL-1 DMA interface (Axon Instruments) and the pClamp software (Version 9.0, Axon Instruments) were used. An Ag-AgCl wire was used as reference electrode. To visualize the cells, an Olympus IX70 microscope was

used. The bath in which the cells were immersed was kept in constant circulation applied by gravity and maintained at 32.5ºC degrees using a Peltier closed-loop system which was also used to apply heat/cold ramp stimuli. Bath solution was composed (in mM) by: 140 NaCl, 10 HEPES, 10 Glucose, 3 KCl, 2.4 $CaCl_2$, 1.3 $MgCl_2$, adjusted to pH 7.4 with NaOH and 290-300 mOsm. All chemicals were purchased from Sigma-Aldrich.

Recordings were sampled without filtering, digitized and stored in a PC for offline analysis. Current injection protocols were recorded at 20 kHz, and stimulation was performed using 10 crescent squared pulses of 2 s duration. Amplitude gain of the pulses was determined for each cell individually to reach evenly spaced voltage changes but default stimulation was set at +10 pA per pulse, starting at -20 pA, thus being the first two pulses hyperpolarizing ones, the third a 0-current pulse, and the seven remaining pulses depolarized the cell. Values were varied together to maintain this distribution. A total of 46 neurons underwent this protocol and were satisfactorily recorded. For temperature ramps and chemical stimulation, a gap-free protocol with 0 current and 50 kHz sampling rate was settled.

Thermal stimulation

Thermal stimulation was applied using the Peltier system of the bath, in the form of ramps reaching 40 ºC for heating and to 17 ªC for cooling, starting at a physiological temperature of 32 ºC with a total heating/cooling time between 2:30 and 3:30 mins.

Data analysis and statistics

Data recorded in pClamp software (Molecular Devices) was converted into Spike 2 (CED) format using a customized Python (Van Rossum and Drake, 2009) script based on the library Neo.Io. Afterwards, homemade scripts programmed in Spike 2 were used to detect depolarizing MPIs based on their amplitude, with a minimum threshold of +1mV, fitting a parabola between each high point (in which data falls before and after it) and the points on either side. Then, the maximum depolarization point of the transient was marked. After maximum detection, the MPI start and ending were determined as follows: first, the minimum voltage value 200 ms before and after the MPI were captured, and baseline for that specific MPI was defined as 80% the average between the "before" and "after" minimums. In case of these two measurements being different in more than ± 5 mV, the measurement closer to that MPI maximum amplitude was used. Then, start and end of the MPI were defined automatically as the first point crossing the baseline starting from the maximum value. Finally, the MPI and the detected limits were presented graphically to the analyst, who had three options: discard it, approve it for event frequency analysis, or approve it both for event frequency and shape analysis (in case that the MPI was perfectly detected). In consequence, every MPI detected was manually supervised to assure accurate detection.

After MPI detection, the data was processed using Python homemade scripts. For shape analysis, arrays were composed by each single MPI trace, and for event frequency and Fourier analysis the basic unit used to compose the analysis array was each 2 s current pulse, minus 0.25 s at the beginning and the end of the pulse, to avoid recording phasic phenomena induced by the current injection. Event-frequency analysis in gap-free recording for chemical and thermic stimulation was carried out manually, while shape analysis was maintained automatized. Each array produced was visually supervised to curate for detection errors. Figures were made using Python MatPlotLib, SeaBorn and SPSS 26 (IBM Corp.). Statistics were performed using SPSS 26, and data is reported as mean ± SEM unless otherwise specified.

RESULTS

1. Location of the ocular surface neurons in the somatosensory thalamus and the primary somatosensory cortex.

To accomplish the first objective *"To determine the stereotaxic coordinates to record neurons receiving information from the ocular surface, in the primary somatosensory cortex and somatosensory thalamus"* we performed a hypothesis-driven screening in these structures, looking for responses to OS sensory stimulation. Screening stimulation consisted in the application of a saline-wet fine brush and drops of ice-cooled saline over the OS while extracellularly recording in different coordinates.

To decide the coordinates to be evaluated, we first localized the alpha or beta whisker functional representation in the structure. Afterwards, we moved the electrode in the direction that, given the somatotopic organization of the structure, corresponded to a posterior and dorsal displacement inside the face representation, as the OS is located immediately dorsal and posterior respect to the whisker pad in the face, in which alpha and beta whiskers are the postero-dorsal "corner".

The aforementioned strategy was fruitful, and based on this procedure, we report that the thalamic coordinate in which we found OS neurons with higher chance was (from bregma): AP -3.5 to -4; ML 3-4; DV 4.5-5.7mm (1/19 animals at DV 6.5) (Figure 10A-B). These coordinates correspond to the posterior medial complex of thalamus (PoM), near the border of the ventral posteromedial nucleus (VPM), as we later confirmed through histological imaging of the electrode track (Figure 10B). In S1 case, the location in which we found more units was AP 3.7-5.7; ML 5.2-7.2; DV 0.32-1.4mm (Figure 10C-D). S1 neurons responding to OS stimulation were sitting between neurons representing the ear and other areas corresponding to the spinal level

C1 and to neurons representing the maxillary branch of the TG (whisker barrels), thus confirming that OS representation was located inside the V1 part of the face in the somatotopic maps of S1 and Th, as it should be expected based on the "ratunculus" organization of these nuclei.

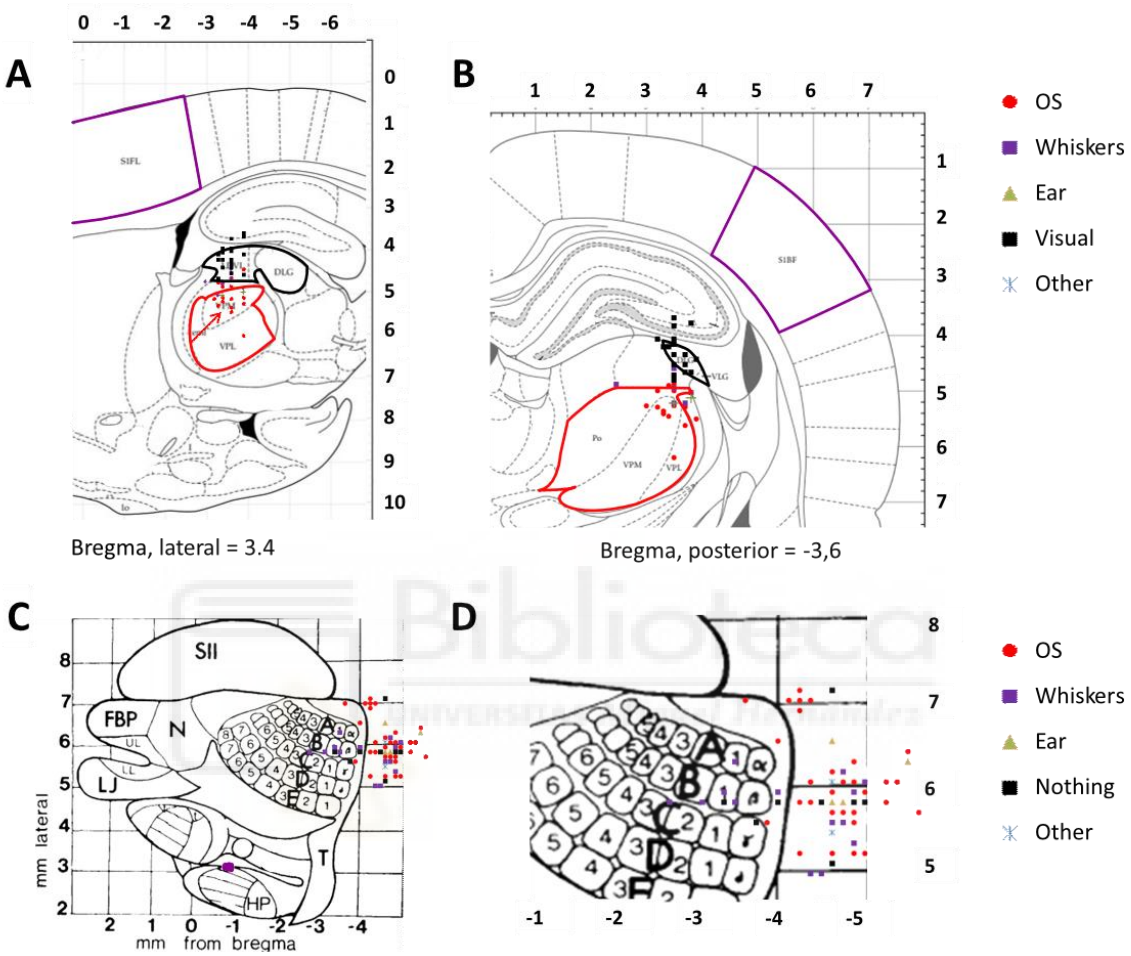

Figure 10. OS has a somatotopic representation in the somatosensory thalamus and primary somatosensory cortex. *Frontal and sagittal drawings of the thalamus (**A-B**) and somatosensory cortex **(C-D)**, with recording sites overdrawn. **A.** The arrow indicates the coordinates suggested in the, near α and β vibrissae coordinates and immediately ventral to visual thalamus* [37]. *In fact, OS responses started just when visual responses disappeared during electrode lowering. **B.** Once inside somatosensory thalamus, the distribution of sites where OS responses were recorded was narrow in the vertical axis, functionally located between visual and vibrissae responses. **C.** Trigeminal V1 representation (ophthalmic) was caudal respect to V2 in S1, close to α and β whiskers. This is consistent with previous evidence showing that V2 representation (maxillary branch of the trigeminal ganglion, innervating the whiskers) is caudal respect to*

V3 (mandibular, jaw) in this structure [35,36]. ***D.*** *Zoom in of C. Total number of recordings represented: Thalamus, 47; S1, 58. Schemes of the thalamus and brain primary somatosensory brain cortex from Paxinos and Watson (2007) and Chapin and Lin (1984), used with permission of copyright holders. "Other" classifier was applied to paws, trunk, tail, and facial areas not included in other categories.*

2. Time course of the ocular TG, Th and S1 neuron population response to different stimulus modalities.

The next objective was to *"To characterize the population and single unit responses of trigeminal ganglion, thalamus and primary somatosensory cortex neurons to stimuli of different modalities delivered to the ocular surface, and to investigate how modality is processed along the somatosensory pathway"*. Therefore, we first analyzed the multiunit activity (MUA) elicited by all stimulus modalities, averaging across trials and animals for representation (Figure 11) and summarizing the numerical data (Table 1).

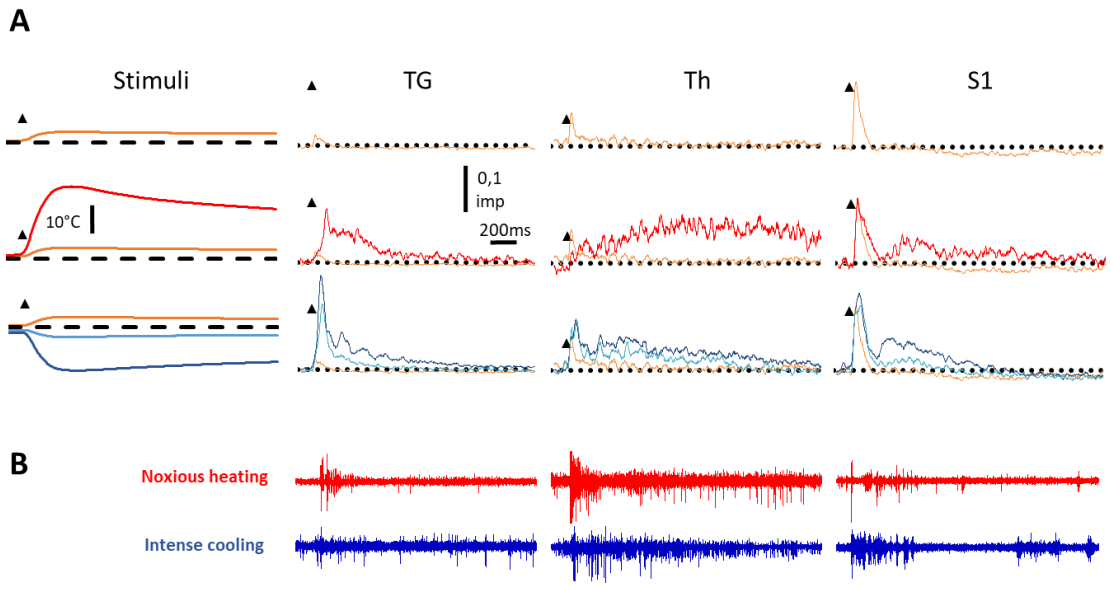

Figure 11. The modality of the OS stimuli is encoded by CNS neurons with different time components and noxious stimuli produce qualitatively different responses. A. *Average of OS temperature change*

produced by each stimulus type respect to basal temperature (dotted line) using 20ms bins. The artifact produced by the drop instillation was used as initiation of the stimulus (black triangles). Numerical summary of these responses is available at Table 1. ***B.*** *Representative filtered (300-3000Hz) MUA recordings at each structure in response to intense cold (blue) or noxious heat (red). Stimulus onset is aligned to the other figures.*

Table 1. Characteristics of the population response of neurons recorded in the trigeminal ganglion, thalamus and primary somatosensory cortex to different thermal stimuli.

		Initial Component				**Second Component**		
		Warming	**Noxious heating**	**Mild cooling**	**Intense cooling**	**Noxious heating**	**Mild cooling**	**Intense cooling**
Trigeminal ganglion (V1)	**Firing rate (spikes/ms)**	0,13±0,1	0,13±0,1	0,13±0,1	0,14±0,1	0,62±0,2	0,42±0,2	0,53±0,2
	Latency (ms)	9,4±3,8	7±3,5	8,1±4,1	7,8±2,4	114,1±58,1	56±20,4	52,1±16,4
Thalamic nuclei	**Firing rate (spikes/ms)**	0,21±0,1	0,31±0,1	0,25±0,1	0,21±0,1	0,53±0,2	0,31±0,1	0,31±0,2

	Latency (ms)	20,9±5,5	21,8±5,3	21,9±7,3	19,6±5,7	726,8±277,3	121±104,5	138,7±144,3
Somatosensory cortex (S1)	**Firing rate (spikes/ms)**	0,23±0,1	0,41±0,1	0,23±0,1	0,21±0,1	0,45±0,2	0,19±0,1	0,23±0,1
	Latency (ms)	24,7±6	24,5±6,1	25,8±6,1	26,5±5,8	302,6±57,5	297,3±60,4	278,8±74,3

Latency, in *ms*, represents the time from the stimulus initiation to the peak of the response. Data are presented as mean±SD.

We observed that warming produced a fast increase in the firing rate at all recorded structures (Figure 11, orange traces*)*. This fast response was present, with the same latency and duration, in all responses evoked by other stimulus modalities, and we called it "initial component" ($p>0.05$, Table 1). The main difference in warming stimulation respect to other stimuli was that warmth response consisted only in this initial component, while in other stimulus modalities a second component of the response was observed. Taking this into account, and considering that warm thermoreceptors sensory endings have not been identified in the OS (Gallar et al., 1993; González-González et al., 2017), we considered this response as the mechanical activation of mechanosensory nerves produced by the saline drop, as this mechanical stimulus is constant for all modalities. Consequently, we used the latency of this fast response/component to determine conduction velocity of the TG units which are directly innervating the OS (Figure 12).

Nonetheless, when comparing our conduction velocities to the usually reported ones, a potential bias should be considered: conduction velocity is to be generally calculated using electrical stimulation, and here we used a mechanical stimulus. Therefore, sensory transduction of the mechanical force in the nerve ending is a potential source of increased delay between stimulation and recording of the response, resulting in a probable underestimation of the conduction velocities reported in this work.

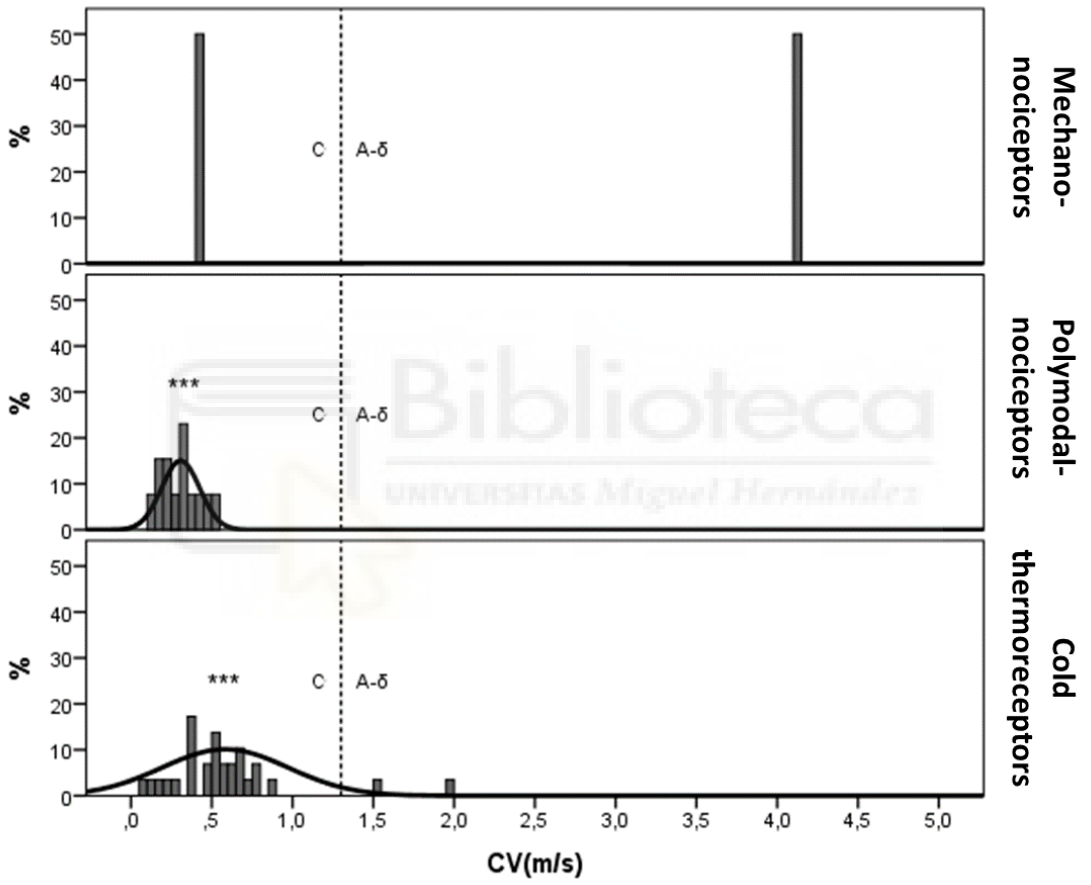

Figure 12*. *Conduction velocity of the different functional types of ocular TG neurons. *Conduction velocity (CV, m/s) of the axons of the primary TG neurons that innervate the OS. CV was calculated using the time between onset of the stimulus and beginning of the positive response in the recording, divided by the estimated anatomical distance between the ocular surface and the TG in the rat (20mm), which was expected to be homogeneous given the similitude in size between animals. Consistently with previous works, CVs of OS-innervating nociceptors are inside the C-fiber range, presenting lower CVs than cold sensory neurons (***p<0.01, independent t-Test), which included fibers falling into C and A-δ categories.*

The number of pure mechanosensitive neurons innervating the OS was low (n=2), and one of them was a C-fiber and the other the fastest A-δ fiber in our sample.

Noxious heating induced a quite different response formed by two components (Figure 11, red traces). The initial component was similar to warmth response. On the other hand, the second component presented different dynamics in the CNS compared to TG: in Th and S1 it appeared as a long-lasting activation, while in TG it was shorter. As this stimulus activates OS nociceptors, this second component could be considered as containing nociceptive information. Nevertheless, a contribution of cold thermoreceptors displaying paradoxical response cannot be ruled out. Such paradoxical response is the response of cold primary sensory neurons to heat stimulation, that has been previously described in the OS innervation (Acosta et al., 2014).

Respect to cold stimulation, both mild and intense cooling produced similar temporal profiles, with two components forming the response (Figure 11, blue traces). As stated before, the initial component was similar to warming and noxious heating while the second component of the cooling response presented greater amplitude for intense cooling than for mild cooling in all structures ($p<0.05$ in TG and Th; $p<0.01$ in S1), suggesting that it could contain information about intensity discrimination of the stimulus. Moreover, the second component latency was faster for cooling than for noxious heating (Table 1, Figure 11).

3. Time course of the ocular TG, Th and S1 single neuron responses to different modalities of stimulus.

To complete the second objective *"To characterize the population and single unit responses of trigeminal ganglion, thalamus and primary somatosensory cortex neurons to stimuli of different modalities delivered to the ocular surface, and to investigate how modality is processed along the somatosensory pathway"* we analyzed single unit responses evoked by our stimulation

modalities when applied over the OS. MUA activity was sorted in single unit spikes and three response dynamics were identified; 1) Initial phase: responses matching the initial component of the population response*;* 2) Second phase: responses matching the second/late component of the population response 3) Biphasic: responses with both components (Figure 13A).

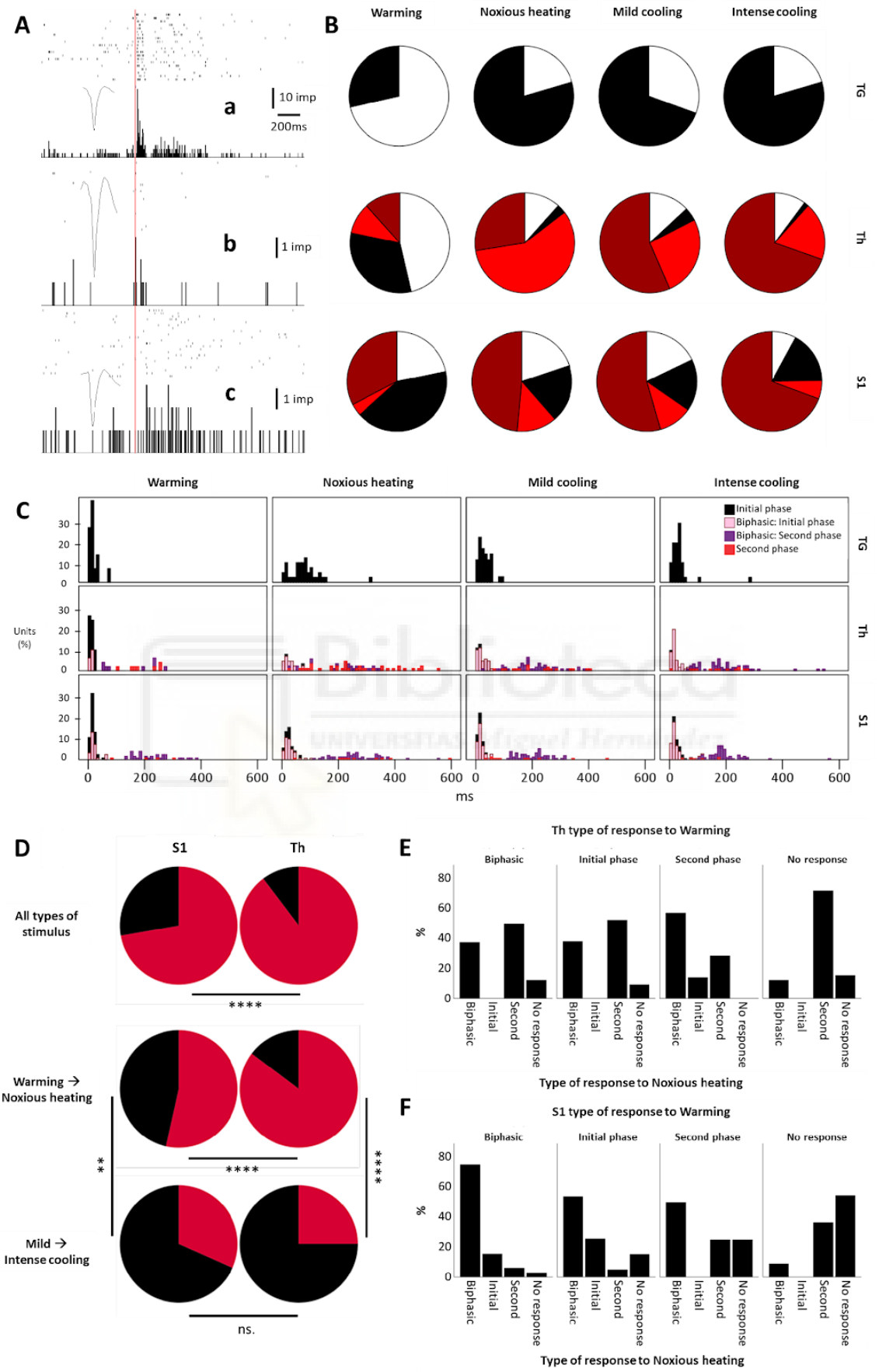
A
a
10 imp
200ms
b
1 imp
c
1 imp
B
Warming
Noxious heating
Mild cooling
Intense cooling
TG
Th
S1
C
Warming
Noxious heating
Mild cooling
Intense cooling
Initial phase
Biphasic: Initial phase
Biphasic: Second phase
Second phase
Units (%)
ms
D
S1
Th
All types of stimulus
****
Warming → Noxious heating
**
****
****
Mild → Intense cooling
ns.
E
Th type of response to Warming
Biphasic
Initial phase
Second phase
No response
%
Type of response to Noxious heating
F
S1 type of response to Warming
Type of response to Noxious heating

Figure 13. Single neurons from the CNS receive multimodal inputs, producing different response dynamics. A. *Peristimulus time histograms from three different S1 units' response to intense cold stimulation. Note the three different dynamics of the response, being from top to bottom: biphasic (a), initial (b) and second phase responses (c). Insets: averaged waveform of the corresponding unit.* ***B.*** *Percentage of TG (n=49), Th (n=69) and S1 neurons (n=101 units) presenting biphasic response (dark red), initial phase (black), second phase (bright red) or no response (white).* ***C****. Latency histograms (5ms bins) displaying when each unit started firing after OS stimulation.* ***D.*** *Percentage of CNS units that maintained the same response dynamic to every stimulation modality (Constant) or presented different dynamics to different modalities (Variable). In the thalamus, variable responses were more abundant than in S1 when considering all modalities (top charts "All"; ***p<0.01, Fisher's exact test), and specifically comparing the difference in response dynamics between warming and noxious heating (middle charts "Warmth-> Noxious Heating"; ****p<0.001). Otherwise, both CNS structures where similar in proportion when considering how many neurons changed their response dynamic between mild and intense cooling (low charts "Mild-> Intense Cooling"; ns= not significant).* ***E,F.*** *Percentage of the units that either maintained or changed their "response profile" between warming and noxious heating stimulation in Th and S1. Every unit was classified as biphasic, initial or second phase, or no response according to their response to warming (upper labels); then, the dynamics displayed when responding to noxious heating were shown at the X axis. Therefore, each column represents the percentage of neurons that presented a specific pair of response dynamics to warming (upper label) and to noxious heating stimulation (X axis).*

The initial phase of the response was present in most neurons and might be evoked by the mechanical stimulation produced by saline drop instillation (Figure 13B). Biphasic and second phase responses, on the other hand, were induced by noxious heat and both cooling stimuli. We speculate that the second component of the population response is formed by the summation of the late response of units displaying biphasic responses combined with the units displaying second phase responses. Moreover, in the case of noxious heating, Th units showed the higher proportion of second phase responses, reaching 58%, while in S1, biphasic responses were predominant. The Th neurons with second phase responses to noxious heating remained active

even after S1 and TG activity had returned to basal levels (data not shown), maybe related with nociceptive-specific processing (Figure 13C).

The fact that biphasic responses were present in the CNS, while in TG units responded with a single initial phase could be attributed to the convergence in CNS units of peripheral pathways with different latencies (i.e. mechanical and nociceptive pathway). For example, a noxious heat drop will first activate mechanosensory receptors in the OS but also heat nociceptors. The mechanosensory input will reach CNS faster than the nociceptive one, and if they converge at some point in a single neuron, two components will be generated, with each of them representing information from different modalities segregated in time, integrating in a single neuron two originally separated inputs without losing information. This convergence could occur in the ascending pathway of the information, when "peripheral" information of the two modalities arrives to the thalamus, or by descending projections arriving to the thalamus by means of a top-down projection coming, for example, from S1 to the Th (Bourassa et al., 1995). Finally, it is also possible that the excitability of single CNS neurons obliges them to generate such biphasic, initial or second phase only responses, simply by an adequate constellation of voltage-gated channels and biophysical properties that produce different response shapes. In this latter case, response dynamics should be independent of the stimulus modality that activated the neuron, as said dynamic would not be determined by the input that activates the neuron, but by the neuron autonomous excitability itself.

Next, we studied if the single unit responses varied in function of the modality of the stimulus applied over the OS. As shown in Figure5D, most of the neurons varied their response dynamics between warming to noxious heat at thalamus and S1 (Figure 13D). More specifically, neurons displaying initial phase responses to warming turned into biphasic against noxious heating, and neurons unresponsive to warming showed second phase responses upon noxious heating application (Figure 13E). Conversely, response dynamics were similar when comparing mild and

intense cooling. These results are consistent with OS-representing units in S1 and sensory Th receive convergent inputs from different modalities.

4. Response to stimuli of multiple modalities increased along the OS somatosensory pathway.

In order to complete the second objective *"To characterize the population and single unit responses of trigeminal ganglion, thalamus and primary somatosensory cortex neurons to stimuli of different modalities delivered to the ocular surface, and to investigate how modality is processed along the somatosensory pathway"*. we analyzed in more depth the multimodality of the single units by grouping them in distinct functional type. As we used 4 modalities (mechano, warmth, heat, cold) for classification, the theoretical maximal number of functional types is 4^2 (16 profiles) (Figure 14A). Moreover, the number of functional types present in a nucleus was also increased along the OS ascending pathway (TG<Th<S1, Figure 14B).

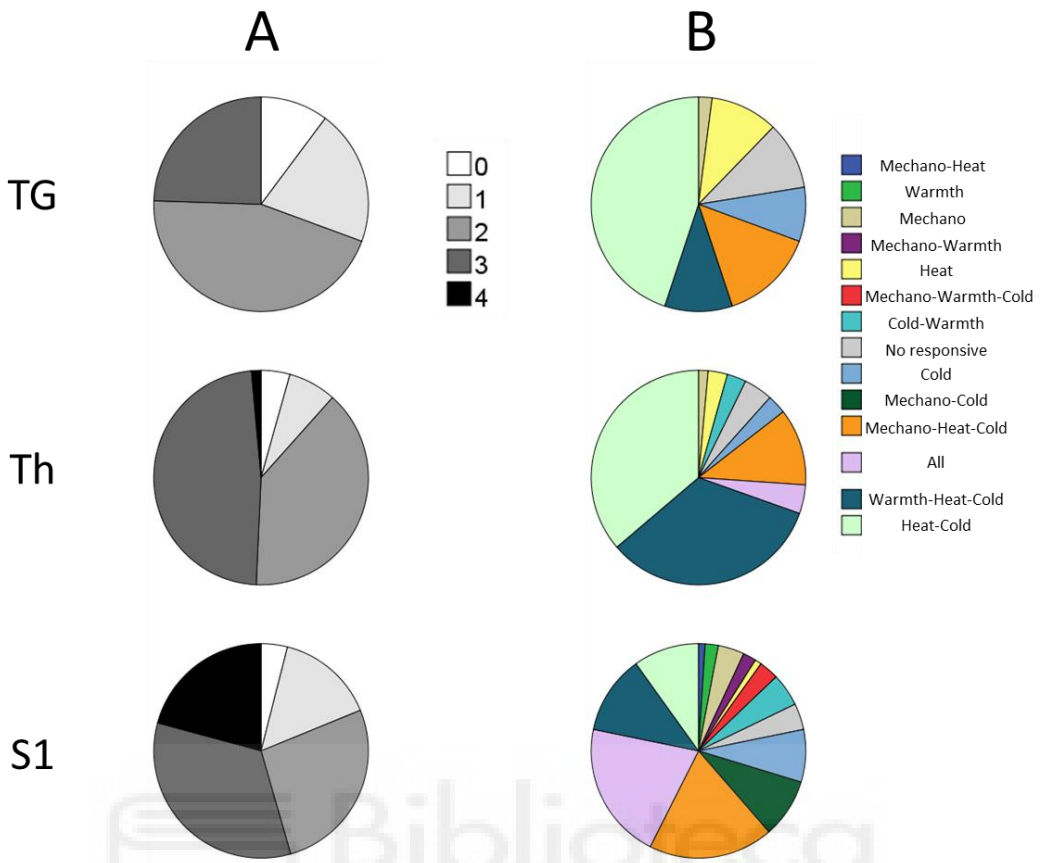

Figure 14. Functional diversity in single neurons is increased along the OS somatosensory pathway. A. *Pie charts representing the number of modalities that a neuron is responding to in all structures. The range goes from 0 (unresponsive) to 4 (neuron responding to every tested modality).* ***B.*** *Distribution of single units responding to the different possible combinations of modalities. Neurons responding to all possible combinations of modalities were found, except for Warmth-Heat and Mechano-Warmth-Heat neurons.*

More specifically, TG presented 7/16 possible functional types, and the most predominant type were cold and noxious heat sensitive units (~45%) (Figure 14B). It might be possible that these units are polymodal nociceptor neurons (Belmonte et al., 2017), but once their ongoing and stimulus-evoked firing activity were studied, about 68% of these units (15/22) were identified as cold thermoreceptor neurons with paradoxical response to intense heat (Acosta et al., 2014). Regarding the CNS, in Th 9/16 different functional types were found and in S1 this number

increased to 14/16, with a prominent quantity of units responding to all stimulus modalities (Figure 14B).

Altogether, these results suggest convergence in the OS central pathway (a single second order neuron receives inputs from at least more than one first order neuron), in such a way that neurons might tend to response to more modalities as they are located more centrally in the somatosensory pathway, given that many pathways would be coinciding in single units

5. Spatial organization of the different functional types of neurons in the thalamus and primary somatosensory cortex.

Next, we asked whether convergence of sensory modalities along the OS somatosensory pathway followed spatial organization. For this purpose, we analyzed if similar functional types of units were clustered in space or, in a different manner, if functional type was independent of location. To this end, we compared each neuron with every other neuron recorded at the same structure and labelled the pairs as "equal" or "not-equal" in terms of modality responsiveness. We then compared the probability of finding two "equal" neurons in the same (P_{near}) and in a different (P_{far}) recording location. We named the ratio between these probabilities *spatial tuning index (STI)*, a quantitative variable indicating how much probable is to find two equal neurons in the same recordings, that we created with this objective in mind. In other words, a value of 2 in STI indicates that it is twice as probable to find two similar neurons in the same recordings than in different recordings ($Spatial\ tuning\ index = Pnear/Pfar$).

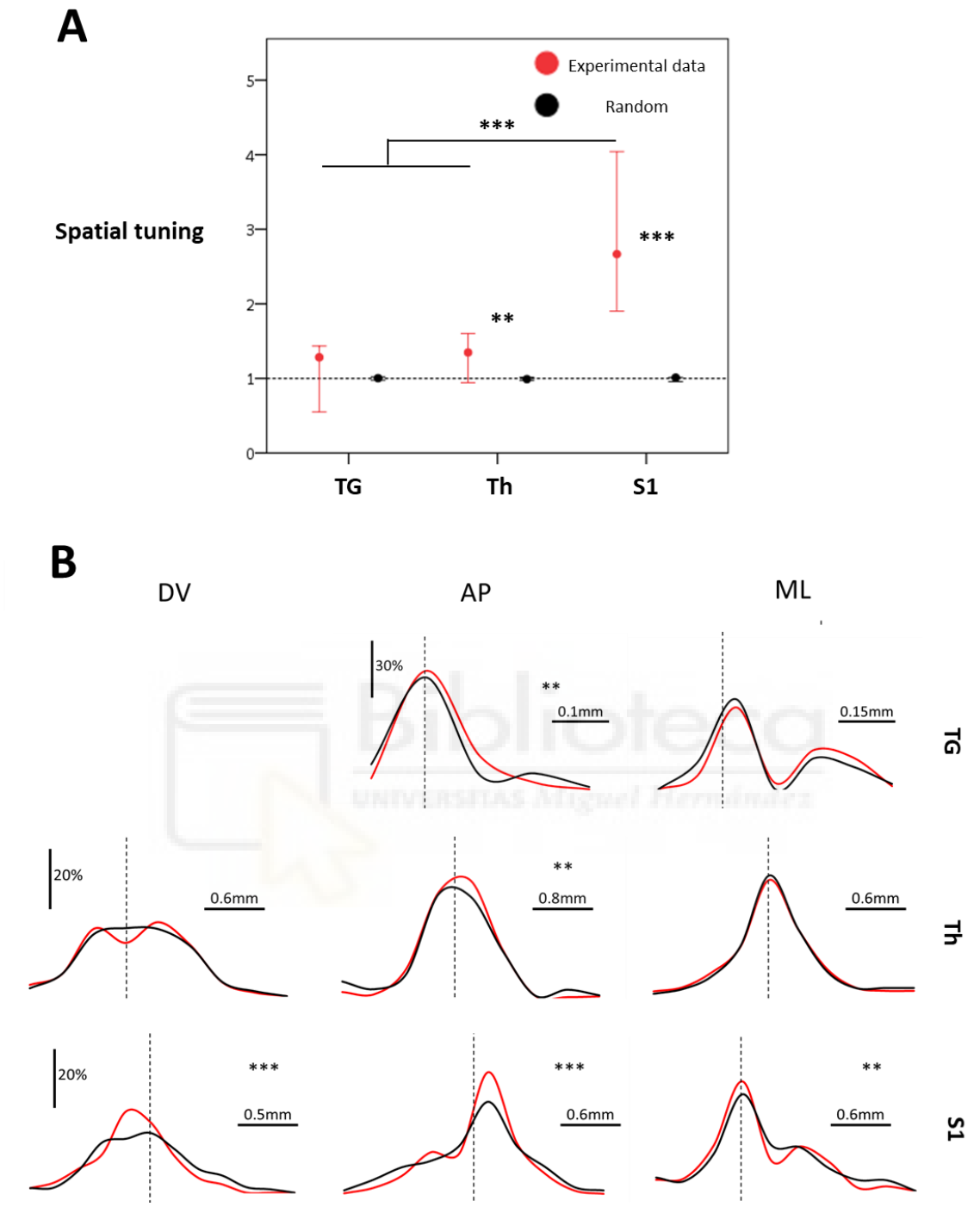

Figure 15. Spatial organization of the functional type appears in the thalamus and is increased in the cortex. A. *Spatial tuning index (STI) of the experimental data compared with bootstrapping of all the data recorded at all structures. STIs from the recorded data were compared with STIs of the same units redistributed into random recordings (100 times shuffling). Median ± CI95% are represented. **p<0.05, ***p<0.01; Mann-Whitney's U test in Data vs. Random, Kruskal-Wallis plus post-hoc Bonferroni test for comparisons between structures.* ***B.*** *Spatial distribution of neurons of the same functional type (red line)*

*and with different type (black line) in all structures and at the different spatial axes (DV, AP and ML). For the TG, DV is not depicted because recordings were consistently performed at 10mm depth to avoid breaking the electrode against the ventral part of the skull under the ganglion. 0 is represented by the dotted line. For comparisons, Levene's equality of variance test was used, **p<0.05, ***p<0.01.*

TG displayed spatial an STI around 1, indicating no spatial organization. Meanwhile, Th and S1 displayed STIs around 1.5 and 2.5, respectively (Figure 15A), meaning that similar units were found closer and implying spatial organization arising inside the CNS and being increased along the OS somatosensory pathway, reaching a maximum in S1 (TG<Th<S1).

As a complementary analysis regarding spatial organization of the functional types, we quantified the distance between the recording coordinates of each pair of neurons, and represented the distribution of equal and not-equal pairs of units. This analysis revealed that TG and Th present DV organization, while S1 is organized in the three axes of space (Fig 15B). Therefore, this results further confirm spatial organization of the functional type in the OS central pathway. This spatial organization was also present when comparing each modality individually (Figure 16-19).

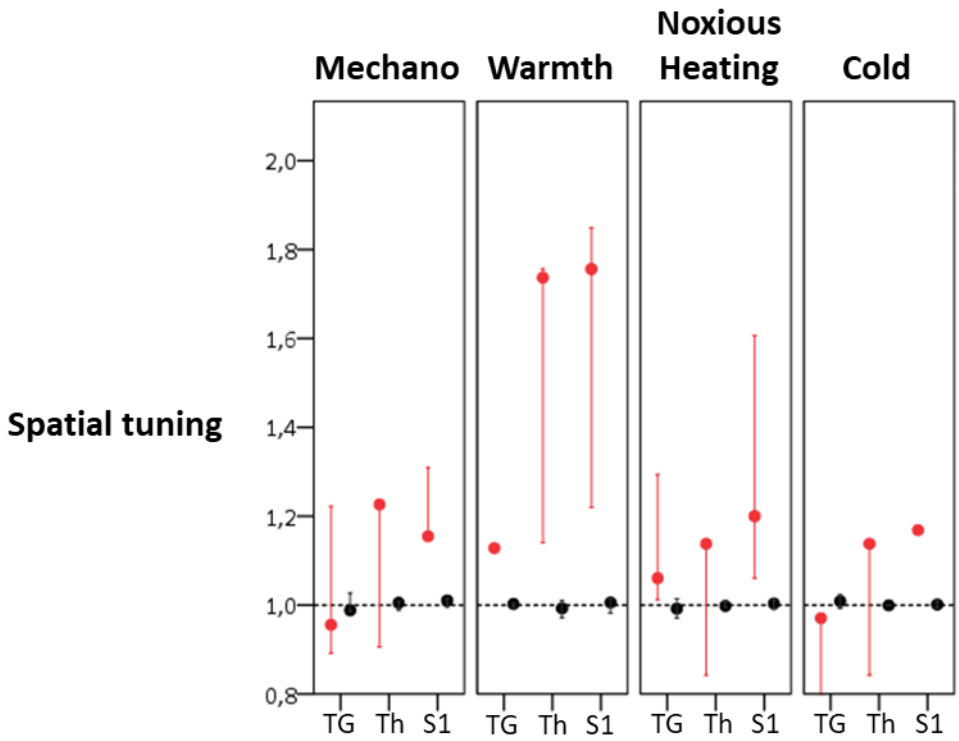

Figure 16. Spatial tuning per modality in each structure. *Data is presented as median ± CI95%.*

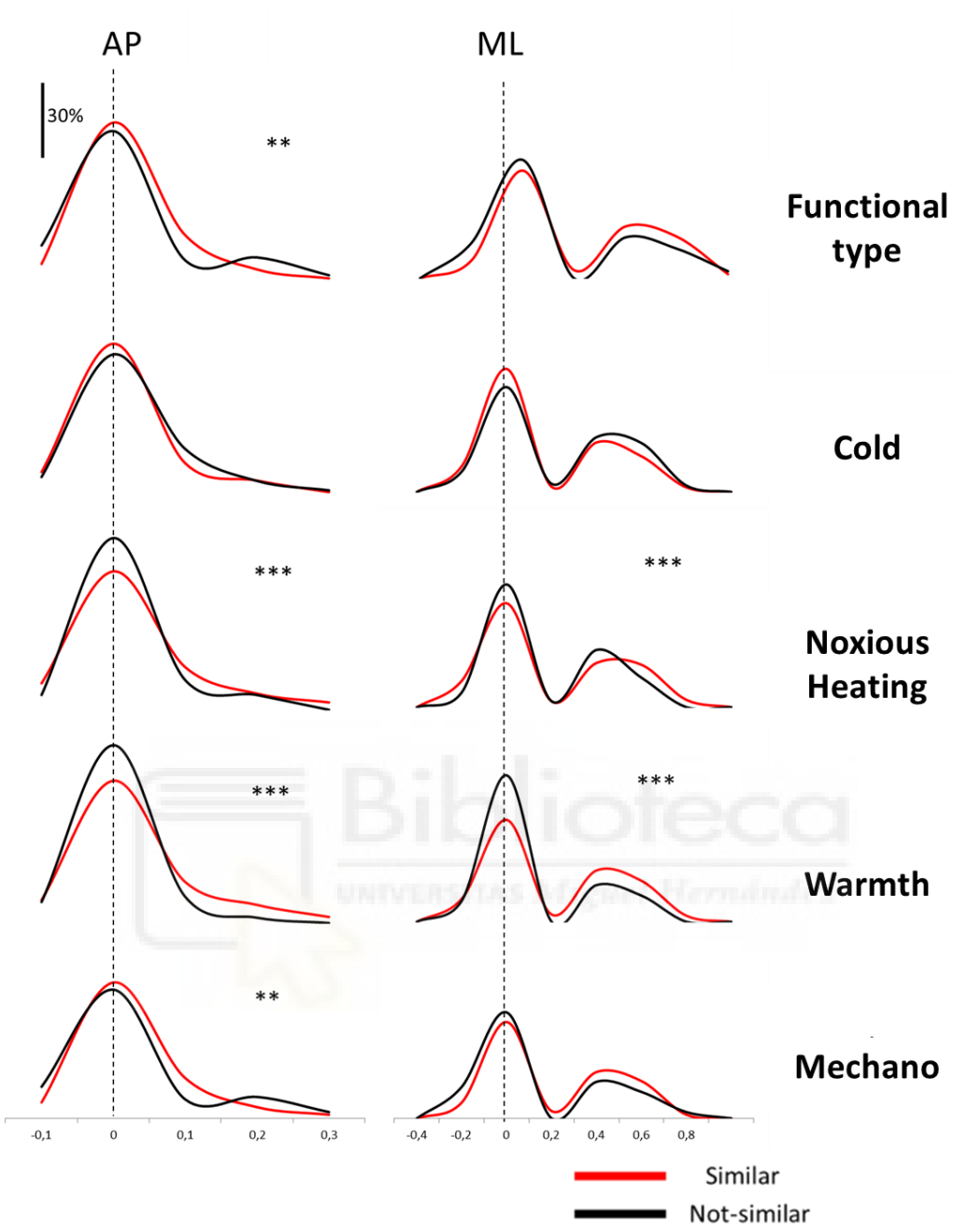

Figure 17. Spatial functional similarity analysis of the TG single units per modality in each spatial axis. *In red, distribution of equal type neurons, in black, non-equal neurons. **p<0.05; ***p<0.01, Levene's equality of variance test was used.*

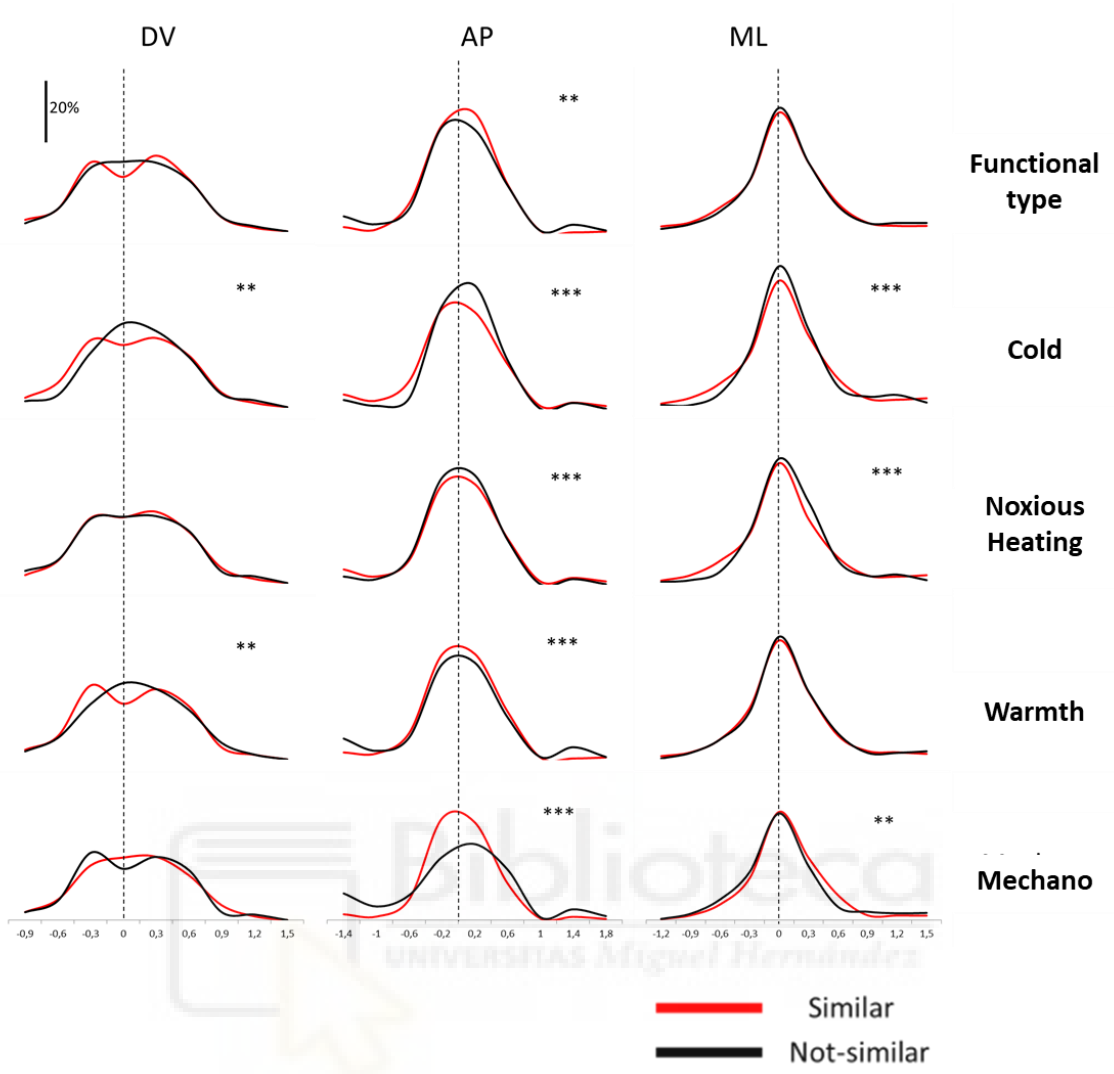

Figure 18 Spatial functional similarity analysis of the thalamic single units per modality in each spatial axis. *In red, distribution of equal type neurons, in black, non-equal neurons. **p<0.05; ***p<0.01, Levene's equality of variance test was used.*

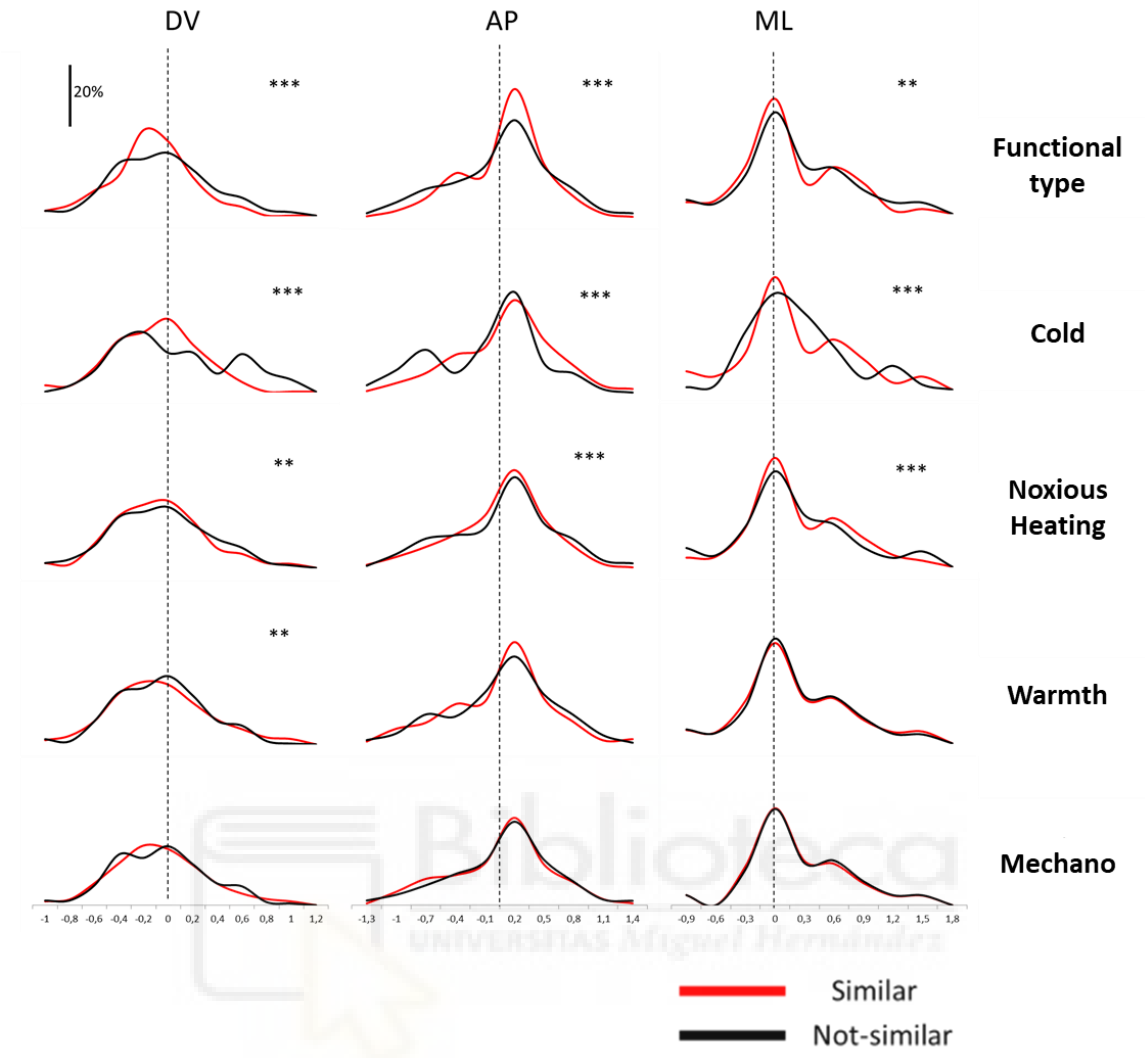

Figure 19. Spatial functional similarity analysis of the cortical single units per modality in each spatial axis. *In red, distribution of equal type neurons, in black, non-equal neurons. **p<0.05; ***p<0.01, Levene's equality of variance test was used.*

6. Ongoing activity of the different functional types of OS neurons.

Neuronal ongoing activity is fundamental to shape the circuits ultimately processing information in the CNS (ref). To accomplish the third objective *"To analyze the spontaneous activity of cortical, thalamic and trigeminal neurons responding to ocular surface stimulation with different modalities of stimulus"* we compared the ongoing activity of the OS neurons on the three

recorded structures, prior to any stimulus application. Th was the most active structure (3.9 ± 4.7, median spikes/sec ± IQR), above S1 (3 ± 3.2) and TG (1.6 ± 2.1) (S1-Th $p<0.05$; S1-TG and Th-TG $p<0.01$).

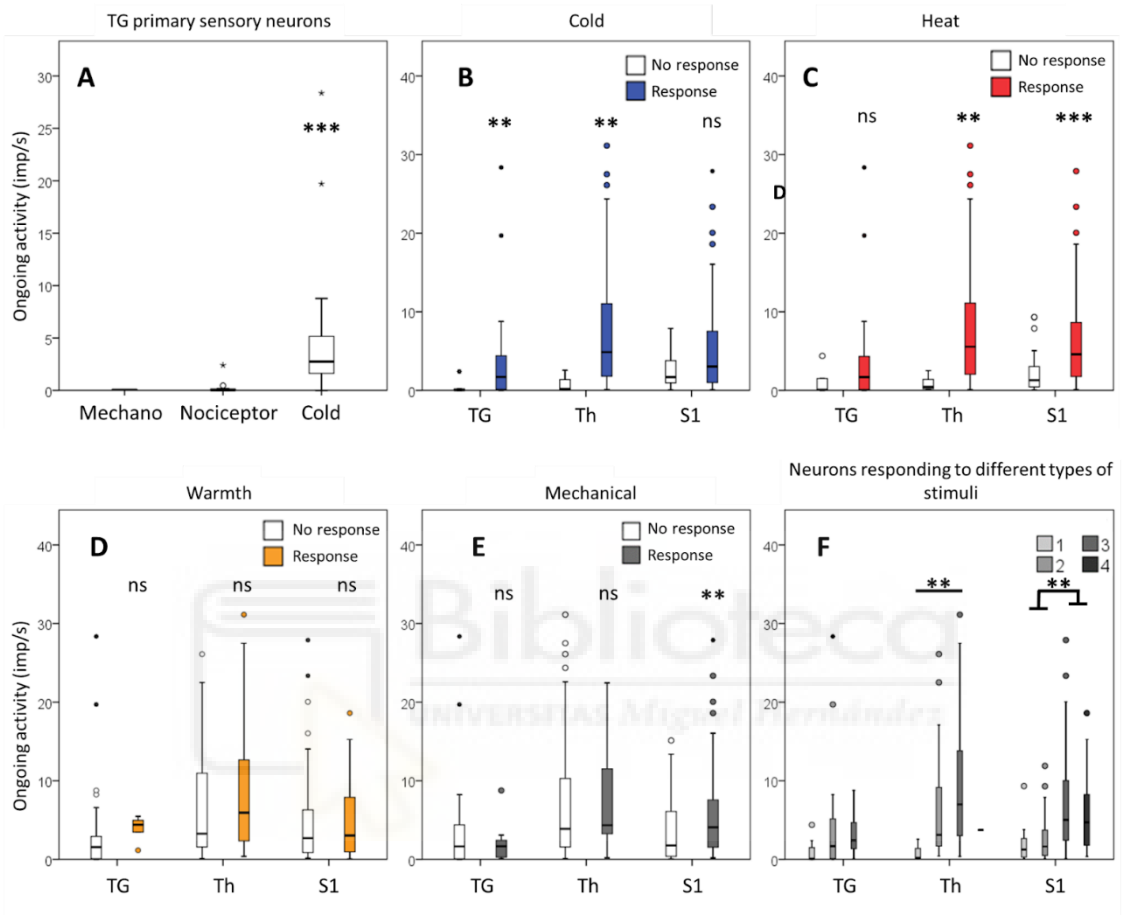

Figure 20. Ongoing activity of trigeminal, thalamic and S1 units responding or not to stimuli of different modalities. A. *Ongoing activity of TG units functionally classified in canonical groups of OS-innervating trigeminal neurons.* ***B-E.*** *Ongoing activity of TG, Th and S1 units innervating the OS.* ***F.*** *Ongoing activity of TG, Th and S1 neurons in function of the number of modalities that a given neuron is responsive to. **p<0.01; ***p<0.001, Mann-Whitney's U tests with Bonferroni correction for multiple comparisons.*

It has been previously documented that OS-innervating trigeminal primary sensory neurons display distinct levels of ongoing activity, both in isolated cultured cells and in sensory nerve terminals directly recorded in the OS (Belmonte et al., 2017; Gallar et al., 1993; González-González et al., 2017). Our results confirm these previous works *in vivo* (Figure 20A). When

considering the three structures, results show that neurons responding to cold display greater ongoing activity in TG and Th, but not in S1 (Figure 20B). Nociceptive neurons responding to noxious heating show higher levels of ongoing activity in the CNS (Th and S1) but not in the periphery (TG) (Figure 20C). On the other hand, warm and mechano-sensitive neurons showed no difference in ongoing activity compared to neurons not responding to these modalities, except for mechanosensitive neurons in S1 (Figure 20D-E). It seems that neurons responding to a specific modality tend to have more ongoing activity than those not responding to that modality. We analyzed if the number of modalities a neuron is responding to (degree of multimodality) is related with the ongoing activity recorded in that neuron. Indeed, this is the case, and more multimodal neurons display higher ongoing activity in the central OS pathway (Th and S1, Figure 20F).

Ongoing activity varies in neurons receiving different peripheral information. Depending on the OS neural pathway structure, each modality seems to account for different weights in determining ongoing activity, with nociceptive neurons displaying greater activity in the CNS and cold neurons being more active in TG and Th. In S1 and Th, the more polymodal neurons displayed greater ongoing activity.

7. Characterization of membrane potential instabilities in trigeminal neurons

To fulfill the fourth objective "*To characterize the membrane potential instabilities of trigeminal ganglion neurons, and their role in action potential generation"* we performed membrane potential measurements in mouse TG neurons using whole-cell patch-clamp. Cells were stimulated by injecting 2 s-long current pulses, both in the hyper- and depolarizing directions, graded in amplitude. This procedure revealed that the membrane potential becomes unstable

upon depolarization in many neurons (Figure 21A). This instability is biased towards positive deflections at physiological potentials between -45 and -25 mV (Figure 21B-C). Consistently, normalized power spectral density (PSD) of the recordings is displaced toward high frequencies (15-50 Hz) upon depolarization (Figure 21D-E). We decided to refer to this phenomenon as Membrane Potential Transients (MPTs). The increase in frequency of MPTs with membrane depolarization occurs at about 30 mV more negative potentials than the increase in AP firing (Figure 21F). The majority of TG neurons recorded produced MPTs when depolarized (115/140). A smaller proportion of the neurons presented spontaneous oscillations at resting Vm (85/140), which was normally slightly depolarized compared to non-spontaneously oscillating ones (-48.2 vs -54 mV, respectively; $p<0.001$, independent t-test). Almost all neurons were able to generate ongoing activity displayed some form of MPT when depolarized (98.1%). Another subset of neurons (19/140), usually the bigger ones, displayed morphologically different MPTs, with lower amplitudes and faster oscillations, ~100 Hz (not shown). A few neurons of this subset produced repetitive firing when depolarized (5/19).

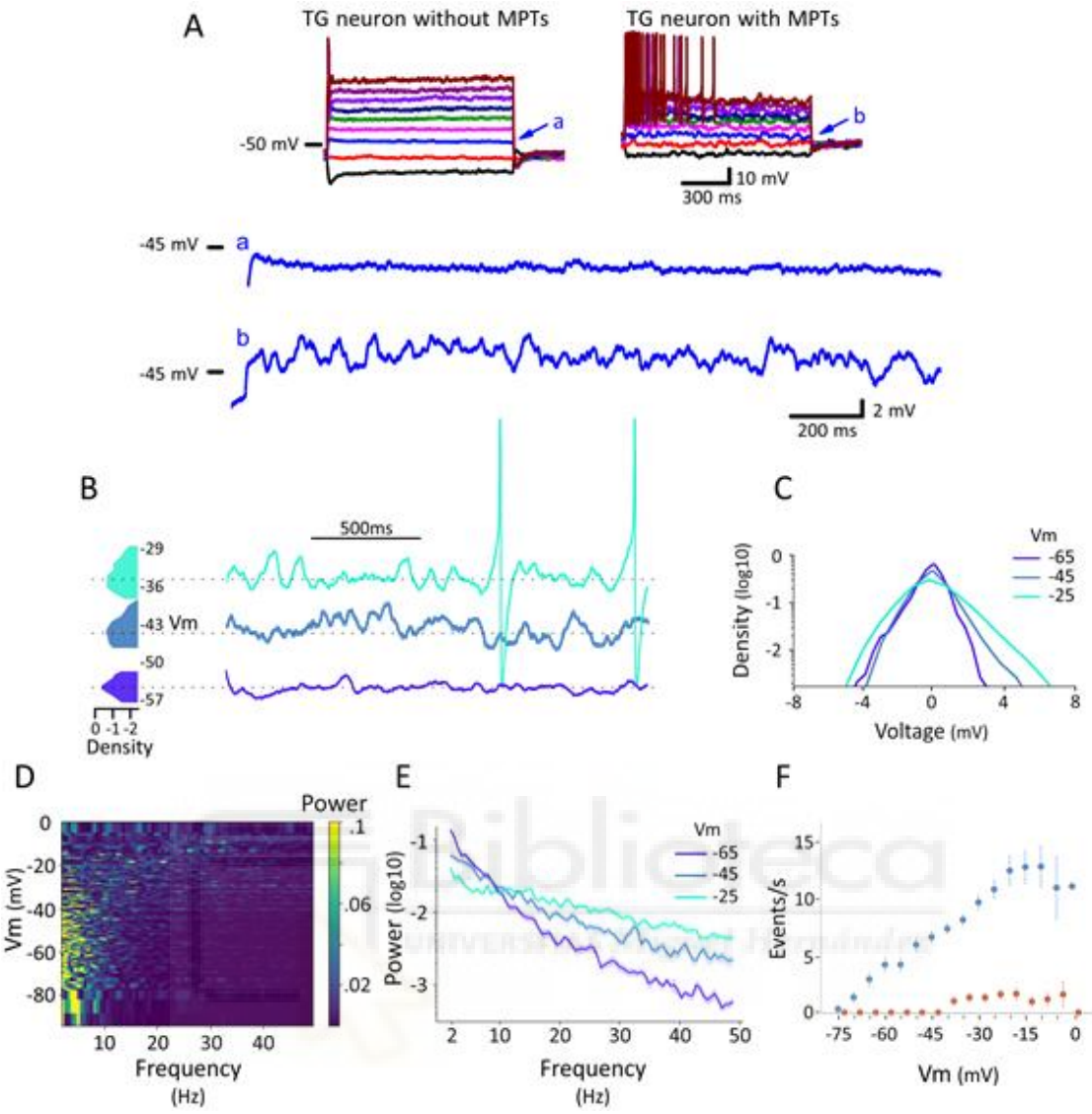

Figure 21. Voltage-dependent membrane potential instabilities in trigeminal neurons. *A) Characteristic recordings of two TG neurons, one without and another with MPTs. B) Representative recording with its respective histograms. Note how the distribution of points is symmetrical at potentials around -65 mV and becomes asymmetrical towards depolarization at potentials near action potential threshold (-28.5 mV). C) Normalized histogram for all pulses grouped in three Vm windows. For better comparison each histogram was centred along the voltage axis at the zero value by subtracting the corresponding median. D) Normalized power spectral density (PSD) distribution from each current injection pulse (389 pulses, 46 neurons). E) Grouped mean of the PSDs plotted in D, for three Vm windows (-70 to -60, -50 to -40 and -30 to -20 mV, respectively). The PSD is displaced to higher frequencies at depolarized potentials. F) Voltage dependence of MPT (blue) and APs (orange) frequency (389 pulses, 46 neurons).*

The morphology of MPTs, described by their maximal amplitude, duration, and negative/positive maximum slopes, was dependent on the Vm (Figure 22A-B). Generally, the amplitude and maximal positive and negative slopes tend to increase with more depolarized potentials, whereas the duration of the transients is progressively reduced. All these dependences can be well-described by Boltzmann functions (Table 2), suggesting that the morphology of MPTs depends on voltage-gated ion channels.

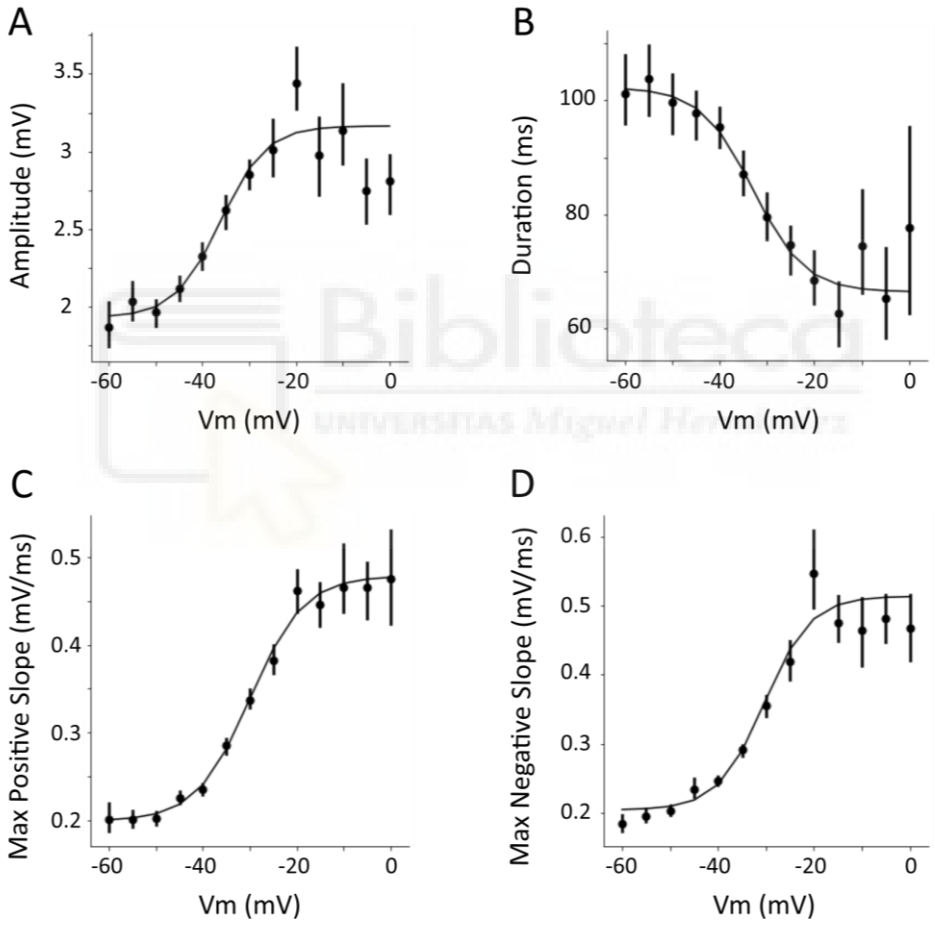

Figure 22. Voltage dependence of the parameters describing the morphology of MPTs*. Mean ± SEM of the amplitude (A), duration (B) and maximal positive (C) and negative slope (D) of the MPTs, binned in 5 mV intervals. The data were fit by Boltzmann functions. Data was computed from 3189 MPTs detected in 46 neurons.*

Variable/parameter	L	x0	k	b
Amplitude	*1.23*	*-36.15*	*0.20*	*1.93*
Duration	*-35.81*	*-32.95*	*0.18*	*102.27*
Max Positive Slope	*-0.28*	*-29.93*	*-0.17*	*0.48*
Max Negative Slope	*0.31*	*-30.32*	*0.21*	*0.20*

Table 2 Parameter estimates *for functions depicted in Figure 14, using a Sigmoid function (Equation 2)*

Equation 1:

$$y = \frac{L}{1 + e^{-k*(x-x0)}} + b$$

- L is responsible for scaling the output range from [0,1] to [0,L]

- b adds bias to the output and changes its range from [0,L] to [b,L+b]

- k is responsible for scaling the input, which remains in (-inf,inf)

- x0 is the point in the middle of the Sigmoid, i.e. the point where Sigmoid should originally output the value 1/2 [since if x=x0, we get 1/(1+exp(0)) = 1/2]

8. MPTs as triggers of action potential firing

To further accomplish the objective 4 *"*To characterize the membrane potential instabilities of trigeminal ganglion neurons, and their role in action potential generation*"*, we explored the relationship between MPT properties and the initial depolarization phase (IDP) of the action potentials. For this, we compared the properties of the MPT depolarizing arm with those of the first depolarization that gives rise to APs produced during tonic current injection (Figure 23A-B). The main result of this analysis is that amplitudes and maximum slopes of the MPT

depolarization and of the IDPs of the APs produced during tonic firing form a continuum (Figure 23C). Subsequently, we modelled the probability of a given spontaneous depolarization to result in an MPT or an AP using a logistic Boltzmann equation of the form:

Equation 2:

$$pAP(Amp, Der) = \frac{1}{1 + e^{8.2 - 0.2Amp - 9.7Der}}$$

where pAP is the probability of a given depolarization to generate an AP, Amp is the maximal amplitude of the event and Der is the maximal positive derivative of the event.

The resultant model is strongly predictive (**Equation 2**), showing that MPTs with faster and larger depolarizing limb have higher probability of generating an AP. This was largely independent of the Vm at which the MPT is generated, probably because the effect of Vm is already recapitulated in the amplitude and depolarization rate of the MPT, as they depend on it.

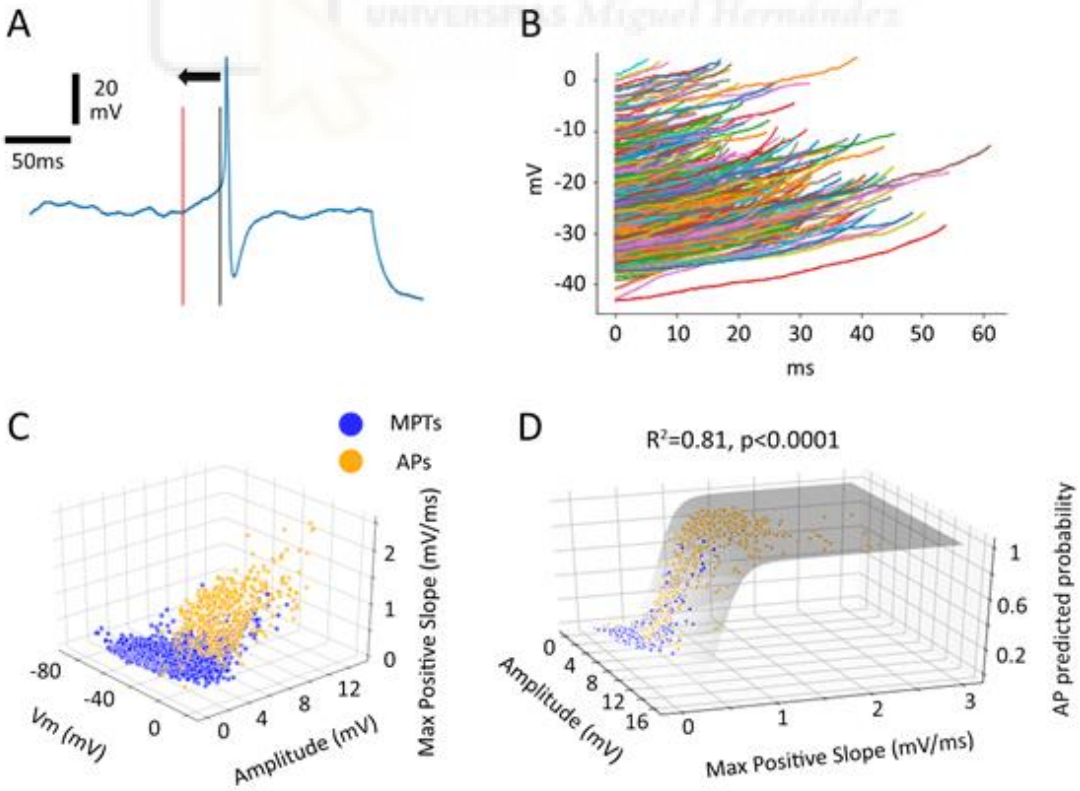

***Figure 23. MPTs as triggers of action potential firing**. A) Graphical scheme illustrating the method used to dissect the initial depolarization phase (IDP) of APs. Starting from the maximal positive peak of the AP and looking backwards, the IDP was defined as the fragment of the voltage trace between the first 0 value of the second derivative (black line) and the first 0 value in the first derivative (red line). B) Superposition of 476 isolated IDPs recorded in the same 46 WT neurons used to characterize the MPTs. Note that IDPs and MPTs are shorter and steeper at depolarized Vm. C) Combined plot of all MPTs and IDPs in function of their amplitude, maximal depolarization slope and Vm at which they are produced. D) The gray shade and vertical axis represent the logistic regression (see Equation 2) predicting the probability of a given depolarization to become an AP, attending to its amplitude and maximal derivative. Individual MPTs not converting into APs are represented as blue data points and the initial depolarizing phase of successfully generated APs are represented in orange.*

Interestingly, main role being proposed for MPTs is to generate repetitive ongoing activity during the application of tonic or slow-ramp stimuli, a hypothesis supported by our results. However, MPTs have not been studied during natural stimulation in PNS. We tackled this question by determining the properties of MPTs during stimulation with chemical (capsaicin or menthol; Figure 24) and thermal (heat or cold; Figure 25) stimuli. The cumulative application of capsaicin (Figure 24A-B) or menthol (Figure 24D-E) induced concentration-dependent increases in the frequency of MPTs and eventually led to the firing of APs. Notably, the MPTs triggered by capsaicin and menthol showed relationships to the IDPs of APs that were similar to that of MPTs elicited by depolarizations induced by current injection (Figure 24C-F). This is confirmed by the fact that the data for capsaicin and menthol could be well-described by the regression model obtained for MPIs triggered by current injection. Moreover, similar results were obtained when TG neurons were stimulated by heat (Figure 25A-C) or by cold (Figure 25D-F). Taken together these results reveal that the ability to generate MPTs is an intrinsic property of the TG neurons that does not depend on the type of stimulation causing the depolarization, but on the

membrane potential itself. Furthermore, irrespective of the stimulus applied MPTs retained a causal relationship with APs.

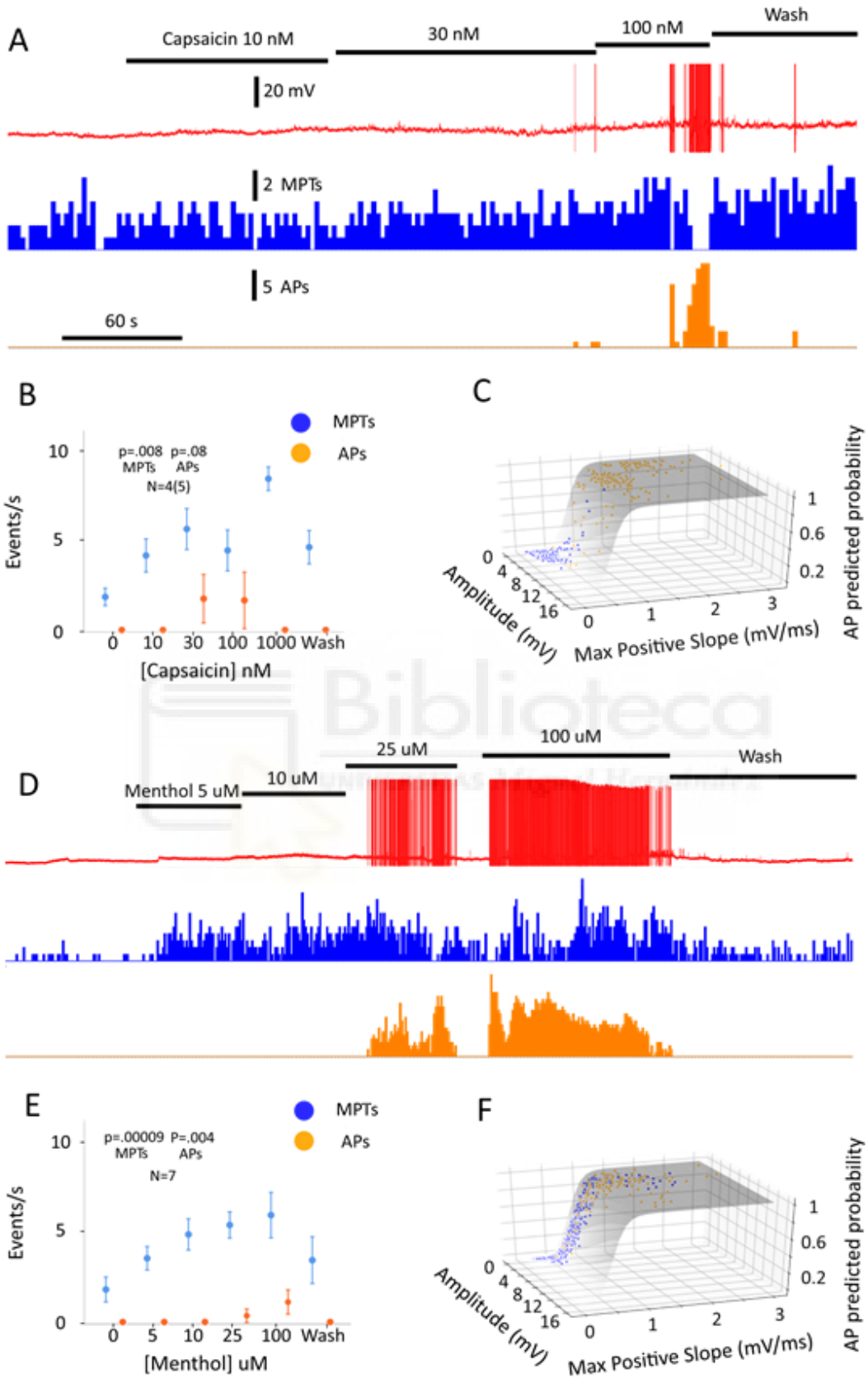
A
Capsaicin 10 nM
30 nM
100 nM
Wash
20 mV
2 MPTs
5 APs
60 s
B
MPTs
APs
p=.008 p=.08
MPTs APs
N=4(5)
Events/s
[Capsaicin] nM
0 10 30 100 1000 Wash
C
AP predicted probability
Amplitude (mV)
Max Positive Slope (mV/ms)
D
Menthol 5 uM
10 uM
25 uM
100 uM
Wash
E
MPTs
APs
p=.00009 P=.004
MPTs APs
N=7
Events/s
[Menthol] uM
0 5 10 25 100 Wash
F
AP predicted probability
Amplitude (mV)
Max Positive Slope (mV/ms)

Figure 24. Chemical stimulation enhances MPIs. *A, D) representative current-clamp recordings showing the effects of capsaicin (A) and menthol (D) on Vm (red), MPI frequency (blue) and APs (orange). Notice MPI being produced at concentrations that do not induce APs. B, E) Mean ± SEM of event frequency for each concentration and statistical values resulting from ANOVA analyses. C, F) Fit of the data by a Boltzmann function (Equation 1). The data presented was collected from 5 capsaicin-sensitive neurons and 7 menthol-sensitive neurons.*

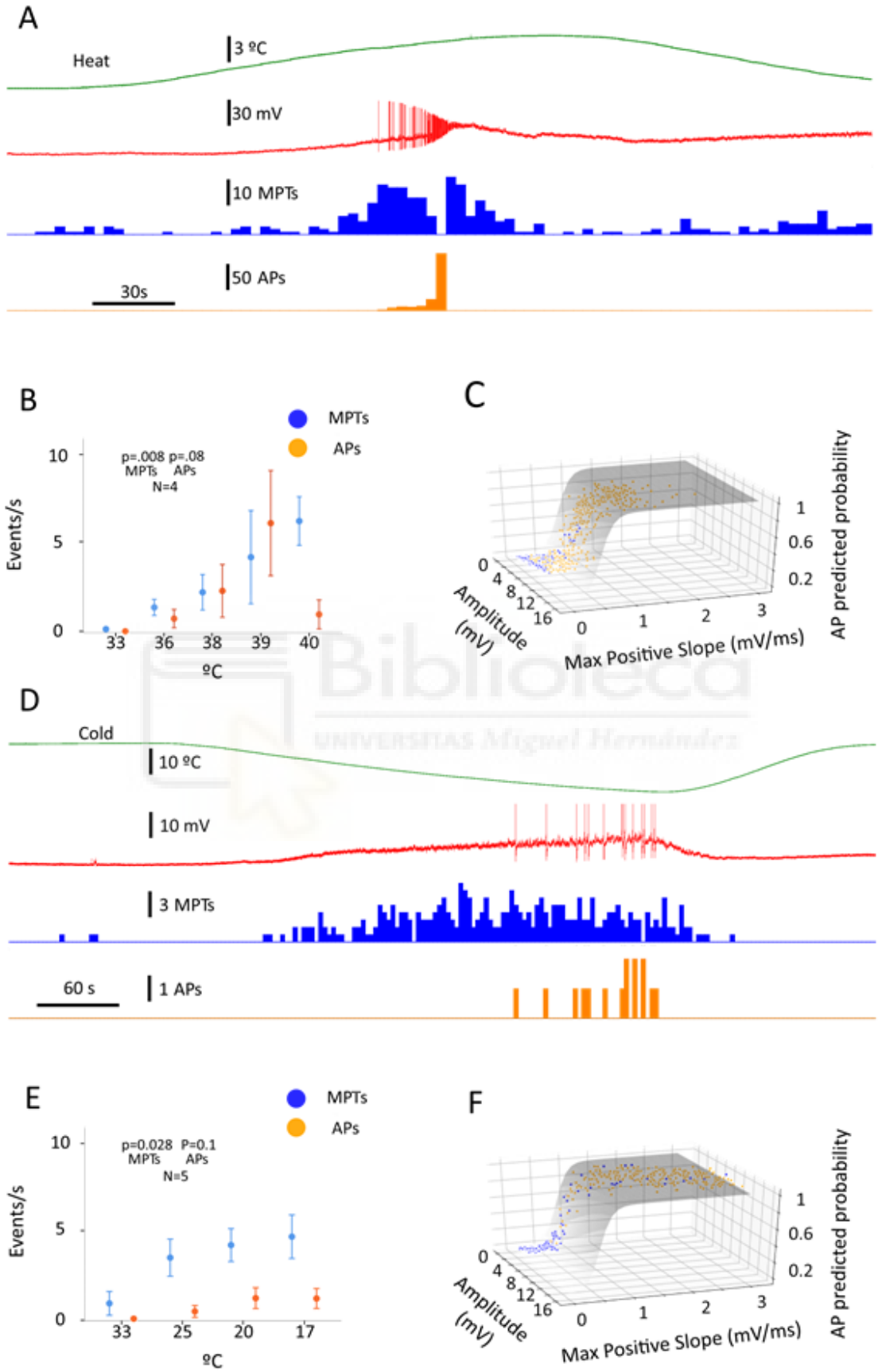

Figure 25. Thermal stimulation enhances MPIs. *A, D) representative current-clamp recordings showing the effects of heat (A) and cold (D) on Vm (red), MPI frequency (blue) and APs (orange). Notice MPI being produced at temperatures at which no APs are elicited. B, E) Mean ± SEM of event frequency as a function of temperature and statistical values resulting from ANOVA analyses. C, F) Fit of the data by a Boltzmann function (Equation 1). The data presented was collected from 5 heat-sensitive neurons and 7 cold-sensitive neurons.*

Discussion

This work provides, for the first time, anatomical locations and physiological characterization in the somatosensory thalamus and cortex of sensory stimuli originated in the OS. For the OS, sensory modalities have higher degree of multimodality at single neuron level along the ascending sensory structures, creating new functional types and conditioning spontaneous activity of the units that form the system. Furthermore, here we thoroughly characterize TG neuron MPIs and demonstrate their key role in ongoing activity generation and responses towards tonic and slow-ramp stimulation.

1. Functional representation of OS at thalamic and cortical level

Regarding the first objective of this thesis work, *"To determine the stereotaxic coordinates to record neurons receiving information from the ocular surface, in the primary somatosensory cortex and somatosensory thalamus"*, we have documented that the anatomical representation of the OS in the thalamus and cortex are consistent with general somatotopic arrangement of the body surface and the structure of the trigeminal subsystem. Previous works have described that there is a spatial organization of the three trigeminal branches inside the TG (Leiser and Moxon, 2006). Therefore, somatotopic arrangement starts early in the ascending pathway, and it will be preserved along the entire somatosensory system: brainstem, thalamus, and cortex. Until now, whiskers (trigeminal branches V2 and V3; (Chapin and Lin, 1984; Clemens et al., 2018; Deschênes et al., 2005; Furuta et al., 2009; Urbain and Deschênes, 2007)), trunk and extremities (Diamond et al., 1992a) representations were well known, but OS has been almost neglected. The only exception is the brainstem, in which solid works have been performed, mainly in the spinal nucleus of the trigeminus, SpV (Marfurt, 1981; Meng et al., 1997; Pozo and Cervero, 1993).

In thalamus, OS and periocular representation coordinates have been reported in the cat (Yokota et al., 1985). In rats, some authors found representation of the eyebrow's guard hair as the first sensory response in PoM/VPM thalamic complex after entering it dorsally immediately after LGN visual responses were extinguished (Diamond et al., 1992a).

There is a complete lack of information about OS representation in the primary somatosensory cortex, to the best of our knowledge, except for a case report in a human, in which authors report pain related activation of S1 using fMRI (Moulton et al., 2012). Therefore, our results are consistent with previously described somatotopic organization (Chapin and Lin, 1984), but with this data, we cannot rule out other possible coordinates in which OS positive or negatively responding neurons could be found.

2. Functional profiles of the OS neuronal populations along the somatosensory pathway

We addressed the second objective of this thesis work, "*To characterize the population and single unit responses of trigeminal ganglion, thalamus and primary somatosensory cortex neurons to stimuli of different modalities delivered to the ocular surface, and to investigate how modality is processed along the somatosensory pathway".* Based on our data, we now know that the profile of temporal activation of Th and S1 usually showed two different components: an early (short/phasic) and a late (long-lasting) response. Single unit analysis revealed that each component was built up by different neuron dynamics depending on stimulation modality. In other words, the same neuron could be participating only in the initial, the second or both components depending on stimulation modality. This could be due in principle to the polymodal responses of corneal innervation (Gallar et al., 1993; González-González et al., 2017). However, a detailed study of each single unit indicates that a different and precise composition of

sensitivity to different stimulus modalities identify separate neuronal populations inside the somatosensory thalamus and cortex.

Warming stimulation produced a fast, initial component that was found in every stimulus modality and has been considered as a mechanical response. This interpretation is based on the absence of warm receptors on the OS, where this stimulus could be just codified by the decrease in the spontaneous activity of cold thermoreceptors (Paricio-Montesinos et al., 2020). Nevertheless, latencies for this response were slow compared to whisker latencies produced when mechanoreceptors of the whisker pad were stimulated (Minnery et al., 2003; Minnery and Simons, 2003; Plomp et al., 2014). This is consistent with mechanosensitive primary receptors of the OS being slow A-Delta and C nociceptive fibers, previously classified as mechano- or polymodal nociceptors by other authors, that produce irritation or pain upon activation (Acosta et al., 2001a; Belmonte et al., 1991, 2017; Gallar et al., 1993). Also, classical literature suggests that nociceptive information is conveyed in thalamic PoM (Mo et al., 2017) and this pathway (paralemniscal) is slower than the lemniscal pathway (Diamond et al., 1992a). Paralemniscal pathway latencies for whisker stimulation to PoM (10-30 ms) closely resemble our reported latencies in thalamus (19-22 ms) in contrast to fast VPM lemniscal responses (4-6ms). Additionally, all corneal afferents are entering the CNS through the Sp5, the first nuclei in the paralemniscal pathway (Marfurt, 1981). Therefore, we propose that the input coming from the OS is being represented mainly in PoM, ascending to somatosensory cortex through the paralemniscal pathway.

All other stimulus modalities tested (noxious heating and mild and intense cold) were characterized by a long-lasting second component, produced after the first one, which matched previous works reported cortical latencies for thermal responses using MEG and EEG in humans (Fardo et al., 2017; Jin et al., 2018; Wang et al., 2016)**.** Furthermore, said latencies and response durations are consistent with cortical synaptic inputs and depolarization time measured

intracellularly *in vivo* (Bokiniec et al., 2018; Milenkovic et al., 2014). Interestingly, mild and intense cooling stimulation produced similar profiles differing only in their amplitude, but warming and noxious heating produced qualitatively different responses. In line with this, other authors have demonstrated that cold intensity is being codified as a continuous increase in activity both in primary (Yarmolinsky et al., 2016) and dorsal horn central neurons (Ran et al., 2016), while noxious heat is differentiated from innocuous warmth by a discrete threshold that activates a new population of noxious sensing neurons (Vandewauw and Voets, 2016). Our results suggest that this operating concept of thermosensation is extensible to OS representation in thalamo-cortical processing, differentiating noxious and non-noxious stimulation of the same modality.

3. The importance of neuronal identity in the population responses.

Still tackling the second thesis objective, "*To characterize the population and single unit responses of trigeminal ganglion, thalamus and primary somatosensory cortex neurons to stimuli of different modalities delivered to the ocular surface, and to investigate how modality is processed along the somatosensory pathway",* we discovered that there is a convergence of stimulus modalities (or multimodality) as we "go up" in the pathway. Consequently, new combinations of modalities sensitivity render more diverse functional types in Th and S1 units, not present in TG. Indeed, this result make us propose that S1 could potentially discriminate the modality/ies of a stimulus. Subsequently, this phenomenon could contribute to the integration of the "labeled" peripheral modalities processed by the TG. This has been barely explored in other works, probably due to a bias in the way to explore the whisker system, classically tactile. We reported a spatial clustering of functionality attending to stimulus modality responsiveness, which is increased along the somatosensory pathway as convergence and functional diversity increases. A conceptual illustration of our interpretative proposal could be found at Figure 26.

Whether these local circuits are determined by common afferent projections (Casas-Torremocha et al., 2019) or by local connectivity which communicates different modalities between neurons is yet to be resolved.

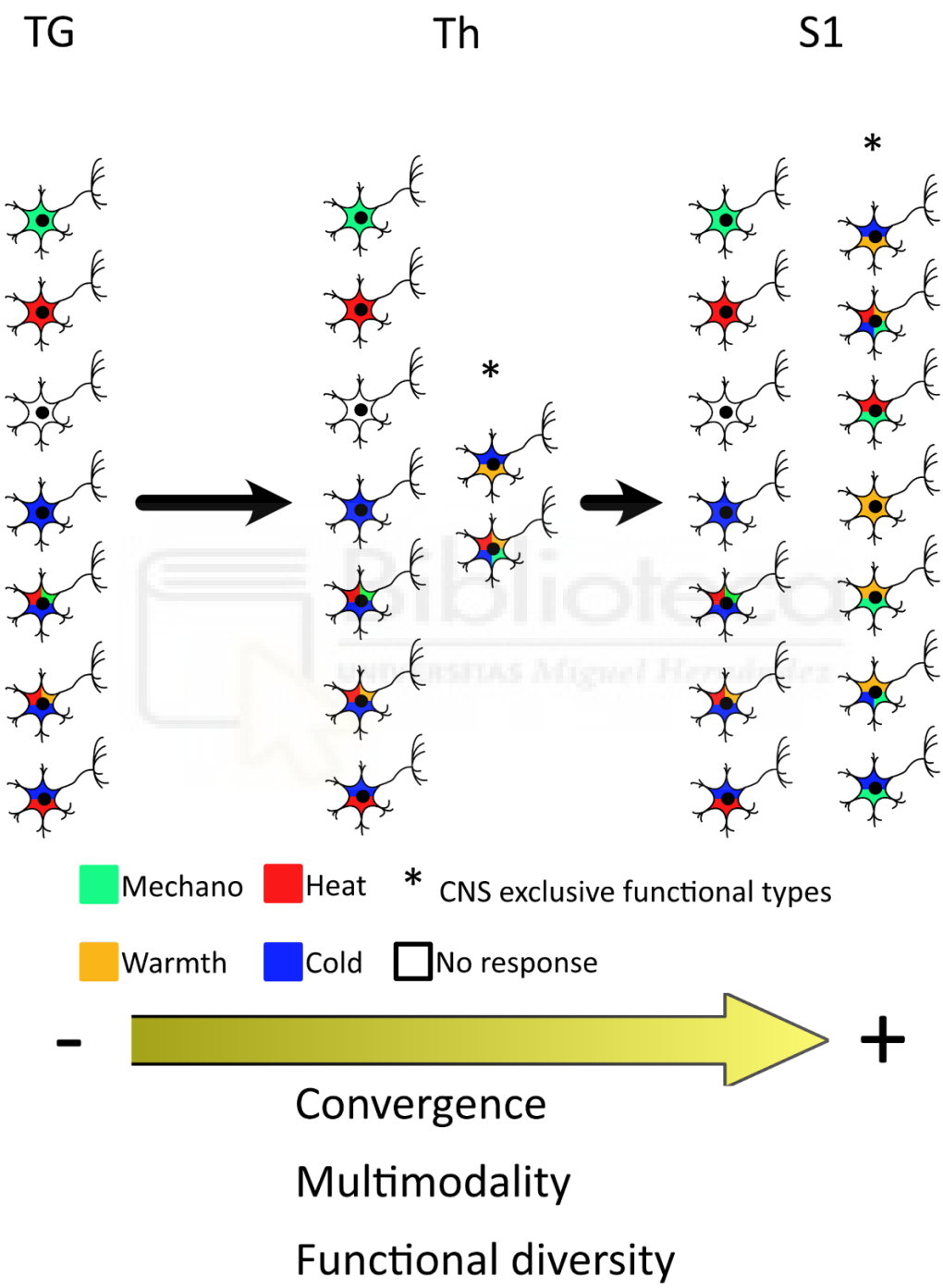

Figure 26. Schematic drawing representing the increasing neural functional variety along the somatosensory axis, *in which both divergence and convergence are produced along the somatosensory pathway inside the CNS: information that was originally segregated in the periphery (TG) gets mixed in*

*single neurons in the CNS (mixed color units), ultimately increasing multimodality and functional diversity. This creates clusters of neurons of a similar functional profile integrating different combinations of input modalities. Therefore, divergency of the connectivity between neurons (one single neuron connects with many) creates convergence of labelled lines of information. * marks new functional types appearing in the CNS, not present in the periphery.*

4. Spatial organization of neurons clustered by sensory modalities.

When analyzing the shape of the aforementioned spatial clusters of functional types, we found that the anteroposterior axis is the only one organizing TG and Th, while S1 is organized in the three spatial axes, with the DV axis being predominant. This finding in TG is not surprising, as moving in the ML quickly takes the electrode outside the ophthalmic branch, no longer representing OS [56]. In Th, this result is coincident with the AP organization of noxious, mixed and non-noxious units innervating the face reported for cats by Yokota et al., in 1985 (Yokota et al., 1985). In S1, the strong influence of the DV axis could be attributed to the different afferents received by each cortical layer from primary (VPM) and higher order thalamic nuclei (PoM) (Mo et al., 2017). These differing projections of the lemniscal (IV) and paralemniscal (I, II/III, V) pathways to S1 could be conferring spatially distributed multimodality along DV axis (Sherman, 2017). To better characterize this local circuit function, shape, and spatial organization, specific experimental approaches such as high-density electrophysiological recordings and functional imaging should be performed.

5. Neuronal ongoing activity differences across modalities and structures

The third thesis objective was to *"To analyze the spontaneous activity of cortical, thalamic and trigeminal neurons responding to ocular surface stimulation with different modalities of stimulus"*. The relevance of this objective is based in the fact that spontaneous activity determines functional states of thalamo-cortical networks, which are a key factor for information processing (Castro-Alamancos, 2004). Spontaneous activity emerges from a combination of intrinsic properties of neurons, neuronal networking (excitatory and inhibitory balance) and sensory inputs received. Here, we report differences in spontaneous activity of neurons in TG, Th and S1, depending on the type and number of modalities they are responsive to. This suggests that afferent inputs play an important role in the generation and modulation of spontaneous activity in thalamocortical units, which is in agreement with experiments studying the consequences of the interruption of ascending pathways or peripheral deafferentation (Aguilar et al., 2010; Alonso-Calviño et al., 2016; Bishop and Zito, 2013; Fernández-López et al., 2019; Hengen et al., 2013; Teichert et al., 2017). Our results suggest that modality-specific features could be involved in spontaneous activity of different neuronal populations. This opens new ways to understand how chronic unbalance of modalities inputs due to peripheral damage or pharmacological treatment interferes with perception, by modifying the "resting state" of the thalamocortical network. In addition, changes in spontaneous activity due to the behavioral states of an individual could increase or reduce OS processing of sensory afferences (Acosta et al., 1999).

6. MPIs as generators of peripheral ongoing activity in trigeminal sensory neurons

In order to complete the fourth and last objective of this thesis, "*To characterize the membrane potential instabilities of trigeminal ganglion neurons, and their role in action potential generation*" we conducted a series of patch-clamp recordings on *cultured TG neurons*. Furthermore, to adequately interpret those results, we first reviewed and organized all the bibliography related with MPIs in primary sensory neurons, since the first publications in the topic in the 80s. This revision led to a paper recently published in *Pain* (Velasco et al., 2022a).

Regarding the interpretation of our experiments, it should be noted that one of the most surprising characteristics of MPIs is the great heterogeneity that they present. According to the current literature, they can be divided in fast Spontaneous Membrane Potential Oscillations (SMPOs) and slow, non-continuous Depolarizing Spontaneous Fluctuations (DSFs). The frequency of the oscillations varies greatly across cell types, being ~100 Hz and above in fast conducting A-Type neurons displaying frequencies, and 10-20 Hz in C-type cells. Furthermore, the molecular basis of MPI is distinct in different ganglia (TG, DRG, Mes-V), as TTX blocks SMPOs both in DRG and Mes-V but not in TG, and TEA blocks SMPOs in TG, but upregulates them in other ganglia (Amir et al., 1999; Pedroarena et al., 1999; Puil and Spigelman, 1988). Given that fast oscillations in A-type neurons are the only ones described in the TG, we decided to focus our work in small/mid-sized cells mostly displaying a slow instability biased towards depolarization, similar to DSFs and/or slow SMPOs, described in DRG neurons (Lopez et al., 2021; North et al., 2019; Odem et al., 2018). We considered small/mid-sized neurons of special relevance due to their prominent role in nociception, thermosensation and pruriception (Lawson et al., 2019). As the terminology and separation between slow SMPOs and DSFs is confusing, we chose to use the term membrane potential instabilities (MPIs) to refer to all of them, and the term MPT (membrane potential transient) to refer to the most common form

found in our recordings. We belief that MPT is a better term because it reflects that the events are transient and not always spontaneous, in the sense that they are mainly elicited by membrane depolarization. For the sake of symmetry with respect to the term SMPO, it could be considered to use the name Subthreshold Membrane Potential Transients (SMPT), but prefer not to use the term Subthreshold because the MPTs can be recorded at voltage more positive than the threshold of AP firing.

Most cells we recorded displayed slow MPIs, although some of them exhibit the traditional fast-oscillation SMPOs profile or did not exhibit potential instability at all. When originally describing oscillations in TG neurons, Puil et al. stated that "almost every neuron" exhibited this behavior (Puil and Spigelman, 1988). Odem et al., reported that the majority of C-cells in DRG exhibit at least some form of DSFs, in line with the observations of Puil et al. (Odem et al., 2018). On the other hand, SMPOs are a rarer phenomenon in the DRG, being produced in approximately 25% of the neurons when depolarized (Amir et al., 1999; Li et al., 2007). Putting all together, we conclude that our great percentage of neurons displaying MPI is due to be recording in the TG and because MPTs (or DSFs) are quite common in small/mid-sized cells.

The high correlation between the capability to generate MPIs and repetitive firing present in primary sensory neurons (Amir et al., 1999; Amir and Devor, 1997; Pedroarena et al., 1999; Verdier et al., 2004) has led the field to propose that MPIs enable the neurons to generate such activity, because they prevent or remove membrane accommodation resulting from the voltage-dependent inactivation of the Na_V channels required for AP firing (Kovalsky et al., 2008, 2009; Wang et al., 2011). This acquires special significance when considering pathological states such as axonal neuropathic injury, in which local axonal MPIs induce spontaneous, ectopic firing (Kapoor et al., 1997). Other pathological models produce increased MPIs in the soma of rodent and human cells (Djouhri et al., 2018; Liu et al., 2000; North et al., 2019; Odem et al., 2018; Xing et al., 2001b; Zhang et al., 1999). Here, we obtained an equation predicting the probability of a

given depolarization to trigger an AP, based solely on its amplitude and maximal rate of depolarization. This was previously suggested by Kovalsky et al. (2008), under the theoretical rationale of MPIs promoting firing through the overcoming of accommodation (inactivation) of ionic channels during a tonic or ramp-like stimulation. We experimentally confirm this proposal and report for the first time that MPTs are generated during physiological responses towards diverse chemical and thermal stimuli. Moreover, the equation accounting for the relationship between MPTs and APs is equally valid for these stimulations. This is of great relevance for physiological contexts of stimulus transduction and encoding, but also for many pathological states featuring hyperexcitability and exacerbated responses, e.g., in allergy (Velasco et al., 2022b).

As future steps to be taken in this field, it is crucial to further investigate in more detail the relationship between MPIs and APs generation. Sensory nerve endings are the actual location in which transduction takes place in primary sensory neurons. Although MPIs are possible bases of ongoing activity in peripheral nerve endings (Olivares et al., 2015), this has not been tested experimentally. However, this door is now open, thanks to recently available new methodologies, such as genetically encoded fluorescent voltage indicators (Bando et al., 2019) that can be used for optical *in vivo* recordings of single sensory terminals (Aleixandre-Carrera et al., 2021). At the molecular level, the precise nature of MPIs remains far from being unraveled. It is clear that a single ion channel type is not enough to explain the generation and shaping of MPIs and is therefore necessary to test multiple KO animals and combinations of specific blockers. Another pending issue is to elucidate the K^+ channels implicated in the MPIs, as they are known to be crucial for all fast SMPOs reported in primary sensory neurons (Amir et al., 2002a; Pedroarena et al., 1999; Puil et al., 1989), but have not being investigated in slow oscillations or MPTs (DSFs). Finally, trigeminal MPIs have not been characterized in any pathological model, contrary to MPIs of DRGs. This challenge should be taken, given that

multiple sensory disorders related with the trigeminal innervation are currently a burden for our society (e.g., oral cancer (Warnakulasuriya, 2009), dry eye (Stapleton et al., 2017), trigeminal neuralgia (De Toledo et al., 2016) or allergic rhinitis/conjunctivitis (Mims, 2014)).

7. The relationship between OS somatosensory representation and MPIs

The available evidence demonstrates that peripheral inputs, especially ongoing activity, play a role in shaping the function and connectivity of CNS circuits (Aguilar et al., 2010; Antón-Bolaños et al., 2019; Humanes-Valera et al., 2013; Martini et al., 2021; Yagüe et al., 2014), and our results reveal that neurons in the CNS receiving information from distinct primary afferents vary in their own ongoing activity. These two ideas indicate that MPIs constitute the link between molecular expression in a primary sensory neuron (a sensor) and the shaping of the circuits in the CNS, which have the task of processing the peripheral input and generating conscious perception and motor actions (a processor driving actuators). In a poetical way, the expression of a single molecule in the tip of a minuscule sensory receptor, can be shaping our brains. This hypothesis remains to be tested experimentally.

Indeed, this hypothesis is not only relevant due to the beautiful scenario it poses in terms of basic sciences, reuniting molecular biology with systems neuroscience, but has also an enormous translational potential. Central sensitization is defined as a potentiated state of the CNS nociceptive circuit, and it is considered a potential contributor to pain perpetuation beyond the damage of peripheral tissues, in other words, chronic pain (Woolf, 1983, 2011). As MPIs are enhanced an even generated *de novo* in injured sections of the primary sensory neurons (Kapoor et al., 1997; Liu et al., 2002), their continuous afference towards CNS circuits in pain-related states could induce plastic changes in the nociceptive circuit, ultimately linking peripheral and

central sensitization, and contributing to chronic pain maintenance. Moreover, MPIs have been also documented in the central nervous system (Fry and Ferguson, 2007; Psarropoulou and Avoli, 1995; Sanhueza and Bacigalupo, 2005; Schmitz et al., 1998; Yoshida et al., 2011), so their study in primary sensory neurons (a more "simpler" scenario) opens the door to deeper understanding on how neural networks are functioning in the brain. If they are so relevant in determining ongoing activity in primary sensory neurons, do not we expect them to have key roles also the generation of ongoing activity in central neurons? Furthermore, knowing that MPIs may be coupled to cross-excitation in the peripheral sensory ganglia (Amir et al., 1996) and being cross-excitation a slight subthreshold depolarization produced by neuron-to-neuron communication, one cannot avoid to wonder if MPIs and membrane resonance have a role in synaptic integration between neurons in the CNS, as a synaptic potential is, after all, a slight subthreshold depolarization, too.

8. Impact and consequences of the thesis work

All the objectives initially proposed for this thesis work were accomplished. Our work revealed and characterized the somatotopic representation of the ocular surface thalamic and primary cortical somatosensory areas. These findings are crucial for the field of ophthalmology, in which a myriad of highly prevalent somatosensory alterations have unsatisfactory treatments, such as dry eye disease or ocular trigeminal neuralgia. These pathologies presumably produce relevant, and unknown, plastic changes in the thalamo-cortical circuits, such as the ones reported for dry eye disease in the brainstem. Now it is possible to venture into characterizing these central consequences and discover new physiopathological mechanisms, inspiring innovative therapeutic approaches.

Furthermore, in this work we provide new insights in a poorly explored field in somatosensory neuroscience: modality organization in a highly multimodal tissue such as the ocular surface. Our results in this topic provide new principles of organization of the ocular surface somatosensory system, which should be further explored and are potentially crucial for the understanding of the integration of sensations modalities resulting in a unified conscious perception. Whether these results are generalizable for all structures represented in the primary somatosensory cortex or only applicable to ocular surface representation is a question still to be addressed.

During the performance of my doctoral thesis, we generated a compendium of the available knowledge regarding Membrane Potential Instabilities, along more than 30 years of research (Velasco et al, 2022a). We found that MPIs are the strongest candidate mechanism to underly the generation of ongoing activity, and here we characterize them in detail in TG neurons. Furthermore, we demonstrate their role in ongoing activity generation, which is crucial for the correct formation and function of the somatosensory circuits in the central nervous system. Modification of MPIs and the consequent alterations in ongoing activity could be a crucial contributor to pathological states encompassing pain and aberrant sensory perceptions.

Conclusions

1) There is a somatotopic representation of the ocular surface in the somatosensory thalamus and primary somatosensory cortex, whose coordinates we have reported in rats.
2) Multimodality (that is, the positive response to stimuli of different modalities) and functional diversity (that is, the presence of neurons responding to multiple combinations of stimulus modalities) of the neurons innervating the ocular surface increase from the trigeminal ganglion to the thalamus and cortex. Neurons functionally similar cluster at the thalamus and the primary somatosensory cortex.
3) The time course of the population and single unit responses evoked in trigeminal ganglion, somatosensory thalamus and S1 cortex neurons by ocular surface stimulation depends on the intensity and modality of the applied stimulus.
4) The ongoing activity of thalamic and cortical neurons innervating the eye surface increases with the degree of multimodality, being higher in multimodal neurons.
5) The frequency and shape of membrane potential instabilities depend on the membrane voltage of TG neurons at which they are generated, near the threshold of action potential firing.

Conclusiones

1) Existe una representación somatotópica de la superficie ocular en el tálamo somatosensorial y el cortex somatosensorial primario, cuyas coordenadas en la rata reportamos.
2) La multimodalidad (es decir, la respuesta positiva a estímulos de distinta modalidad) y la diversidad funcional (es decir, la presencia de neuronas respondiendo a varias combinaciones de modalidades de estímulo) de las neuronas que inervan la superficie ocular se incrementa desde el ganglio trigémino al córtex, pasando por el tálamo. Las neuronas funcionalmente similares se encuentran agrupadas en el espacio.
3) El curso temporal de las respuestas poblacionales y unitarias evocadas mediante estimulación de la superficie ocular en el ganglio trigémino, el tálamo somatosensorial y la corteza somatosensorial primaria dependen de la intensidad y la modalidad del estímulo aplicado.
4) La actividad basal de las neuronas talámicas y corticales que inervan la superficie del ojo se es mayor cuánto más multimodales son dichas neuronas.
5) La frecuencia y la forma de las inestabilidades del potencial de membrana dependen del potencial de membrana de las neuronas trigeminales que las generan, siendo máximas a medida que este se aproxima al umbral de disparo de los potenciales de acción.

References

Acosta, Belmonte, Gallar (2001a). Sensory experiences in humans and single-unit activity in cats evoked by polymodal stimulation of the cornea. *J Physiol* 534, 511–525.

Acosta, Luna, Quirce, Belmonte, Gallar (2014). Corneal sensory nerve activity in an experimental model of UV keratitis. *Invest Ophthalmol Vis Sci* 55, 3403–3412.

Acosta, M.C., Gallar, J., Belmonte, C. (1999). The influence of eye solutions on blinking and ocular comfort at rest and during work at video display terminals. *Exp Eye Res* 68, 663–669.

Acosta, M.C., Tan, M.E., Belmonte, C., Gallar, J. (2001b). Sensations evoked by selective mechanical, chemical, and thermal stimulation of the conjunctiva and cornea. *Investig Ophthalmol Vis Sci* 42, 2063–2067.

Aguilar, J., Humanes-Valera, D., Alonso-Calviño, E., Yague, J.G., Moxon, K.A., Oliviero, A., Foffani, G. (2010). Spinal cord injury immediately changes the state of the brain. 30, 7528–7537.

Aicher, S.A., Hermes, S.M., Hegarty, D.M. (2013). Corneal afferents differentially target thalamic- and parabrachial-projecting neurons in spinal trigeminal nucleus caudalis. *Neuroscience* 232, 182–193.

Aleixandre-Carrera, F., Engelmayer, N., Ares-Suárez, D., Acosta, M. del C., Belmonte, C., Gallar, J., Meseguer, V., Binshtok, A.M. (2021). Optical assessment of nociceptive TRP channel function at the peripheral nerve terminal. *Int J Mol Sci* 22, 1–20.

Alonso-Calviño, E., Martínez-Camero, I., Fernández-López, E., Humanes-Valera, D., Foffani, G., Aguilar, J. (2016). Increased responses in the somatosensory thalamus immediately after spinal cord injury. *Neurobiol Dis* 87, 39–49.

Amir, R., Devor, M. (1997). Spike-evoked suppression and burst patterning in dorsal root

ganglion neurons of the rat. *J Physiol* 501, 183–196.

Amir, R., Devor, M., Kocsis, J., Wall, P.D. (1996). *Chemically Mediated Cross-Excitation in Rat Dorsal Root Ganglia*.

Amir, R., Kocsis, J.D., Devor, M. (2005). Multiple interacting sites of ectopic spike electrogenesis in primary sensory neurons. *J Neurosci* 25, 2576–2585.

Amir, R., Liu, C.N., Kocsis, J.D., Devor, M. (2002a). Oscillatory mechanism in primary sensory neurones. *Brain* 125, 421–435.

Amir, R., Michaelis, M., Devor, M. (1999). Membrane potential oscillations in dorsal root ganglion neurons: Role in normal electrogenesis and neuropathic pain. *J Neurosci* 19, 8589–8596.

Amir, R., Michaelis, M., Devor, M. (2002b). Burst discharge in primary sensory neurons: Triggered by subthreshold oscillations, maintained by depolarizing afterpotentials. *J Neurosci* 22, 1187–1198.

Antón-Bolaños, N., Espinosa, A., López-Bendito, G. (2018). Developmental interactions between thalamus and cortex: a true love reciprocal story. *Curr Opin Neurobiol* 52, 33–41.

Antón-Bolaños, N., Sempere-Ferràndez, A., Guillamón-Vivancos, T., Martini, F.J., Pérez-Saiz, L., Gezelius, H., Filipchuk, A., Valdeolmillos, M., López-Bendito, G. (2019). Prenatal activity from thalamic neurons governs the emergence of functional cortical maps in mice. *Science (80-)* 364, 987–990.

Azarfar, A., Calcini, N., Huang, C., Zeldenrust, F., Celikel, T. (2018). Neural coding: A single neuron's perspective. *Neurosci Biobehav Rev* 94, 238–247.

Baccei, M.L., Kocsis, J.D. (2000). Voltage-gated calcium currents in axotomized adult rat cutaneous afferent neurons. *J Neurophysiol* 83, 2227–2238.

Baker, M.D., Nassar, M.A. (2020). Painful and painless mutations of SCN9A and SCN11A voltage-gated sodium channels. *Pflugers Arch* 472, 865–880.

Bandell, M., Story, G.M., Hwang, S.W., Viswanath, V., Eid, S.R., Petrus, M.J., Earley, T.J., Patapoutian, A. (2004). Noxious cold ion channel TRPA1 is activated by pungent compounds and bradykinin. *Neuron* 41, 849–857.

Bando, Y., Grimm, C., Cornejo, V.H., Yuste, R. (2019). Genetic voltage indicators. *BMC Biol* 17.

Basso, L., Serhan, N., Tauber, M., Gaudenzio, N. (2019). Peripheral neurons: Master regulators of skin and mucosal immune response. *Eur J Immunol* 49, 1984–1997.

Bautista, D.M., Jordt, S.E., Nikai, T., Tsuruda, P.R., Read, A.J., Poblete, J., Yamoah, E.N., Basbaum, A.I., Julius, D. (2006). TRPA1 mediates the inflammatory actions of environmental irritants and proalgesic agents. *Cell* 124, 1269–1282.

Bautista, D.M., Siemens, J., Glazer, J.M., Tsuruda, P.R., Basbaum, A.I., Stucky, C.L., Jordt, S.E., Julius, D. (2007). The menthol receptor TRPM8 is the principal detector of environmental cold. *Nature* 448, 204–208.

Bech, F., González-González, O., Artime, E., Serrano, J., Alcalde, I., Gallar, J., Merayo-Lloves, J., Belmonte, C. (2018). Functional and morphologic alterations in mechanical, polymodal, and cold sensory nerve fibers of the cornea following photorefractive keratectomy. *Investig Ophthalmol Vis Sci* 59, 2281–2292.

Belmonte, C., Acosta, M.C., Gallar, J. (2004a). Neural basis of sensation in intact and injured corneas. *Exp Eye Res* 78, 513–525.

Belmonte, C., Acosta, M.C., Merayo-Lloves, J., Gallar, J. (2015). What Causes Eye Pain? *Curr Ophthalmol Rep* 3, 111–121.

Belmonte, C., Aracil, A., Acosta, M.C., Luna, C., Gallar, J. (2004b). Nerves and sensations from

the eye surface. *Ocul Surf* 2, 248–253.

Belmonte, C., Brock, J.A., Viana, F. (2009). Converting cold into pain. *Exp Brain Res* 196, 13–30.

Belmonte, C., Giraldez, F. (1981). Responses of cat corneal sensory receptors to mechanical and thermal stimulation. *J Physiol* 321, 355–368.

Belmonte, C., Nichols, J.J., Cox, S.M., Brock, J.A., Begley, C.G., Bereiter, D.A., Dartt, D.A., Galor, A., Hamrah, P., Ivanusic, J.J., Jacobs, D.S., McNamara, N.A., Rosenblatt, M.I., Stapleton, F., Wolffsohn, J.S. (2017). TFOS DEWS II pain and sensation report. *Ocul Surf* 15, 404–437.

Belmonte, Gallar, Pozo, Rebollo (1991). Excitation by irritant chemical substances of sensory afferent units in the cat's cornea. *J Physiol* 437, 709–725.

Bennett, D.L., Clark, X.A.J., Huang, J., Waxman, S.G., Dib-Hajj, S.D. (2019). The role of voltage-gated sodium channels in pain signaling. *Physiol Rev* 99, 1079–1151.

Bennett, D.L.H., Woods, C.G. (2014). Painful and painless channelopathies. *Lancet Neurol* 13, 587–599.

Berry, M.J., Meister, M. (1998). Refractoriness and neural precision. *J Neurosci* 18, 2200–2211.

Bishop, H.I., Zito, K. (2013). The downs and ups of sensory deprivation: Evidence for firing rate homeostasis in vivo. *Neuron* 80, 247–249.

Blair, N.T., Bean, B.P. (2002). Roles of tetrodotoxin (TTX)-sensitive Na+ current, TTX-resistant Na+ current, and Ca2+ current in the action potentials of nociceptive sensory neurons. 22, 10277–10290.

Boivie, J. (1979). An anatomical reinvestigation of the termination of the spinothalamic tract in the monkey. *J Comp Neurol* 186, 343–369.

Bokiniec, P., Zampieri, N., Lewin, G.R., Poulet, J.F. (2018). The neural circuits of thermal

perception. *Curr Opin Neurobiol* 52, 98–106.

Bourassa, J., Pinault, D., Deschênes, M. (1995). Corticothalamic projections from the cortical barrel field to the somatosensory thalamus in rats: a single-fibre study using biocytin as an anterograde tracer. *Eur J Neurosci* 7, 19–30.

Bron, R., Wood, R.J., Brock, J.A., Ivanusic, J.J. (2014). Piezo2 expression in corneal afferent neurons. *J Comp Neurol* 522, 2967–2979.

Buchan, M.J., Gothard, G., von Klemperer, A., van Rheede, J. (2021). Diverse roles for the posteromedial thalamus in sensory-evoked cortical plasticity. *J Neurophysiol* 125, 537–539.

Buzsáki, G., Anastassiou, C.A., Koch, C. (2012). The origin of extracellular fields and currents-EEG, ECoG, LFP and spikes. *Nat Rev Neurosci* 13, 407–420.

Casas-Torremocha, D., Porrero, C., Rodriguez-Moreno, J., García-Amado, M., Lübke, J.H.R., Núñez, Á., Clascá, F. (2019). Posterior thalamic nucleus axon terminals have different structure and functional impact in the motor and somatosensory vibrissal cortices. *Brain Struct Funct* 224.

Castro-Alamancos, M.A. (2004). Dynamics of sensory thalamocortical synaptic networks during information processing states. *Prog Neurobiol* 74, 213–247.

Caterina, M.J., Leffler, A., Malmberg, A.B., Martin, W.J., Trafton, J., Petersen-Zeitz, K.R., Koltzenburg, M., Basbaum, A.I., Julius, D. (2000). Impaired nociception and pain sensation in mice lacking the capsaicin receptor. *Science* 288, 306–313.

Cechetto, D.F., Standaert, D.G., Saper, C.B. (1985). Spinal and trigeminal dorsal horn projections to the parabrachial nucleus in the rat. *J Comp Neurol* 240, 153–160.

Cen, X., Nitta, A., Ibi, D., Zhao, Y., Niwa, M., Taguchi, K., Hamada, M., Ito, Y., Ito, Y., Wang, L., Nabeshima, T. (2008). Identification of Piccolo as a regulator of behavioral plasticity and dopamine transporter internalization. *Mol Psychiatry* 13, 451–463.

Chao, C., Golebiowski, B., Stapleton, F. (2014). The role of corneal innervation in LASIK-induced neuropathic dry eye. *Ocul Surf* 12, 32–45.

Chapin, J.K., Lin, C. -S (1984). Mapping the body representation in the SI cortex of anesthetized and awake rats. *J Comp Neurol* 229, 199–213.

Chen, Q.L., Heinricher, M.M. (2019). Descending Control Mechanisms and Chronic Pain. *Curr Rheumatol Rep* 21.

Chiang, M.C., Bowen, A., Schier, L.A., Tupone, D., Uddin, O., Heinricher, M.M. (2019). Parabrachial Complex: A Hub for Pain and Aversion. *J Neurosci* 39, 8225–8230.

Chung, M.K., Wang, S. (2011). Cold suppresses agonist-induced activation of TRPV1. *J Dent Res* 90, 1098–1102.

Clemens, A.M., Fernandez Delgado, Y., Mehlman, M.L., Mishra, P., Brecht, M. (2018). Multisensory and Motor Representations in Rat Oral Somatosensory Cortex. *Sci Rep* 8.

Colburn, R.W., Lubin, M. Lou, Stone, D.J., Wang, Y., Lawrence, D., D'Andrea, M.R.R., Brandt, M.R., Liu, Y., Flores, C.M., Qin, N. (2007). Attenuated cold sensitivity in TRPM8 null mice. *Neuron* 54, 379–386.

Colgin, L.L. (2016). Rhythms of the hippocampal network. *Nat Rev Neurosci* 17, 239–249.

Corniani, G., Saal, H.P. (2020). Tactile innervation densities across the whole body. *J Neurophysiol* 124, 1229–1240.

Coste, B., Mathur, J., Schmidt, M., Earley, T.J., Ranade, S., Petrus, M.J., Dubin, A.E., Patapoutian, A. (2010). Piezo1 and Piezo2 are essential components of distinct mechanically activated cation channels. *Science* 330, 55–60.

DelMonte, D.W., Kim, T. (2011). Anatomy and physiology of the cornea. *J Cataract Refract Surg*

37, 588–598.

Deschênes, M., Timofeeva, E., Lavallée, P., Dufresne, C. (2005). The vibrissal system as a model of thalamic operations. In *Progress in Brain Research*, (Prog Brain Res), pp. 31–40.

Descoeur, J., Pereira, V., Pizzoccaro, A., Francois, A., Ling, B., Maffre, V., Couette, B., Busserolles, J., Courteix, C., Noel, J., Lazdunski, M., Eschalier, A., Authier, N., Bourinet, E. (2011). Oxaliplatin-induced cold hypersensitivity is due to remodelling of ion channel expression in nociceptors. *EMBO Mol Med* 3, 266–278.

Devor, M. (1999). Unexplained peculiarities of the dorsal root ganglion. *Pain* 82.

Dhaka, A., Murray, A.N., Mathur, J., Earley, T.J., Petrus, M.J., Patapoutian, A. (2007). TRPM8 is required for cold sensation in mice. *Neuron* 54, 371–378.

Diamond, M.E., Armstrong-James, M., Budway, M.J., Ebner, F.F. (1992a). Somatic sensory responses in the rostral sector of the posterior group (POm) and in the ventral posterior medial nucleus (VPM) of the rat thalamus: Dependence on the barrel field cortex. *J Comp Neurol* 319, 66–84.

Diamond, M.E., Armstrong-James, M., Ebner, F.F. (1992b). Somatic sensory responses in the rostral sector of the posterior group (POm) and in the ventral posterior medial nucleus (VPM) of the rat thalamus. *J Comp Neurol* 318, 462–476.

Diamond, M.E., Von Heimendahl, M., Knutsen, P.M., Kleinfeld, D., Ahissar, E. (2008). “Where” and “what” in the whisker sensorimotor system. *Nat Rev Neurosci* 9, 601–612.

Djouhri, L., Smith, T., Alotaibi, M., Weng, X. (2018). Membrane potential oscillations are not essential for spontaneous firing generation in L4 Aβ-afferent neurons after L5 spinal nerve axotomy and are not mediated by HCN channels. *Exp Physiol* 103, 1145–1156.

Doan, T.N., Stephans, K., Ramirez, A.N., Glazebrook, P.A., Andresen, M.C., Kunze, D.L. (2004).

Differential distribution and function of hyperpolarization-activated channels in sensory neurons and mechanosensitive fibers. *J Neurosci* 24, 3335–3343.

Dong, H., Fan, Y.-H., Wang, Y.-Y., Wang, W.-T., Hu, S.-J. (2008). Lidocaine Suppresses Subthreshold Oscillations by Inhibiting Persistent Na + Current in Injured Dorsal Root Ganglion Neurons.

Dreyer, D.A., Loe, P.R., Metz, C.B., Whitsel, B.L. (1975). Representation of head and face in postcentral gyrus of the macaque. *J Neurophysiol* 38, 714–733.

Dubin, A.E., Patapoutian, A. (2010). Nociceptors: the sensors of the pain pathway. *J Clin Invest* 120, 3760–3772.

Efron, N., Al-Dossari, M., Pritchard, N. (2009). In vivo confocal microscopy of the bulbar conjunctiva. *Clin Exp Ophthalmol* 37, 335–344.

Eguchi, H., Hiura, A., Nakagawa, H., Kusaka, S., Shimomura, Y. (2017). Corneal Nerve Fiber Structure, Its Role in Corneal Function, and Its Changes in Corneal Diseases. *Biomed Res Int* 2017.

El-Boustani, S., Sermet, B.S., Foustoukos, G., Oram, T.B., Yizhar, O., Petersen, C.C.H. (2020). Anatomically and functionally distinct thalamocortical inputs to primary and secondary mouse whisker somatosensory cortices. *Nat Commun* 11.

Emery, E.C., Luiz, A.P., Sikandar, S., Magnúsdóttir, R., Dong, X., Wood, J.N. (2016). In vivo characterization of distinct modality-specific subsets of somatosensory neurons using GCaMP. *Sci Adv* 2.

Fakih, D., Zhao, Z., Nicolle, P., Reboussin, E., Joubert, F., Luzu, J., Labbé, A., Rostène, W., Baudouin, C., Mélik Parsadaniantz, S., Réaux-Le Goazigo, A. (2019). Chronic dry eye induced corneal hypersensitivity, neuroinflammatory responses, and synaptic plasticity in the mouse trigeminal brainstem. *J Neuroinflammation* 16.

Fardo, F., Vinding, M.C., Allen, M., Jensen, T.S., Finnerup, N.B. (2017). Delta and gamma oscillations in operculo-insular cortex underlie innocuous cold thermosensation. *J Neurophysiol* 117, 1959–1968.

Fernández-López, E., Alonso-Calviño, E., Humanes-Valera, D., Foffani, G., Aguilar, J. (2019). Slow-wave activity homeostasis in the somatosensory cortex after spinal cord injury. *Exp Neurol* 322.

Fernández-Trillo, J., Florez-Paz, D., Íñigo-Portugués, A., González-González, O., del Campo, A.G., González, A., Viana, F., Belmonte, C., Gomis, A. (2020). Piezo2 Mediates Low-Threshold Mechanically Evoked Pain in the Cornea. *J Neurosci* 40, 8976–8993.

Francis, J.T., Xu, S., Chapin, J.K. (2008). Proprioceptive and cutaneous representations in the rat ventral posterolateral thalamus. *J Neurophysiol* 99, 2291–2304.

Frangeul, L., Porrero, C., Garcia-Amado, M., Maimone, B., Maniglier, M., Clascá, F., Jabaudon, D. (2014). Specific activation of the paralemniscal pathway during nociception. *Eur J Neurosci* 39, 1455–1464.

Friedberg, M.H., Lee, S.M., Ebner, F.F. (1999). Modulation of receptive field properties of thalamic somatosensory neurons by the depth of anesthesia. *J Neurophysiol* 81, 2243–2252.

Friedberg, M.H., Lee, S.M., Ebner, F.F. (2004). The contribution of the principal and spinal trigeminal nuclei to the receptive field properties of thalamic VPM neurons in the rat. *J Neurocytol* 33, 75–85.

Fry, M., Ferguson, A. V. (2007). Subthreshold oscillations of membrane potential of rat subfornical organ neurons. *Neuroreport* 18, 1389–1393.

Fukuoka, T., Kobayashi, K., Yamanaka, H., Obata, K., Dai, Y., Noguchi, K. (2008). Comparative study of the distribution of the α-subunits of voltage-gated sodium channels in normal and axotomized rat dorsal root ganglion neurons. *J Comp Neurol* 510, 188–206.

Furuta, T., Kaneko, T., Deschênes, M. (2009). Septal neurons in barrel cortex derive their receptive field input from the lemniscal pathway. *J Neurosci* 29, 4089–4095.

Gallar, Acosta, Moilanen, Holopainen, Belmonte, Tervo (2004). Recovery of corneal sensitivity to mechanical and chemical stimulation after laser in situ keratomileusis. *J Refract Surg* 20, 229–235.

Gallar, J., Pozo, M.A., Tuckett, R.P., Belmonte, C. (1993). Response of sensory units with unmyelinated fibres to mechanical, thermal and chemical stimulation of the cat's cornea. *J Physiol* 468, 609–622.

Garcia-Larrea, L., Bastuji, H. (2018). Pain and consciousness. *Prog Neuropsychopharmacol Biol Psychiatry* 87, 193–199.

Gauriau, C., Bernard, J.F. (2004). A comparative reappraisal of projections from the superficial laminae of the dorsal horn in the rat: the forebrain. *J Comp Neurol* 468, 24–56.

George, A.L. (2005). Inherited disorders of voltage-gated sodium channels. *J Clin Invest* 115, 1990–1999.

Gipson, I.K. (2007). The ocular surface: The challenge to enable and protect vision. The Friedenwald lecture. In *Investigative Ophthalmology and Visual Science*, (NIH Public Access), pp. 4391–4398.

Golan, O., Randleman, J.B. (2018). Pain management after photorefractive keratectomy. *Curr Opin Ophthalmol* 29, 306–312.

Gold, M.S., Shuster, M.J., Levine, J.D. (1996). Characterization of six voltage-gated K+ currents in adult rat sensory neurons. *J Neurophysiol* 75, 2629–2646.

González-González, O., Bech, F., Gallar, J., Merayo-Lloves, J., Belmonte, C. (2017). Functional properties of sensory nerve terminals of the mouse cornea. *Investig Ophthalmol Vis Sci* 58, 404–

415.

González, A., Herrera, G., Ugarte, G., Restrepo, C., Piña, R., Pertusa, M., Orio, P., Madrid, R. (2017). IKD Current in Cold Transduction and Damage-Triggered Cold Hypersensitivity. *Adv Exp Med Biol* 1015, 265–277.

Goodwin, G., McMahon, S.B. (2021). The physiological function of different voltage-gated sodium channels in pain. *Nat Rev Neurosci* 22, 263–274.

Grillner, S., Markram, H., De Schutter, E., Silberberg, G., LeBeau, F.E.N. (2005). Microcircuits in action--from CPGs to neocortex. *Trends Neurosci* 28, 525–533.

Guerrero-Moreno, A., Baudouin, C., Melik Parsadaniantz, S., Réaux-Le Goazigo, A. (2020). Morphological and Functional Changes of Corneal Nerves and Their Contribution to Peripheral and Central Sensory Abnormalities. *Front Cell Neurosci* 14.

Guillery, R.W., Sherman, S.M. (2002). Thalamic relay functions and their role in corticocortical communication: Generalizations from the visual system. *Neuron* 33, 163–175.

Haidarliu, S., Yu, C., Rubin, N., Ahissar, E. (2008). Lemniscal and extralemniscal compartments in the VPM of the rat. *Front Neuroanat* 2.

Hengen, K.B., Lambo, M.E., VanHooser, S.D., Katz, D.B., Turrigiano, G.G. (2013). Firing rate homeostasis in visual cortex of freely behaving rodents. *Neuron* 80, 335–342.

Herman, A.M., Palmer, C., Azevedo, R.T., Tsakiris, M. (2021). Neural divergence and convergence for attention to and detection of interoceptive and somatosensory stimuli. *Cortex* 135, 186–206.

Hirata, H., Dallacasagrande, V., Mizerska, K., Ivakhnitskaia, E., Rosenblatt, M.I. (2018). Ambient air currents activate corneal nerves during ocular desiccation in rats: Simultaneous recordings of neural activity and corneal temperature. *Investig Ophthalmol Vis Sci* 59, 4031–4043.

Hirata, H., Takeshita, S., Hu, J.W., Bereiter, D.A. (2000). Cornea-responsive medullary dorsal horn neurons: modulation by local opioids and projections to thalamus and brain stem. *J Neurophysiol* 84, 1050–1061.

Hodgkin, A.L., Huxley, A.F. (1952). A quantitative description of membrane current and its application to conduction and excitation in nerve. *J Physiol* 117, 500.

Huang, S.M., Li, X., Yu, Y.Y., Wang, J., Caterina, M.J. (2011). TRPV3 and TRPV4 ion channels are not major contributors to mouse heat sensation. *Mol Pain* 7.

Huang, W., Liu, M., Yan, S.F., Yan, N. (2017). Structure-based assessment of disease-related mutations in human voltage-gated sodium channels. *Protein Cell* 8, 401–438.

Humanes-Valera, D., Aguilar, J., Foffani, G. (2013). Reorganization of the intact somatosensory cortex immediately after spinal cord injury. *PLoS One* 8.

Humanes-Valera, D., Foffani, G., Alonso-Calviño, E., Fernández-López, E., Aguilar, J. (2017). Dual Cortical Plasticity After Spinal Cord Injury. *Cereb Cortex* 27, 2926–2940.

Hwang, S.J., Min Oh, J., Valtschanoff, J.G. (2005). Expression of the vanilloid receptor TRPV1 in rat dorsal root ganglion neurons supports different roles of the receptor in visceral and cutaneous afferents. *Brain Res* 1047, 261–266.

Iggo, A., Andres, K.H. (1982). Morphology of cutaneous receptors. *Annu Rev Neurosci* 5, 1–31.

Jacquin, M.F., Renehan, W.E., Mooney, R.D., Rhoades, R.W. (1986). Structure-function relationships in rat medullary and cervical dorsal horns. I. Trigeminal primary afferents. *J Neurophysiol* 55, 1153–1186.

Jin, Q.Q., Wu, G.Q., Peng, W.W., Xia, X.L., Hu, L., Iannetti, G.D. (2018). Somatotopic representation of second pain in the primary somatosensory cortex of humans and rodents. *J Neurosci* 38, 5538–5550.

Johnson, K.O. (2001). The roles and functions of cutaneous mechanoreceptors. *Curr Opin Neurobiol* 11, 455–461.

Julius, D. (2013). TRP channels and pain. *Annu Rev Cell Dev Biol* 29, 355–384.

Kaas, J.H., Nelson, R.J., Sur, M., Dykes, R.W., Merzenich, M.M. (1984). The somatotopic organization of the ventroposterior thalamus of the squirrel monkey, Saimiri sciureus. *J Comp Neurol* 226, 111–140.

Kanellopoulos, A.H., Matsuyama, A. (2016). Voltage-gated sodium channels and pain-related disorders. *Clin Sci (Lond)* 130, 2257–2265.

Kapoor, R., Li, Y.G., Smith, K.J. (1997). Slow sodium-dependent potential oscillations contribute to ectopic firing in mammalian demyelinated axons. *Brain* 120, 647–652.

Karashima, Y., Talavera, K., Everaerts, W., Janssens, A., Kwan, K.Y., Vennekens, R., Nilius, B., Voets, T. (2009). TRPA1 acts as a cold sensor in vitro and in vivo. *Proc Natl Acad Sci U S A* 106, 1273–1278.

Kasetsuwan, N., Satitpitakul, V., Changul, T., Jariyakosol, S. (2013). Incidence and pattern of dry eye after cataract surgery. *PLoS One* 8.

Kato, K., Miyake, K., Hirano, K., Kondo, M. (2019). Management of Postoperative Inflammation and Dry Eye after Cataract Surgery. *Cornea* 38, S25–S33.

Ke, C.B., He, W.S., Li, C.J., Shi, D., Gao, F., Tian, Y.K. (2012). Enhanced SCN7A/Nax expression contributes to bone cancer pain by increasing excitability of neurons in dorsal root ganglion. *Neuroscience* 227, 80–89.

Knowlton, W.M., Bifolck-Fisher, A., Bautista, D.M., McKemy, D.D. (2010). TRPM8, but not TRPA1, is required for neural and behavioral responses to acute noxious cold temperatures and cold-mimetics in vivo. *Pain* 150, 340–350.

Kobayashi, K., Fukuoka, T., Obata, K., Yamanaka, H., Dai, Y., Tokunaga, A., Noguchi, K. (2005). Distinct expression of TRPM8, TRPA1, and TRPV1 mRNAs in rat primary afferent neurons with adelta/c-fibers and colocalization with trk receptors. *J Comp Neurol* 493, 596–606.

Koch, S.C., Acton, D., Goulding, M. (2018). Spinal Circuits for Touch, Pain and Itch. *Annu Rev Physiol* 80, 189.

Kovács, I., Luna, C., Quirce, S., Mizerska, K., Callejo, G., Riestra, A., Fernández-Sánchez, L., Meseguer, V.M., Cuenca, N., Merayo-Lloves, J., Acosta, M.C., Gasull, X., Belmonte, C., Gallar, J. (2016). Abnormal activity of corneal cold thermoreceptors underlies the unpleasant sensations in dry eye disease. *Pain* 157, 399–417.

Kovalsky, Y., Amir, R., Devor, M. (2008). Subthreshold oscillations facilitate neuropathic spike discharge by overcoming membrane accommodation. *Exp Neurol* 210, 194–206.

Kovalsky, Y., Amir, R., Devor, M. (2009). Simulation in Sensory Neurons Reveals a Key Role for Delayed Na^+ Current in Subthreshold Oscillations and Ectopic Discharge: Implications for Neuropathic Pain. *J Neurophysiol* 102, 1430–1442.

Kurose, M., Meng, I.D. (2013). Corneal dry-responsive neurons in the spinal trigeminal nucleus respond to innocuous cooling in the rat. *J Neurophysiol* 109, 2517–2522.

Labetoulle, M., Baudouin, C., Calonge, M., Merayo-Lloves, J., Boboridis, K.G., Akova, Y.A., Aragona, P., Geerling, G., Messmer, E.M., Benítez-del-Castillo, J. (2019). Role of corneal nerves in ocular surface homeostasis and disease. *Acta Ophthalmol* 97, 137–145.

Launay, P.S., Godefroy, D., Khabou, H., Rostene, W., Sahel, J.A., Baudouin, C., Melik Parsadaniantz, S., Reaux-Le Goazigo, A. (2015). Combined 3DISCO clearing method, retrograde tracer and ultramicroscopy to map corneal neurons in a whole adult mouse trigeminal ganglion. *Exp Eye Res* 139, 136–143.

Laverdet, B., Danigo, A., Girard, D., Magy, L., Demiot, C., Desmoulière, A. (2015). Skin innervation: important roles during normal and pathological cutaneous repair. *Histol Histopathol* 30, 875–892.

Lawson, S.N., Fang, X., Djouhri, L. (2019). Nociceptor subtypes and their incidence in rat lumbar dorsal root ganglia (DRGs): focussing on C-polymodal nociceptors, Aβ-nociceptors, moderate pressure receptors and their receptive field depths. *Curr Opin Physiol* 11, 125–146.

Lazarov, N. (2000). The mesencephalic trigeminal nucleus in the cat. *Adv Anat Embryol Cell Biol* 153, 1–103.

Leiser, S.C., Moxon, K.A. (2006). Relationship between physiological response type (RA and SA) and vibrissal receptive field of neurons within the rat trigeminal ganglion. *J Neurophysiol* 95, 3129–3145.

Levin, L.A., Adler, F.H. (2011). *Adler's physiology of the eye.* (Edingburg: Saunders/Elsevier).

Li, C.X., Jing, Y.L., Xie, Y.K. (2007). Glycosylation-induced depolarization facilitates subthreshold membrane oscillation in injured primary sensory neurons. *Brain Res* 1139, 201–209.

Li, J.N., Ren, J.H., Zhao, L.J., Wu, X.M., Li, H., Dong, Y.L., Li, Y.Q. (2021). Projecting neurons in spinal dorsal horn send collateral projections to dorsal midline/intralaminar thalamic complex and parabrachial nucleus. *Brain Res Bull* 169, 184–195.

Li, L., Rutlin, M., Abraira, V.E., Cassidy, C., Kus, L., Gong, S., Jankowski, M.P., Luo, W., Heintz, N., Koerber, H.R., Woodbury, C.J., Ginty, D.D. (2011). The functional organization of cutaneous low-threshold mechanosensory neurons. *Cell* 147, 1615–1627.

Lieberman, A. (1976). Sensory ganglia. In: Landon DN, ed. The peripheral nerve. London, United Kingdom. 188–278.

Liu, C.N., Devor, M., Waxman, S.G., Kocsis, J.D. (2002). Subthreshold oscillations induced by

spinal nerve injury in dissociated muscle and cutaneous afferents of mouse DRG. *J Neurophysiol* 87, 2009–2017.

Liu, C.N., Michaelis, M., Amir, R., Devor, M. (2000). Spinal nerve injury enhances subthreshold membrane potential oscillations in DRG neurons: Relation to neuropathic pain. *J Neurophysiol* 84, 205–215.

Liu, F., Wuni, G.Y., Bahuva, R., Shafiq, M.A., Gattas, B.S., Ibetoh, C.N., Stratulat, E., Gordon, D.K. (2020). Pacemaking Activity in the Peripheral Nervous System: Physiology and Roles of Hyperpolarization Activated and Cyclic Nucleotide-Gated Channels in Neuropathic Pain. *Cureus* 12.

Lopez, E.R., Carbajal, A.G., Tian, J. Bin, Bavencoffe, A., Zhu, M.X., Dessauer, C.W., Walters, E.T. (2021). Serotonin enhances depolarizing spontaneous fluctuations, excitability, and ongoing activity in isolated rat DRG neurons via 5-HT4 receptors and cAMP-dependent mechanisms. *Neuropharmacology* 184.

Lu, J., Hathaway, C.B., Bereiter, D.A. (1993). Adrenalectomy enhances Fos-like immunoreactivity within the spinal trigeminal nucleus induced by noxious thermal stimulation of the cornea. *Neuroscience* 54, 809–818.

Lum, E., Corbett, M.C., Murphy, P.J. (2019). Corneal Sensitivity After Ocular Surgery. *Eye Contact Lens* 45, 226–237.

Lumpkin, E.A., Caterina, M.J. (2007). Mechanisms of sensory transduction in the skin. *Nature* 445, 858–865.

Luna, Mizerska, Quirce, Belmonte, Gallar, Acosta, Meseguer (2021). Sodium Channel Blockers Modulate Abnormal Activity of Regenerating Nociceptive Corneal Nerves After Surgical Lesion. *Invest Ophthalmol Vis Sci* 62.

Ma, Q. (2010). Labeled lines meet and talk: Population coding of somatic sensations. *J Clin Invest* 120, 3773–3778.

Ma, Q. (2012). Population coding of somatic sensations. *Neurosci Bull* 28, 91–99.

Marfurt, C.F. (1981). The somatotopic organization of the cat trigeminal ganglion as determined by the horseradish peroxidase technique. *Anat Rec* 201, 105–118.

Marfurt, C.F., Cox, J., Deek, S., Dvorscak, L. (2010). Anatomy of the human corneal innervation. *Exp Eye Res* 90, 478–492.

Martinez, L.M., Molano-Mazón, M., Wang, X., Sommer, F.T., Hirsch, J.A. (2014). Statistical wiring of thalamic receptive fields optimizes spatial sampling of the retinal image. *Neuron* 81, 943–956.

Martinez, S., Belmonte, C. (1996). C-Fos expression in trigeminal nucleus neurons after chemical irritation of the cornea: reduction by selective blockade of nociceptor chemosensitivity. *Exp Brain Res* 109, 56–62.

Martini, F.J., Guillamón-Vivancos, T., Moreno-Juan, V., Valdeolmillos, M., López-Bendito, G. (2021). Spontaneous activity in developing thalamic and cortical sensory networks. *Neuron* 109, 2519–2534.

Mathers, D.A., Barker, J.L. (1984). Spontaneous voltage and current fluctuations in tissue cultured mouse dorsal root ganglion cells. *Brain Res* 293, 35–47.

McEchron, M.D., McCabe, P.M., Green, E.J., Hitchcock, J.M., Schneiderman, N. (1996). Immunohistochemical expression of the c-Fos protein in the spinal trigeminal nucleus following presentation of a corneal airpuff stimulus. *Brain Res* 710, 112–120.

McGivern, J.G., McDonough, S.I. (2004). Voltage-gated calcium channels as targets for the treatment of chronic pain. *Curr Drug Targets CNS Neurol Disord* 3, 457–478.

McKemy, D.D. (2013). The molecular and cellular basis of cold sensation. *ACS Chem Neurosci* 4, 238–247.

McKemy, D.D., Neuhausser, W.M., Julius, D. (2002). Identification of a cold receptor reveals a general role for TRP channels in thermosensation. *Nature* 416, 52–58.

Meacham, K., Shepherd, A., Mohapatra, D.P., Haroutounian, S. (2017). Neuropathic Pain: Central vs. Peripheral Mechanisms. *Curr Pain Headache Rep* 21.

Megat, S., Ray, P.R., Tavares-Ferreira, D., Moy, J.K., Sankaranarayanan, I., Wanghzou, A., Lou, T.F., Barragan-Iglesias, P., Campbell, Z.T., Dussor, G., Price, T.J. (2019). Differences between Dorsal Root and Trigeminal Ganglion Nociceptors in Mice Revealed by Translational Profiling. *J Neurosci* 39, 6829–6847.

Menétrey, D., Basbaum, A.I. (1987). Spinal and trigeminal projections to the nucleus of the solitary tract: a possible substrate for somatovisceral and viscerovisceral reflex activation. *J Comp Neurol* 255, 439–450.

Meng, Hu, Benetti, Bereiter (1997). Encoding of corneal input in two distinct regions of the spinal trigeminal nucleus in the rat: cutaneous receptive field properties, responses to thermal and chemical stimulation, modulation by diffuse noxious inhibitory controls, and projections to the p. *J Neurophysiol* 77, 43–56.

Meng, I.D., Bereiter, D.A. (1996). Differential distribution of Fos-like immunoreactivity in the spinal trigeminal nucleus after noxious and innocuous thermal and chemical stimulation of rat cornea. *Neuroscience* 72, 243–254.

Meseguer, V., Alpizar, Y.A., Luis, E., Tajada, S., Denlinger, B., Fajardo, O., Manenschijn, J.A., Fernández-Peña, C., Talavera, A., Kichko, T., Navia, B., Sánchez, A., Señarís, R., Reeh, P., Pérez-García, M.T., López-López, J.R., Voets, T., Belmonte, C., Talavera, K., Viana, F. (2014). TRPA1

channels mediate acute neurogenic inflammation and pain produced by bacterial endotoxins. *Nat Commun* 5.

Mezzera, C., López-Bendito, G. (2016). Cross-modal plasticity in sensory deprived animal models: From the thalamocortical development point of view. *J Chem Neuroanat* 75, 32–40.

Milenkovic, N., Zhao, W.J., Walcher, J., Albert, T., Siemens, J., Lewin, G.R., Poulet, J.F.A. (2014). A somatosensory circuit for cooling perception in mice. *Nat Neurosci* 17, 1560–1566.

Millan, M.J. (2002). Descending control of pain. *Prog Neurobiol* 66, 355–474.

Mims, J.W. (2014). Epidemiology of allergic rhinitis. *Int Forum Allergy Rhinol* 4.

Minnery, B.S., Bruno, R.M., Simons, D.J. (2003). Response transformation and receptive-field synthesis in the lemniscal trigeminothalamic circuit. *J Neurophysiol* 90, 1556–1570.

Minnery, B.S., Simons, D.J. (2003). Response properties of whisker-associated trigeminothalamic neurons in rat nucleus principalis. *J Neurophysiol* 89, 40–56.

Mo, C., Petrof, I., Viaene, A.N., Sherman, S.M. (2017). Synaptic properties of the lemniscal and paralemniscal pathways to the mouse somatosensory thalamus. *Proc Natl Acad Sci U S A* 114, E6212–E6221.

Moulton, E.A., Becerra, L., Rosenthal, P., Borsook, D. (2012). An Approach to Localizing Corneal Pain Representation in Human Primary Somatosensory Cortex. *PLoS One* 7.

Munger, B.L., Halata, Z. (1984). The sensorineural apparatus of the human eyelid. *Am J Anat* 170, 181–204.

Murray Sherman, S., Guillery, R.W. (2011). Distinct functions for direct and transthalamic corticocortical connections. *J Neurophysiol* 106, 1068–1077.

Nelson, R.J., Sur, M., Felleman, D.J., Kaas, J.H. (1980). Representations of the body surface in

postcentral parietal cortex of Macaca fascicularis. *J Comp Neurol* 192, 611–643.

North, R.Y., Li, Y., Ray, P., Rhines, L.D., Tatsui, C.E., Rao, G., Johansson, C.A., Zhang, H., Kim, Y.H., Zhang, B., Dussor, G., Kim, T.H., Price, T.J., Dougherty, P.M. (2019). Electrophysiological and transcriptomic correlates of neuropathic pain in human dorsal root ganglion neurons. *Brain* 142, 1215–1226.

Noseda, R., Monconduit, L., Constandil, L., Chalus, M., Villanueva, L. (2008). Central nervous system networks involved in the processing of meningeal and cutaneous inputs from the ophthalmic branch of the trigeminal nerve in the rat. *Cephalalgia* 28, 813–824.

Odem, M.A., Bavencoffe, A.G., Cassidy, R.M., Lopez, E.R., Tian, J., Dessauer, C.W., Walters, E.T. (2018). Isolated nociceptors reveal multiple specializations for generating irregular ongoing activity associated with ongoing pain. *Pain* 159, 2347–2362.

Olivares, E., Salgado, S., Maidana, J.P., Herrera, G., Campos, M., Madrid, R., Orio, P. (2015). TRPM8-dependent dynamic response in a mathematical model of cold thermoreceptor. *PLoS One* 10.

Olszewski, J. (1950). On the anatomical and functional organization of the spinal trigeminal nucleus. *J Comp Neurol* 92, 401–413.

Ossipov, M.H., Morimura, K., Porreca, F. (2014). Descending pain modulation and chronification of pain. *Curr Opin Support Palliat Care* 8, 143–151.

Pagella, P., Jiménez-Rojo, L., Mitsiadis, T.A. (2014). Roles of innervation in developing and regenerating orofacial tissues. *Cell Mol Life Sci* 71, 2241–2251.

Panzeri, S., Brunel, N., Logothetis, N.K., Kayser, C. (2010). Sensory neural codes using multiplexed temporal scales. *Trends Neurosci* 33, 111–120.

Paricio-Montesinos, Schwaller, Udhayachandran, Rau, Walcher, Evangelista, Vriens, Voets,

Poulet, Lewin (2020). The Sensory Coding of Warm Perception. *Neuron* 106, 830-841.e3.

Parra, A., Gonzalez-Gonzalez, O., Gallar, J., Belmonte, C. (2014). Tear fluid hyperosmolality increases nerve impulse activity of cold thermoreceptor endings of the cornea. *Pain* 155, 1481–1491.

Parra, A., Madrid, R., Echevarria, D., Del Olmo, S., Morenilla-Palao, C., Acosta, M.C., Gallar, J., Dhaka, A., Viana, F., Belmonte, C. (2010). Ocular surface wetness is regulated by TRPM8-dependent cold thermoreceptors of the cornea. *Nat Med* 16, 1396–1399.

Paxinos, G., Watson, C. (2007). The rat brain in stereotaxic coordinates.

Pedroarena, C.M., Pose, I.E., Yamuy, J., Chase, M.H., Morales, F.R. (1999). Oscillatory membrane potential activity in the soma of a primary afferent neuron. *J Neurophysiol* 82, 1465–1476.

Peier, A.M., Moqrich, A., Hergarden, A.C., Reeve, A.J., Andersson, D.A., Story, G.M., Earley, T.J., Dragoni, I., McIntyre, P., Bevan, S., Patapoutian, A. (2002). A TRP channel that senses cold stimuli and menthol. *Cell* 108, 705–715.

Pflugfelder, S.C., Stern, M.E. (2020). Biological functions of tear film. *Exp Eye Res* 197.

Piña, R., Ugarte, G., Campos, M., Íñigo-Portugués, A., Olivares, E., Orio, P., Belmonte, C., Bacigalupo, J., Madrid, R. (2019). Role of TRPM8 Channels in Altered Cold Sensitivity of Corneal Primary Sensory Neurons Induced by Axonal Damage. *J Neurosci* 39, 8177–8192.

Plomp, G., Quairiaux, C., Kiss, J.Z., Astolfi, L., Michel, C.M. (2014). Dynamic connectivity among cortical layers in local and large-scale sensory processing. *Eur J Neurosci* 40, 3215–3223.

Pozo, M.A., Cervero, F. (1993). Neurons in the rat spinal trigeminal complex driven by corneal nociceptors: Receptive-field properties and effects of noxious stimulation of the cornea. *J Neurophysiol* 70, 2370–2378.

Psarropoulou, C., Avoli, M. (1995). Subthreshold membrane-potential oscillations in immature rat CA3 hippocampal neurones. *Neuroreport* 6, 2561–2564.

Puil, E., Gimbarzevsky, B., Spigelman, I. (1988). Primary involvement of K+ conductance in membrane resonance of trigeminal root ganglion neurons. *J Neurophysiol* 59, 77–89.

Puil, E., Miura, R.M., Spigelman, I. (1989). Consequences of 4-aminopyridine applications to trigeminal root ganglion neurons. *J Neurophysiol* 62, 810–820.

Puil, E., Spigelman, I. (1988). Electrophysiological responses of trigeminal root ganglion neurons in vitro. *Neuroscience* 24, 635–646.

Purves, D., Augustine, G.J., Fitzpatrick, D., Katz, L.C., LaMantia, A.-S., McNamara, J.O., Williams, S.M. (2001). Neuroscience. 1–2.

Quallo, T., Vastani, N., Horridge, E., Gentry, C., Parra, A., Moss, S., Viana, F., Belmonte, C., Andersson, D.A., Bevan, S. (2015). TRPM8 is a neuronal osmosensor that regulates eye blinking in mice. *Nat Commun* 6.

Raghavan, M., Fee, D., Barkhaus, P.E. (2019). Generation and propagation of the action potential. *Handb Clin Neurol* 160, 3–22.

Rahman, M., Okamoto, K., Thompson, R., Bereiter, D.A. (2014). Trigeminal pathways for hypertonic saline- and light-evoked corneal reflexes. *Neuroscience* 277, 716–723.

Rahman, M., Okamoto, K., Thompson, R., Katagiri, A., Bereiter, D.A. (2015). Sensitization of trigeminal brainstem pathways in a model for tear deficient dry eye. *Pain* 156, 942–950.

Rahman, M., Shiozaki, K., Okamoto, K., Thompson, R., Bereiter, D.A. (2017). Trigeminal brainstem modulation of persistent orbicularis oculi muscle activity in a rat model of dry eye. *Neuroscience* 349, 208–219.

Ran, C., Hoon, M.A., Chen, X. (2016). The coding of cutaneous temperature in the spinal cord. *Nat Neurosci* 19, 1201–1209.

Rausell, E., Jones, E.G. (1991). Chemically distinct compartments of the thalamic VPM nucleus in monkeys relay principal and spinal trigeminal pathways to different layers of the somatosensory cortex. *J Neurosci* 11, 226–237.

Rossum, G.V., Drake, F.L. (2009). Introduction to Python 3.

Rush, A.M., Cummins, T.R., Waxman, S.G. (2007). Multiple sodium channels and their roles in electrogenesis within dorsal root ganglion neurons. *J Physiol* 579, 1–14.

Sanhueza, M., Bacigalupo, J. (2005). Intrinsic subthreshold oscillations of the membrane potential in pyramidal neurons of the olfactory amygdala. 22, 1618–1626.

Santiago, B., Diaz-Tahoces, A., Gallar, J., Belmonte, C., Acosta, M.C. (2017). Somatotopic organization of the different functional types of trigeminal ganglion neurons innervating the ocular surface and periocular tissues. *Invest Ophthalmol Vis Sci* 58, 1020.

Sanzarello, I., Merlini, L., Rosa, M.A., Perrone, M., Frugiuele, J., Borghi, R., Faldini, C. (2016). Central sensitization in chronic low back pain: A narrative review. *J Back Musculoskelet Rehabil* 29, 625–633.

Sawada, Y., Hosokawa, H., Hori, A., Matsumura, K., Kobayashi, S. (2007). Cold sensitivity of recombinant TRPA1 channels. *Brain Res* 1160, 39–46.

Schmitz, D., Gloveli, T., Behr, J., Dugladze, T., Heinemann, U. (1998). *Subthreshold membrane potential oscillations in neurons of deep layers of the entorhinal cortex* (Elsevier Ltd).

Sherman, S.M. (2017). Functioning of circuits connecting thalamus and cortex. *Compr Physiol* 7, 713–739.

Shin, S.M., Moehring, F., Itson-Zoske, B., Fan, F., Stucky, C.L., Hogan, Q.H., Yu, H. (2021). Piezo2 mechanosensitive ion channel is located to sensory neurons and nonneuronal cells in rat peripheral sensory pathway: implications in pain. *Pain* 162, 2750–2768.

Sinica, V., Zimova, L., Barvikova, K., Macikova, L., Barvik, I., Vlachova, V. (2019). Human and Mouse TRPA1 Are Heat and Cold Sensors Differentially Tuned by Voltage. *Cells* 9.

Sluka, K.A., Frey-Law, L., Bement, M.H. (2018). Exercise-induced pain and analgesia? Underlying mechanisms and clinical translation. *Pain* 159 Suppl 1, S91–S97.

Stapleton, F., Alves, M., Bunya, V.Y., Jalbert, I., Lekhanont, K., Malet, F., Na, K.S., Schaumberg, D., Uchino, M., Vehof, J., Viso, E., Vitale, S., Jones, L. (2017). TFOS DEWS II Epidemiology Report. *Ocul Surf* 15, 334–365.

Story, G.M., Peier, A.M., Reeve, A.J., Eid, S.R., Mosbacher, J., Hricik, T.R., Earley, T.J., Hergarden, A.C., Andersson, D.A., Hwang, S.W., McIntyre, P., Jegla, T., Bevan, S., Patapoutian, A. (2003). ANKTM1, a TRP-like channel expressed in nociceptive neurons, is activated by cold temperatures. *Cell* 112, 819–829.

Syeda, R., Florendo, M.N., Cox, C.D., Kefauver, J.M., Santos, J.S., Martinac, B., Patapoutian, A. (2016). Piezo1 Channels Are Inherently Mechanosensitive. *Cell Rep* 17, 1739–1746.

Syeda, R., Xu, J., Dubin, A.E., Coste, B., Mathur, J., Huynh, T., Matzen, J., Lao, J., Tully, D.C., Engels, I.H., Michael Petrassi, H., Schumacher, A.M., Montal, M., Bandell, M., Patapoutian, A. (2015). Chemical activation of the mechanotransduction channel Piezo1. *Elife* 4.

Tan, C.H., McNaughton, P.A. (2016). The TRPM2 ion channel is required for sensitivity to warmth. *Nature* 536, 460–463.

Teichert, M., Liebmann, L., Hübner, C.A., Bolz, J. (2017). Homeostatic plasticity and synaptic scaling in the adult mouse auditory cortex. *Sci Rep* 7.

Thiel, G., Rubil, S., Lesch, A., Guethlein, L.A., Rössler, O.G. (2017). Transient receptor potential TRPM3 channels: Pharmacology, signaling, and biological functions. *Pharmacol Res* 124, 92–99.

Timofeev, I. (2013). Local origin of slow EEG waves during sleep. *Zh Vyssh Nerv Deiat Im I P Pavlova* 63, 105–112.

Toda, I. (2018). Dry eye after lasik. *Investig Ophthalmol Vis Sci* 59, DES109–DES115.

Todd, A.J. (2010). Neuronal circuitry for pain processing in the dorsal horn. *Nat Rev Neurosci* 11, 823–836.

De Toledo, I.P., Conti Réus, J., Fernandes, M., Porporatti, A.L., Peres, M.A., Takaschima, A., Linhares, M.N., Guerra, E., De Luca Canto, G. (2016). Prevalence of trigeminal neuralgia: A systematic review. *J Am Dent Assoc* 147, 570-576.e2.

Tominaga, M., Caterina, M.J., Malmberg, A.B., Rosen, T.A., Gilbert, H., Skinner, K., Raumann, B.E., Basbaum, A.I., Julius, D. (1998). The cloned capsaicin receptor integrates multiple pain-producing stimuli. *Neuron* 21, 531–543.

Torre, V., Ashmore, J.F., Lamb, T.D., Menini, A. (1995). Transduction and adaptation in sensory receptor cells. *J Neurosci* 15, 7757–7768.

Urbain, N., Deschênes, M. (2007). A new thalamic pathway of vibrissal information modulated by the motor cortex. *J Neurosci* 27, 12407–12412.

Vandewauw, I., De Clercq, K., Mulier, M., Held, K., Pinto, S., Van Ranst, N., Segal, A., Voet, T., Vennekens, R., Zimmermann, K., Vriens, J., Voets, T. (2018). A TRP channel trio mediates acute noxious heat sensing. *Nature* 555, 662–666.

Vandewauw, I., Voets, T. (2016). Heat is absolute, cold is relative. *Nat Neurosci* 19, 1188–1189.

Vangeel, L., Benoit, M., Miron, Y., Miller, P.E., De Clercq, K., Chaltin, P., Verfaillie, C., Vriens, J.,

Voets, T. (2020). Functional expression and pharmacological modulation of TRPM3 in human sensory neurons. *Br J Pharmacol* 177, 2683–2695.

Velasco, E., Alvarez, J.L., Meseguer, V.M., Gallar, J., Talavera, K. (2022a). Membrane potential instabilities in sensory neurons: mechanisms and pathophysiological relevance. *Pain* 163, 64–74.

Velasco, E., Delicado-Miralles, M., Hellings, P.W., Gallar, J., Van Gerven, L., Talavera, K. (2022b). Epithelial and sensory mechanisms of nasal hyperreactivity. *Allergy*.

Venkatachalam, K., Montell, C. (2007). TRP channels. *Annu Rev Biochem* 76, 387–417.

Verdier, D., Lund, J.P., Kolta, A. (2004). Synaptic Inputs to Trigeminal Primary Afferent Neurons Cause Firing and Modulate Intrinsic Oscillatory Activity. *J Neurophysiol* 92, 2444–2455.

Vermeiren, S., Bellefroid, E.J., Desiderio, S. (2020). Vertebrate Sensory Ganglia: Common and Divergent Features of the Transcriptional Programs Generating Their Functional Specialization. *Front Cell Dev Biol* 8.

Viana, F. (2016). TRPA1 channels: molecular sentinels of cellular stress and tissue damage. *J Physiol* 594, 4151–4169.

Vriens, J., Nilius, B., Voets, T. (2014). Peripheral thermosensation in mammals. *Nat Rev Neurosci* 15, 573–589.

Vriens, J., Owsianik, G., Hofmann, T., Philipp, S.E., Stab, J., Chen, X., Benoit, M., Xue, F., Janssens, A., Kerselaers, S., Oberwinkler, J., Vennekens, R., Gudermann, T., Nilius, B., Voets, T. (2011). TRPM3 is a nociceptor channel involved in the detection of noxious heat. *Neuron* 70, 482–494.

Wang, J., La, J.H., Hamill, O.P. (2019). PIEZO1 Is Selectively Expressed in Small Diameter Mouse DRG Neurons Distinct From Neurons Strongly Expressing TRPV1. *Front Mol Neurosci* 12.

Wang, L., Gui, P., Li, L., Ku, Y., Bodner, M., Fan, G., Zhou, Y. Di, Dong, X.W. (2016). Neural correlates of heat-evoked pain memory in humans. *J Neurophysiol* 115, 1596–1604.

Wang, Y.Y., Wen, Z.H., Duan, J.H., Zhu, J.L., Wang, W.T., Dong, H., Li, H.M., Gao, G.D., Xing, J.L., Hu, S.J. (2011). Noise enhances subthreshold oscillations in injured primary sensory neurons. *NeuroSignals* 19, 54–62.

Warnakulasuriya, S. (2009). Global epidemiology of oral and oropharyngeal cancer. *Oral Oncol* 45, 309–316.

Waxman, S.G., Kocsis, J.D., Black, J.A. (1994). Type III sodium channel mRNA is expressed in embryonic but not adult spinal sensory neurons, and is reexpressed following axotomy. *J Neurophysiol* 72, 466–470.

Woo, S.H., Ranade, S., Weyer, A.D., Dubin, A.E., Baba, Y., Qiu, Z., Petrus, M., Miyamoto, T., Reddy, K., Lumpkin, E.A., Stucky, C.L., Patapoutian, A. (2014). Piezo2 is required for Merkel-cell mechanotransduction. *Nature* 509, 622–626.

Woolf, C.J. (1983). Evidence for a central component of post-injury pain hypersensitivity. *Nature* 306, 686–688.

Woolf, C.J. (2011). Central sensitization: Implications for the diagnosis and treatment of pain. *Pain* 152, S2.

Wu, N., Hsiao, C.F., Chandler, S.H. (2001). Membrane resonance and subthreshold membrane oscillations in mesencephalic V neurons: Participants in burst generation. *J Neurosci* 21, 3729–3739.

Xing, J.L., Hu, S.J., Long, K.P. (2001a). Subthreshold membrane potential oscillations of type A neurons in injured DRG. *Brain Res* 901, 128–136.

Xing, J.L., Hu, S.J., Xu, H., Han, S., Wan, Y.H. (2001b). Subthreshold membrane oscillations

underlying integer multiples firing from injured sensory neurons. *Neuroreport* 12, 1311–1313.

Yagüe, J.G., Humanes-Valera, D., Aguilar, J., Foffani, G. (2014). Functional reorganization of the forepaw cortical representation immediately after thoracic spinal cord hemisection in rats. *Exp Neurol* 257, 19–24.

Yarmolinsky, D.A., Peng, Y., Pogorzala, L.A., Rutlin, M., Hoon, M.A., Zuker, C.S. (2016). Coding and Plasticity in the Mammalian Thermosensory System. *Neuron* 92, 1079–1092.

Yin, Y., Le, S.C., Hsu, A.L., Borgnia, M.J., Yang, H., Lee, S.Y. (2019). Structural basis of cooling agent and lipid sensing by the cold-activated TRPM8 channel. *Science* 363.

Yokota, T., Koyama, N., Matsumoto, N. (1985). Somatotopic distribution of trigeminal nociceptive neurons in ventrobasal complex of cat thalamus. *J Neurophysiol* 53, 1387–1400.

Yoshida, M., Giocomo, L.M., Boardman, I., Hasselmo, M.E. (2011). Frequency of subthreshold oscillations at different membrane potential voltages in neurons at different anatomical positions on the dorsoventral axis in the rat medial entorhinal cortex. *J Neurosci* 31, 12683–12694.

Yu, C., Derdikman, D., Haidarliu, S., Ahissar, E. (2006). Parallel thalamic pathways for whisking and touch signals in the rat. *PLoS Biol* 4.

Zemel, B.M., Ritter, D.M., Covarrubias, M., Muqeem, T. (2018). A-Type K V Channels in Dorsal Root Ganglion Neurons: Diversity, Function, and Dysfunction. *Front Mol Neurosci* 11.

Zeng, W.Z., Marshall, K.L., Min, S., Daou, I., Chapleau, M.W., Abboud, F.M., Liberles, S.D., Patapoutian, A. (2018). PIEZOs mediate neuronal sensing of blood pressure and the baroreceptor reflex. *Science* 362, 464–467.

Zhang, H., Wang, X., Guo, W., Li, A., Chen, R., Huang, F., Liu, X., Chen, Y., Li, N., Liu, X., Xu, T., Xue, Z., Zeng, S. (2021). Cross-Streams Through the Ventral Posteromedial Thalamic Nucleus to

Convey Vibrissal Information. *Front Neuroanat* 15.

Zhang, J.-M., Song, X.-J., LaMotte, R.H. (1999). Enhanced Excitability of Sensory Neurons in Rats With Cutaneous Hyperalgesia Produced by Chronic Compression of the Dorsal Root Ganglion. *J Neurophysiol* 82, 3359–3366.

Zheng, Y., Liu, P., Bai, L., Trimmer, J.S., Bean, B.P., Ginty, D.D. (2019). Deep Sequencing of Somatosensory Neurons Reveals Molecular Determinants of Intrinsic Physiological Properties. *Neuron* 103, 598-616.e7.

Zimmerman, A., Bai, L., Ginty, D.D. (2014). The gentle touch receptors of mammalian skin. *Science* 346, 950–954.

Books:

Purves D, Augustine GJ, Fitzpatrick D, et al., editors. Neuroscience. 2nd edition. Sunderland (MA): Sinauer Associates; 2001.

Kandel, E. R., Schwartz, J. H., & Jessell, T. M. (2000). Principles of neural science. New York: McGraw-Hill, Health Professions Division.

Annex 1: Publications

Resting membrane potential instabilities in sensory neurons: mechanisms and pathophysiological relevance

Velasco E[1], Alvarez JL[2], Meseguer VM[1], Gallar J[1,3], Talavera K[2,*]

1-Instituto de Neurociencias, Universidad Miguel Hernández-CSIC, 03550 San Juan de Alicante, Spain.

2-Laboratory of Ion Channel Research, Department of Cellular and Molecular Medicine, KU Leuven, VIB Center for Brain & Disease Research, 3000 Leuven, Belgium.

3-Instituto de Investigación Sanitaria y Biomédica de Alicante, 03550 San Juan de Alicante, Spain

*Corresponding author: Laboratory of Ion Channel Research, Department of Cellular and Molecular Medicine, KU Leuven, VIB Center for Brain & Disease Research, 3000 Leuven, Belgium. karel.talavera@kuleuven.vib.be; Tel.: +32-16-330469; Web: https://www.kuleuven.be/wieiswie/en/person/00033481

Pages: 18

Figures: 4

Tables: 1

Abstract

Peripheral sensory neurons transduce physicochemical stimuli affecting somatic tissues into the firing of action potentials that are conveyed to the central nervous system. This results in conscious perception, adaptation and survival, but alterations of the firing patterns can result in pain and hypersensitivity conditions. Thus, understanding the molecular mechanisms underlying action potential firing in peripheral sensory neurons is essential in sensory biology and pathophysiology. Over the last 30 years it has been consistently reported that these cells can display resting membrane potential instabilities (RMPIs), in the form of subthreshold membrane potential oscillations (SMPOs) or depolarizing spontaneous fluctuations (DSFs). However, research on this subject remains sparse, without a clear conductive thread to be followed. To address this, we here provide a synthesis of the description, molecular bases, mathematical models, physiological roles and pathophysiological implications of RMPIs in peripheral sensory neurons. SMPOs have been reported in trigeminal, dorsal root and Mes-V ganglia, where they are thought to support repetitive firing. They are proposed to have roles also in intercellular communication, ectopic firing and responses to tonic and slow natural stimuli. We highlight how SMPOs are of great interest for the study of sensory transduction physiology and how they may represent therapeutic targets for many pathological conditions, such as acute and chronic pain,

itch and altered sensory perceptions. We identify future research directions, including the elucidation of the underlying molecular determinants and modulation mechanisms, their relation to the encoding of natural stimuli and their implication in pain and hypersensitivity conditions.

Introduction

Peripheral sensory neurons are a special subtype of neurons that detect external and internal stimuli affecting somatic tissues. The cell bodies of these neurons are located in the nodose, vagal, trigeminal (TG) and dorsal root (DRG) ganglia and in the mesencephalic nucleus of the trigeminus (Mes-V). Nodose and vagal ganglia are part of the vagal nerve, implicated in the autonomic system, mainly controlling internal tissues such as visceral and tympanic structures. DRGs are located at each side of the spinal cord, and innervate all the somatic structures corresponding to their medullar level (skin, muscles, bones, etc.). TG ganglia accomplish a similar function, innervating the face, mouth and ocular surface. Mes-V is a curious nucleus with peripheral projections innervating the jaw musculature and periodontal mechanoreceptors, but it is located in the central nervous system (CNS).

The peripheral sensory nerve endings transduce stimuli into local generator potentials finally leading to the firing of action potentials, whose instantaneous frequency encodes the information about the characteristics of the stimuli that is conveyed to the central nervous system. This process allows the organism to adequately respond to changes of external and internal conditions, ultimately allowing for adaptation, survival and conscious perception of the environment [51]. Moreover, alterations of firing patterns, such as the appearance of abnormal of spontaneous, have been related to multiple pathologies featuring aberrant functions of sensory neurons, especially pain. Thus, the understanding of the mechanisms underlying the action potential firing is essential in sensory biology and pathophysiology [13,17,20].

According to the prevalent current view, action potential firing in sensory neurons occurs upon the induction of a sufficiently strong and fast depolarization from a stable membrane potential, by activation of chemo-, thermo- and mechano-sensitive cation channels. However, it has been consistently reported that sensory neurons can display marked resting membrane potential instabilities (RMPIs). One form of this instability manifests as sinusoidal-like oscillations, dubbed subthreshold membrane potential oscillations (SMPOs). SMPOs have been reported in TG, DRG and Mes-V, as well as in many central nervous system (CNS) nuclei, such as the thalamus [2], the inferior olive [18] and the cortex [59]. Another, much less studied type of RMPI has been reported in C-type DRG neurons, showing positive deflections of the membrane potential. This activity is therefore morphologically different from SMPOs and has been referred to as Depolarizing Spontaneous Fluctuations (DSFs) [47,60].

In peripheral sensory neurons, SMPOs were first described in TG neurons in the late 80s [52–54]. Subsequently, SMPOs have been described in DRG neurons [3,9] and in the mesencephalic trigeminal nucleus (Mes-V) [49,50]. SMPOs have been mostly studied in rat DRG neurons, in full mounted ganglia [5,9], slice preparations [49,50,52–54,62], primary cultured neurons [22,30,64,67,71], and in vivo recordings [7,21,34]. They are also described in mice fetal [41] and adult DRGs recordings [36,41]. SMPOs are proposed to have many physiological functions, such as generating repetitive and spontaneous activity and contributing to cell-to-cell communication [3,8,9,49,50,62]. Furthermore, they have been strongly linked in animal studies to different features of peripheral sensitization such as ectopic firing, enhanced excitability and spontaneous activity development in neuropathic injuries [21,29,37,38]. Recent studies describe the SMPOs contribution to pain in other pathological conditions which sensitize peripheral sensory neurons,

such as bone cancer [30]. Also, DSFs display a tight relationship with spontaneous activity and neuropathic damage, even in human DRG cells from patients with neuropathic pain [46] and in rodents with spinal cord injury [12,47,70]. These findings indicate that the study of RMPIs is fundamental for the understanding of peripheral mechanisms of normal sensory function, pain generation and the identification of possible therapeutic targets.

In this review we recapitulate on the description and molecular bases of RMPIs in sensory neurons and on how they have been proposed to trigger action potentials, leading to repetitive firing. We discuss how, in turn, this facilitates intercellular communication, ectopic firing and response to tonic stimuli, and how in consequence, RMPIs are key to understanding of sensory transduction physiology and pathophysiology. Finally, we propose future research directions, with the ultimate purpose of inspiring further exploration of this largely neglected but promising field.

Morphological description and relationship with the membrane potential

SMPOs appear as a constant or briefly interrupted sinusoidal-like waves deflecting the membrane voltage both in the depolarizing and hyperpolarizing directions (**Figure 1**). These waves are distinct in amplitude (1-6 mV) and frequencies (10-200 Hz), depending on the membrane voltage and neuronal type. Neurons that are capable of producing SMPOs can be divided into two groups: one in which oscillations occur at the resting membrane potential and the other in which cells oscillate only when depolarization is applied. Notably, spontaneously-oscillating neurons tend to have resting potentials more depolarized than the neurons that need external depolarization to oscillate, indicating that the membrane potential is a main modulator of SMPOs [9,60]. Accordingly, the frequency of the SMPOs increases monotonously with membrane depolarization. The SMPO amplitude, on the other hand, increases with depolarization only until a certain point and further depolarization renders smaller SMPOs until reaching complete abolition at highly depolarized potentials. The resting potentials at which the amplitude is maximal are generally reported between -50 and -30 mV. Around 25% of DRG neurons *in vitro* and 13% of DRG neurons *in vivo* are capable of producing SMPOs (spontaneous or evoked), whereas 36% of Mes-V neurons are able to oscillate spontaneously or upon depolarization [62]. In contrast, most TG neurons are capable of producing SMPOs when depolarized [55].

The ability to generate SMPOs also varies across the cell type within the same ganglion. The majority of studies have been performed in DRG A-type neurons, which are large neurons with high conduction velocities, roughly categorized as proprio- and mechanoceptors. Twelve percent of these neurons exhibit spontaneous oscillations, while 27% are able to generate SMPOs when depolarized, with a maximum amplitude between 3-6 mV, and high frequencies, ranging from 80 to almost 200 Hz [9]. In contrast, C-type neurons have been rather neglected in the SMPO literature. Those are small neurons with low conduction velocities (< 1m/s) and are a functionally heterogeneous population, mainly composed by nociceptors, but containing also pruriceptors, low and high threshold mechanosensors and thermosensors. These neurons do not exhibit spontaneous oscillations, but 25% of them produce SMPOs when depolarized. Although the SMPOs recorded in C-type neurons are similar in amplitude to the ones produced by A-type neurons, they have markedly lower frequency, ranging between 11-15 Hz [9,34],

suggesting for a disparity in the biophysical mechanisms underlying their production between these cell types.

Moreover, RMPIs observed in C-type cells appear as irregular fluctuations rather than as continuous sinusoids (as is the case for A-type neurons). These previously mentioned DSFs have been recently reported in C-type DRG neurons of rats, mice and humans [12,16,46,47,70]. DSFs, were characterized as deflexions from an apparent voltage median (determined from a sliding median window), which were more frequent in the depolarization direction [47]. They do not occur continuously in time, but isolated or during brief periods. On the other hand, DSFs display a similar amplitude and their duration is similar to the period of SMPOs described in C-type neurons. In addition, DSFs are similarly modulated in amplitude and frequency by membrane voltage **(Figure 2)**.

Although SMPOs are present only in few C-type neurons, significant DSFs are found in most DRG neurons capable to generate ongoing activity, either spontaneously or evoked. This makes us think that this could explain the previously mentioned discrepancy between the low numbers of oscillating DRG neurons and most of TG neurons reported being capable to transiently oscillate on depolarization, potentially confounding DSFs and SMPOs. Consequently, except otherwise stated, in advance we are referring to SMPOs/fluctuations/DSFs as resting membrane potential instabilities (RMPIs) in general. Furthermore, we strongly recommend to review these terms in the future to simplify cross-referencing in the field.

Importantly, the possibility of RMPIs constituting only an artifact due to instability in the recordings or the influence of extrinsic noise sources has raised due to their morphological similarity and small amplitude. However, the sensitivity of these events to the inhibitory action of drugs, their consistent modulation by membrane potential and the dependence of their manifestation on the cell type and pathological states indicate that they are intrinsic cellular properties. Furthermore, the frequencies of RMPIs are not in the range of 50, 60 Hz or their harmonics, discarding electrical artifacts. Mechanical vibrations have also been discarded as a possible source [10].

Molecular bases and electrogenesis of RMPIs

Many studies have aimed at the identification of the molecular players and currents underlying SMPOs generation. Although this is still a topic of discussion, significant advance has been made in the last 30 years in regard to the molecular bases of the oscillations and their differences across cell types. In contrast, virtually nothing is known about the mechanistic basis of DSFs.

Synaptic, Ca^{2+} and I_H currents are not required for SMPOs electrogenesis

SMPOs in peripheral sensory neurons are considered a cell autonomous phenomenon [37], as a contribution of synaptic driven currents has been discarded by primary culture experiments in which the cells were isolated and by the inefficacy of synaptic blockers to alter SMPOs even in the heavily interconnected Mes-V nucleus [62,66]. Also, as described below, depletion of extracellular Ca^{2+} (a key mediator of synaptic transmission) has no effect on SMPOs. Even in the CNS, SMPOs are considered cell autonomous [58,59]. However, this does not imply that SMPOs in peripheral sensory neurons do not play a role in cell-to-cell communication, as they do in the

CNS [61]. This topic is further discussed in the section *"SMPOs physiological implications"*. In the case of DSFs, as they have been recorded in isolated cultured cells, they are also assumed to be cell autonomous[16,39,47].

The contribution of Ca^{2+} currents to the generation and shaping of SMPOs seems to be negligible as neither Cd^{2+}, Mg^{2+}, Co^{2+}, apamin or extracellular Ca^{2+} depletion have an appreciable effect on SMPOs in any of the three sensory ganglia [49,54,71]. Also, although hyperpolarization-gated current (I_H) is a fundamental contributor in many pacemaker-like activities, blockers of this current have no effect on peripheral sensory neurons SMPOs [21,39].

K^+ currents

K^+ currents are, on the other hand, ubiquitously crucial for SMPO generation and frequency determination, but the nature of K^+ current implicated seems to vary across different ganglia. In the TG, TEA application slows down and even abolishes both SMPOs and membrane resonance, whereas 4-AP does not block SMPOs, but enhances them [41,53,54]. These results suggest that K_V3- and K_V7-driven currents, TEA-sensitive and 4-AP-insensitive, are implicated in SMPO generation. However, it should be taken into account that these compounds have low specificity at the high concentrations tested (10 and 1 mM respectively) and more refined experiments should be carried to identify the contributing channel isoform(s) [28]. In contrast, K_V blockers (TEA, 4-AP and intracellular Cs^+) facilitate oscillations in DRG neurons and even induce them in non-oscillating cells. The only effective way of disrupting DRG SMPOs by modulating K^+ currents is increasing the extracellular [K^+], a procedure that globally reduces the driving force of all K^+ currents, thus affecting all of them in a non-specific fashion. This suggests that in DRG the implicated K^+ current is not carried by a K_V channel, but by a leak K^+ channel producing an outward current, such as members of the K_{2P} family [6]. However, specific experiments to determine the role of these channels have not been performed. Finally, in Mes-V, TEA, 4-AP and intracellular Cs^+ reduce the frequency of the oscillations, but do not abolish them [49,66]. Interestingly, in Mes-V TEA effects were modest compared to the effect of 4-AP in reducing SMPOs frequency, contrary to the observed in the TG. In all ganglia, K_V blockers reduced the frequency of the oscillations, which could imply that K_V driven I_K is part of the molecular machinery determining the SMPOs frequency. Whether DSFs/slow oscillating neurons (C-type), and fast oscillating neurons (A-type), do differ in their I_K and in their expression of K_V has not yet been determined (for more detail see below *Models of SMPOs electrogenesis)*.

Na^+ currents

Inward Na^+ currents are required for SMPO generation, as substitution of extracellular Na^+ by the impermeant cation $choline^+$ abolish them in every ganglia and neuron type tested thus far [9,49,54]. But, like in the case of K^+ currents, distinct Na^+ currents appear to be implicated in different ganglia. In the TG, TTX at 1 µM does not affect SMPOs nor membrane resonance, suggesting the implication of TTX-resistant (TTX-R) Na^+ channels [52,54]. Because the oscillations are voltage-dependent , voltage-gated TTX-R channels are plausible candidates, which in peripheral sensory neurons are $Na_V1.8$ and $Na_V1.9$ [14]. In DRG neurons, on the other hand, SMPOs are totally blocked by TTX, pointing to TTX-S voltage-gated Na^+ channels as mechanistic substrate [9,29], which in these neurons are $Na_V1.1$, 1.6 and 1.7. In Mes-V neurons, SMPOs are driven by TTX-S channels, like in the DRG [49,66]. However, up until now no precise Na_V channel

has been implicated in SMPOs generation in peripheral sensory neurons. Interestingly, some works from the group of Stephen Waxman exhibit SMPOs in their recordings of WT and mutant mice. Specifically, Figure 5 of reference [24] shows SMPOs recording in neurons from WT and A1632E mutant mice (a gain of function mutation for NaV1.7 channel) and Figure 9 of reference [56], in which SMPOs could be observed in a recording of a small neuron from a NaV1.8-KO mice. However, the contribution of this channels to SMPOs remains obscure as no formal analysis of them is reported in these works.

Models for SMPOs electrogenesis

The interpretation of these experimental results had led to several theoretical models about SMPO generation.

The principles underlying the occurrence of membrane resonance and oscillatory behaviour where clearly explained by Hutcheon and Yarom [27] (**Figure 3**). Membrane resonance is the ability of a given neuron to amplify a stimulus in a certain range of frequencies, and to filter those stimuli which are not. Such resonance has been demonstrated experimentally in peripheral sensory neurons, in a range of frequencies that is similar to that of the SMPOs [52,66]. Resonance can be produced in a simple electronic circuit featuring a high pass filter and a low pass filter with a non-filtered range between them that defines the resonant frequencies. In the simplest model, the low-pass filter is constituted by the cell membrane capacitor in parallel with leak currents, whereas the high-pass filter is constituted by "generator currents" that oppose the change in voltage, by having the equilibrium potential at the base of its activation curve (such as I_H or outwardly rectifying K^+ currents like I_K). If the time constant for activation of the current is higher than the membrane time constant, this difference will define a window of resonance. These two elements are enough to generate resonance, but are not sufficient to generate a stable oscillatory behaviour such as SMPOs. One more piece is needed: an "amplifying current". Contrary to generator currents, this current should have its equilibrium potential at the top of its activation curve. In this way, the amplifying current will be activated by the generator current, increasing the change in voltage. If the amplification is large enough, this will result in time-stable oscillations, whose frequency will be defined by the time constants of the conductances/currents. Currents susceptible to be amplifying currents are the Na^+ persistent current (I_{NaP}), the synaptic NMDA current (I_{NMDA}), and the L-type Ca^{2+} current. Also, the T-type Ca^{2+} current could be, on its own, both a generator and amplifying current.

Regarding models of primary sensory neurons, it should be noted that the majority of them have been developed based on data of large DRG A-type neurons, and might not be extensible to other cell types like C-type neurons. A relatively easy conceptualization of the mechanisms giving rise to an oscillation could be framed in terms of a dynamic balance between depolarizing and repolarizing currents. When the balance favours depolarization, the corresponding limb of the SMPO is generated, until it turns into the repolarizing direction and so on. Using this concept, Puil et al. [53] proposed a simple model for TG SMPOs in which the depolarizing limb of the oscillation is carried by a voltage gated TTX-R Na^+ current, whereas the repolarizing/hyperpolarizing limb is produced by a TEA-sensitive and 4-AP-insensitive voltage-gated K^+ outward current.

Amir et al. [6] proposed a similar model for DRG neurons, integrating the corresponding differential findings between TG and DRG. In this model, the depolarizing limb of the SMPO is generated by a voltage gated TTX-S Na^+ inward current, while the repolarizing/hyperpolarizing limb is attributed to a K^+ leak outward current with low voltage sensitivity, rendering an ohmic linear behaviour to the repolarization. Finally, the voltage-gated K^+ outward current (I_K) determines the frequency of oscillations in this model, resulting in slower and larger oscillations when blocked. This blockade increases the input resistance (R_{in}), producing larger depolarizations when TTX-S channels open. Moreover, slower oscillations allow more recovery of Na_V channels from inactivation in each cycle, increasing their contribution to the depolarization phase. This model only included a fast Na^+ current, but it was later updated with the incorporation of three additional Na^+ currents: two delayed currents (Late1, with a time window of 2-20 ms, and Late 2, with 20-200 ms) and a persistent current (I_{NaP}) [32]. The resultant model does not oscillate at rest (-57 mV), but starts oscillating upon application of small depolarizations, and fires bursts of action potentials with more intense stimuli. With even stronger depolarization, action potentials are abolished and SMPOs are preserved. Further depolarization increases the frequency of the SMPOs but decrease their amplitude until they disappear. These oscillations had a frequency of 44.7 Hz and an amplitude of 2.3 mV. Oscillatory behaviour occurred in the voltage range between -56 and -37 mV. Altogether, all these characteristics are common with experimentally measured SMPOs. The analysis of the individual contribution of each current to SMPOs revealed that Fast and Late1 determine the membrane potential window for SMPOs, bursting and tonic firing generation, whereas Late1 and Late2 determine the frequency of the oscillations. In brief, fast Na^+ currents determine the initiation of the SMPOs and the slow/persistent currents determine their frequency.

In conclusion, SMPOs constitute a cell-autonomous phenomenon that in peripheral sensory neurons is mainly sustained by voltage-gated K^+ and Na^+ currents. The specific identity of these currents varies across sensory ganglia, which may reflect their differences in function, embryological origins and target tissues. Table 1 shows a summary of the different experimental findings and a comparison between ganglia.

Physiological roles of RMPIs

The main proposed physiological role of RMPIs in peripheral sensory neurons is the triggering of action potentials. More precisely, the support of repetitive action potential firing in response to a tonic stimulus and of spontaneous firing activity. For SMPOs in particular, other proposed functions are inter-neuronal communication and the induction of ectopic firing.

RMPIs as generators of repetitive firing

The hypothesis that RMPIs are the basis of repetitive firing activity is supported on experimental findings that heavily correlate the presence of oscillations to the ability of generating repetitive firing (almost 100% of the neurons accomplish this relationship) [3,9,47,49,62]. This hypothesis is also supported by theoretical models suggesting that oscillations of the membrane increase the probability of surpassing the action potential generation threshold [33,64]. For example, in spontaneously bursting firing neurons, a slow depolarization of the membrane potential leads to SMPOs and, only after SMPOs have been produced, action potentials start being generated. Then a hyperpolarizing shift induced by the burst abolishes both SMPOs and action potentials,

and a subsequent recovery from that hyperpolarization results in the start of another burst cycle (**Figure 4**) [3].

The proposed mechanism by which RMPIs enhances neuronal excitability is the reduction of the membrane accommodation induced by physiological stimuli, which arguably are mostly ramp-like. Voltage-gated Na^+ (Na_V) channels become progressively inactivated by ramp-like depolarizations, rendering the neuron unable to generate an action potential. SMPOs and DSFs reduce this accommodation by adding a fast-depolarizing component to slow ramp depolarizations, thus recruiting available Na_V channels and triggering the action potential [33,47]. A similar mechanism is plausible for ongoing activity, in which the depolarizing limb of the oscillation fires the action potential, and the repolarizing limb removes inactivation from the Na_V channels. From this model we can infer that the probability of a given oscillation to generate an action potential is directly dependent both on the amplitude and on the rate of depolarization of the oscillation. However, this idea remains to be tested experimentally.

There are many situations in which sensory cells may be subjected to a ramp-like stimulation. One example is during progressive pressure increase over a joint like the knee or a nerve like the sciatic, during normal walking, which can be painful in pathological states like osteoarthritis or peripheral nerve compression. Other examples are progressive changes in environmental temperature, which induce ramp-like depolarization in sensory cells through activation of thermosensitive TRP channels [40]. Noteworthy, DRG neurons do not have a blood-brain barrier (BBB) like the rest of the PNS (better called blood-nerve barrier, BNB, in the PNS), which may confer them a role as sensors of the body internal state [19]. Thus, circulating chemical molecules (such as chemokines) may induce slow ramp stimulation in sensory nerves, as well as in neuronal soma. The latter action may also provide an answer to the question on the role of RMPIs in the soma. This latter mechanism is particularly interesting, as it has been demonstrated in rats and humans that after a traumatic spinal cord injury the peripheral sensory cells exhibit enhanced spontaneous activity and RMPIs [46,47,70]. Furthermore, circulating chemokines levels have been correlated with the intensity of pain in spinal cord injury patients during the subacute clinical state [44]. We suggest that, in this scenario, somatic RMPIs may modulate a function of neuronal somas as sensors of central nervous system damage.

In a neuropathic damage model study, different oscillatory modes of the SMPOs have been linked to different repetitive firing patterns [69]. Neurons that generate continuous, regular SMPOs normally fire at a constant frequency that is equal or a fraction of the SMPOs frequency. For example, if in a neuron the frequency of the SMPOs is ~100 Hz and each SMPO has a 10% probability of generating an action potential, the action potentials will display a regular ~10 Hz frequency. This group constitutes 11% of the oscillating A-type DRG neurons. Another SMPO pattern, found in 51% of the neurons, is the one called “spindle-like”, modulated in amplitude, and associated with the production of burst firing. Lastly, the remaining 38% of neurons present irregular SMPOs and similarly irregular action potential generation frequency. It has been shown that bursting is the result of an interaction between SMPOs and action potential after depolarization (DAPs) in which the SMPOs triggers the first action potential, and then, a DAP promotes the generation of the next spikes within the burst [7].

SMPOs as neural activity coordinators and promoters of intercellular communication

Another role proposed for SMPOs is the coordination of neural activity between neurons. Although this is the principal role proposed for SMPOs in the central nervous system (CNS), in peripheral sensory neurons it has been less studied due to the scarcity of synapses [35]. Nevertheless, some communication is present between these neurons, as stimulating one of them with a certain pattern produces a subthreshold depolarization in neighbour cells, a phenomenon called "cross-excitation" [3,4]. The mechanistic basis of cross-excitation in sensory neurons is unclear, but the two main candidates are chemical communication between cells and the elevation of extracellular K^+ concentration produced by the activity of the first cell. This phenomenon is usually not enough to produce action potential firing by itself, but if it is produced in a cell exhibiting SMPOs, both depolarizations may sum together and produce sustained action potential firing [7]. Furthermore, currents driven by NMDA are enough to induce SMPOs in Mes-V cells, which possess effective synaptic communication [50]. Synaptic input evoked by electrical stimulation of different Mes-V-projecting nuclei produce an amplification of the ongoing SMPOs, induce SMPOs in quiescent cells and reset the phase of oscillation, which could be a powerful mechanism of synchronization between neurons [19,62].

Moreover, some signalling molecules are capable of triggering SMPOs in peripheral sensory neurons, such as epinephrine and norepinephrine [68]. It could be envisaged that these molecules could simply depolarize the neurons and consequently produce SMPOs. However, this hypothesis has been discarded, as a current injection equivalent to the depolarization produced by norepinephrine was not able to induce SMPOs in a representative fraction of neurons. Instead, it has been proven that SMPOs induction mediated by norepinephrine depends on a PKA-mediated signalling pathway. These results support the possibility of SMPOs being a mechanism of activity synchronization and communication between peripheral sensory neurons, although this remains an open question that requires further investigation.

SMPOs and ectopic firing

The physiological function of peripheral sensory neurons is the sensing of stimuli at their peripheral endings and the generation and conduction of action potentials encoding the stimulus information to the CNS, where further processing takes place. However, it is known that action potentials can be generated in other subcellular compartments of these neurons, such as the axon and the cell soma [5,63], a phenomenon called ectopic firing. Some studies demonstrated the existence of local SMPOs at these sites of ectopic firing generation, thus proposing them as an inducible mechanism of excitability allowing different subcellular compartments to generate repetitive electrical activity [5,29,42] **(Figure 5)**. This is especially relevant in some pathological conditions, in which ectopic firing is conveying a sensory message that has not been produced at the periphery, ultimately producing abnormal pain, discomfort and perceptions and/or plastic modification of the central pathway.

RMPIs in pathological states

SMPOs are strongly upregulated in pathological conditions featuring neuropathic injuries such as axotomy, axonal compression or constriction and demyelination [29]. Also, non-neuropathic pathologies, specifically bone cancer, upregulate SMPOs [31]. The most common alteration is an increase in the percentage of spontaneously oscillating neurons (i.e. from 5% to 30% in axotomized DRGs). Consequently, the percentage of spontaneously active neurons in terms of

repetitive firing is also increased, together with the proportion of neurons capable of producing repetitive firing when depolarized. These changes are demonstrated to occur as soon as 16-24 h post-injury [38]. Also, in axonal lesions it has been proven that local SMPOs generate repetitive firing both in the soma and the axon (see above *SMPOs and ectopic firing).* In fact, action potentials generated in the axon could interact with the soma and be turned into a burst barrage thanks to DAPs mediated amplification [5,29]. Neurons from axotomized DRGs also exhibit oscillations inducible with lower depolarizing thresholds, with a relationship between SMPOs amplitude and membrane voltage shifted to more negative potentials and a lower frequency of oscillation, although this latter finding seems to be dependent on the specific site in which the axotomy is performed [38].

In animals axotomized at the medullar level L5, also the DRG neurons of the L4 display increased hyperexcitability and spontaneous activity, but, interestingly, only 50%, 43% and 0% of spontaneously active cutaneous L4 Aβ-low threshold mechanoreceptors, Aβ-nociceptors and C-nociceptors, respectively, exhibited SMPOs [21]. This finding apparently represents an exception for the dependence of repetitive firing on the presence of SMPOs. However, it should be considered that the injury in L5 neurons was performed at the axonal level, raising the possibility that the ectopic firing was generated in L4 axons in communication with the injured, degenerating L5 axons. In this case, the repetitive firing could be generated in the axon by local axonal SMPOs and then propagated into the cell soma that is being recorded *in vivo*, a phenomenon already reported by other authors (see above *SMPOs and ectopic firing)*.

Although the molecular mechanisms underlying the upregulation of SMPOs remain poorly understood, it was demonstrated that glycosylation of the exoplasmic side of transmembrane proteins, mainly by negatively charged sugars such as sialic acid, depolarizes the neurons and induces SMPOs both in A and C-neurons. This process is reversible by application of neuraminidase, which removes the sialic acid, suggesting for a possible therapeutic option [34]. The effect of glycosylation may be mediated by the increase of extracellular membrane surface charges, which directly leads to membrane depolarization and a consequent increase of SMPOs. Another milestone in the determination of the molecular substrate of the pathologically increased SMPOs is the finding that I_{NaP} is increased in neurons of injured animals in comparison to healthy controls. Specific blockade of this current with 100 nM TTX, the antagonist riluzole, gabapentin or low doses of lidocaine abolishes SMPOs without affecting the capability of the neurons to fire action potentials in the injured neurons [22,64,67,71]. Further theoretical support for a capital role of slow Na^+ depolarizing currents in SMPOs upregulation in pathological states comes from the dynamical systems-based modelling [57]. It was concluded that the minimum change required for SMPOs induction, threshold lowering and repetitive firing in pathological conditions is a change in the voltage for half-maximal activation of the Islow from -21 to -13 mV. The possible contribution of I_{NaP} to SMPO generation in healthy animal remains, however, unexplored.

Surprisingly, the only channel for which its relationship with SMPOs has been characterized is a quite non-conventional voltage-insensitive channel named SCN7A/NaX. This channel is preferentially expressed in glial cells, is sensitive to the Na^+ concentration and has a role in salt ingesting behaviours and in the regulation of Na^+ concentration in the cerebrospinal fluid [45]. NaX is upregulated in DRG neurons of animals with bone cancer, and cells expressing this

channel had more depolarized resting membrane potential, lower rheobase and most of them exhibited SMPOs. Knocking down NaX prevented this hyperexcitability features and decreased the painful symptomatology associated with the sarcoma, suggesting that the NaX and SMPOs relationship is part of the pathological changes sustaining the painful phenotype of this condition [31].

Spinal cord injury (SCI) sensitizes peripheral sensory neurons, in part through DSFs enhancement in C-type neurons, which ultimately produce increased spontaneous and evoked repetitive firing. This has been proven, as stated before, in mice, rats and human preparations [12,37,46,47,70]. The mechanism underlying this phenomenon is still unknown, although it has been demonstrated that isoforms 1 and 2 of the exchange factor directly activated by cAMP (EPAC) could play a role in it, as its pharmacological inactivation prevented the increase in DSFs produced by SCI, and its activation slightly increased their amplitude in naïve rats. Interestingly, the individual KOs for EPAC 1 and 2 had no effect on DFS, suggesting a redundant role of both isoforms [16]. Serotonin, an acute inflammatory mediator, also has the property of increasing DSFs in C-type neurons [47], through a molecular signalling pathway implying cAMP, PKA and EPAC [39]. In fact, a cAMP analogous is sufficient to enhance DSFs, potentially implying that any mediator/process increasing cAMP in C-type nociceptors would lead to DSFs upregulation.

The clinical relevance of RMPIs remains largely unexplored. A recent report [43] documented the effects of low concentrations of local anaesthetics, not able to block action potential generation and conduction, in pain symptomatology from back pain patients, arguing that these concentrations could be able to block SMPOs [22]. The local anaesthetics were administered by a combination of intraepidermal proximal and distal injections in the affected dermatomes, intraepithelial injections in the palatal velum and periosteal injections in the vertebral body of the affected dermatomes. After 4-8 sessions of local anaesthetic injections, 42%, 18% and 40% of the patients displayed total, 90-100% and 30%–90% pain remission, respectively. However, these results are difficult to interpret because the study lacked a control group and, therefore, confounding factors such as spontaneous pain remission, regression to the mean and placebo response cannot be ruled out as contributors to the clinical output of the treatment. Future clinical possibilities of blocking RMPIs could be the targeting of molecular determinants predominantly expressed in the peripheral nervous system, such as some NaV channels isoforms, noting that these may also have crucial roles in the CNS [15]. Thus, an interesting supplementary approach consists in taking profit of the absence of BNB in the DRG to deliver peripheralized antagonists to avoid CNS toxicity [19].

In conclusion for this part, it has been proposed that the repetitive firing produced by upregulated RMPIs could contribute to the development of several symptoms associated with neuropathic injuries, especially mechanical allodynia, paraesthesia and spontaneous pain, both in rodents and humans. This claim is mainly (but not exclusively) based on studies performed in A-type neurons, which are principally mechano- and proprioceptors. This relates to the fact that in neuropathy models, known to feature mechanical allodynia, the percentage of these neurons exhibiting RMPIs is increased. Furthermore, it is known that in this kind of pain models non-nociceptive A-type neurons may signal pain to the CNS through a plastic process called central sensitization, whereby previously pain-unrelated neurons could start triggering the activation of the nociceptive central pathway [65]. In this context, spontaneous repetitive firing induced by

SMPOs in non-nociceptor cells could contribute to spontaneous pain and abnormal sensory experiences such as paraesthesia. Recently, new research about spontaneous depolarizations (DSFs) in C-type DRG nociceptors has emerged, demonstrating a more direct link between this phenomenon and pain, both in normal sensory transmission and pathological situations [46,47]. Furthermore, the knowledge of the molecular mechanism implied in RMPIs generation, although still incipient, offers new therapeutic targets for varied severe clinical painful conditions.

Unsolved questions and new directions in RMPIs research

Several groups have recently stablished that RMPIs in peripheral sensory neurons are relevant for signal transduction. However, some methodological limitations hinder the generalization of the results, and multiple questions remain unsolved. For instance, the thus far predominant use of rats as animal model has limited the use of modern genetic tools to decipher the underlying molecular mechanisms of RMPIs that are otherwise more tractable in mice. For instance, molecular mechanisms generating RMPIs are largely unknown, and the use of genetic tools and models, until now minoritarian in the field, could help assessing the exact identity of the channels participating in RMPIs in a complementary way to pharmacological approaches adopted until now. It should be noted that these pharmacological approaches have been quite generalists, in the sense that specific channel blockers have not been used in peripheral sensory neurons RMPIs research (with the exception of the NaX channel). Other molecules with a possible implication in RMPIs due to their relationship with excitability, such as ion exchangers (i.e. Na^{+}-Ca^{2+}) and TRP channels, should be also tested for their implication in RMPIs.

As stated above, RMPIs have been studied almost exclusively in A-type DRG neurons, mainly due to the role of these cells in allodynia. Although some work has been conducted in C-type neurons, many RMPIs properties in these cells remain obscure, e.g., the source of their lower frequency. An in-depth characterization of RMPIs in C-type neurons would be of great value, because these cells are mainly nociceptors, thermosensors and pruriceptors, and are therefore largely implicated in many severe acute and chronic pathologies. Another interesting point is whether the physiological situation in which RMPIs are recorded could modify them: marking a specific cell type and recording it *in vivo* with the full ganglia and *in vitro* in primary cultures could illustrate if cell communication has an influence in RMPIs or they are a completely cell-autonomous phenomenon.

Another limitation of the research on RMPIs performed so far is that peripheral sensory neurons are extremely functionally diverse. Hence, they could be classified in many ways, of which classical conduction velocity (A/C cell types) is only one of them. Functional classification based on the responsiveness to specific thermal, mechanical and chemical stimuli may be useful to compare the properties of RMPIs across distinct groups of sensory neurons, which in turn may help to better understand their functional roles. For example, corneal nociceptors exhibit very low levels of spontaneous activity, while cold receptors have a characteristically high spontaneous activity, finely tuned by temperature [26]. Do their RMPIs differ, accounting for their distinct spontaneous activities? Also, classifications guided by gene and protein expression patterns could be of great value to further investigate the molecular determinants of RMPIs properties in different cell types (i.e. CGRP+ peptidergic nociceptors and IB4+ non-peptidergic

nociceptors). Furthermore, no studies on RMPIs in the peripheral sensory neurons of the nodose and vagal ganglia have been reported until now. In these ganglia, RMPIs could be implicated in the detection of inner conditions, and thereby in the mechanisms of body homeostasis.

Another point that has not been considered thus far is that, despite the fact that the main proposed role for the RMPIs is the reduction of membrane accommodation during natural ramp and hold stimulation (e.g., a heating ramp), the presence of RMPIs during this kind of stimulus has not been assessed. Instead, all studies so far have used step or ramp current injections to stimulate sensory neurons.

In the pathology domain, the majority of studies on RMPIs have been performed in neuropathic conditions that imply direct neuronal injury. Although this is an important condition, it must not be forgotten that peripheral sensory neurons detect the damage of other cell types as well. This opens a myriad of opportunities related of multiple relevant pathologies, such as inflammatory bowel syndrome, dry eye disease, acute inflammation, chronic itch and many more. In all these pathologies peripheral sensory neurons RMPIs could play a crucial role in regulating the peripheral input that triggers constant pain and discomfort.

Last but not least, it should be noted that sensory transduction is usually not occurring in the soma of peripheral sensory neurons, but in the sensory terminals. This raises the evergreen question of how well we could translate the findings in the soma to the actual transduction and codification. In this sense, some authors have proposed RMPIs to be the base of ongoing activity on, for example, peripheral cold sensory terminals [48]. The topic of whether or not sensory terminals do generate RMPIs is even more relevant when we consider RMPIs as a local phenomenon, whereby a neuron could present a RMPI-generating sensory terminal and a non-generating soma, rendering the ability of repetitive firing. This opens the possibility that, in a physiological situation, the percentages of neurons capable of generating RMPIs is totally different from the ones reported until now. Even more, it would imply that RMPIs generated in the soma are part of the information processing inside the cell, distributed in different subcellular compartments, as others authors have previously suggested [19,23]. Until now, intracellular recordings of a sensory terminal have not been reported due to its technical difficulty. In the closest approximation A-fibers are possible to impale and neuromas could be recorded intracellularly [29]. Thus, we are still limited to extrapolation of results acquired in other subcellular compartments. Hopefully, new methodologies will make possible to optically record from sensory endings even *in vivo* [1,25], with the use of dyes sufficiently sensitive to detect subthreshold membrane potential instabilities [11].

Conclusions

RMPIs appear as a fundamental phenomenon for the normal physiology of peripheral sensory neurons. They allow repetitive firing through the decrease of membrane accommodation, which is crucial for spontaneous activity generation and response to slow or tonic stimulation. They could be also implicated in various forms of cell-to-cell communication, including synaptic and non-synaptic transmission, allowing interactions between cells of different types. RMPIs are enhanced in pathological states and they appear to be fundamental for the tonic activity of primary mechanoreceptors that is the basis of mechanical allodynia. Furthermore, RMPIs

promote ectopic firing, both in the axon and the soma, a distinctive feature of epidemiologically relevant pathologies, such as neuropathic pain.

The molecular basis of RMPIs generation varies in the different studied ganglia (TG, DRG, Mes-V) and it is not yet fully understood in any of them. Nevertheless, it is known that Na^+ and K^+ currents are the main generators of RMPIs, whereas Ca^{2+}, I_H and synaptic currents do not seem to be critically implicated. Specifically, voltage-gated Na^+ and K^+ currents, together with leak K^+ currents are the main candidates for RMPIs generation. RMPIs are proposed to be associated to a particular configuration of membrane resonance, which is the property allowing a neuron to respond preferentially to stimulus in a certain frequency range.

The study of RMPIs in peripheral sensory neurons has walked a long path in the last 30 years, but there are still more questions than answers. These questions could be of invaluable relevance for the advance of many fields in which these neurons play a role, such as pain, itch, mechanosensation and thermoregulation.

Acknowledgements and conflict of interest

The authors want to express their gratitude to Miguel Delicado, Raquel García and Nuria Viudes for they helpful comments and suggestions on the manuscript. Also, to Vicente Alepuz and Reinaldo Valle, that as engineers specialized in electrical and mechanical oscillations assisted us in our understanding of this fascinating phenomenon. There is no conflict of interests to be declared.

Bibliography

[1] Aleixandre-Carrera F, Engelmayer N, Ares-Suárez D, Acosta M del C, Belmonte C, Gallar J, Meseguer V, Binshtok AM. Optical assessment of nociceptive TRP channel function at the peripheral nerve terminal. Int J Mol Sci 2021;22:1–20. doi:10.3390/ijms22020481.

[2] Amarillo Y, Zagha E, Mato G, Rudy B, Nadal MS. The interplay of seven subthreshold conductances controls the resting membrane potential and the oscillatory behavior of thalamocortical neurons. J Neurophysiol 2014;112:393–410. doi:10.1152/jn.00647.2013.

[3] Amir R, Devor M. Spike-evoked suppression and burst patterning in dorsal root ganglion neurons of the rat. J Physiol 1997;501:183–196. doi:10.1111/j.1469-7793.1997.183bo.x.

[4] Amir R, Devor M, Kocsis J, Wall PD. Chemically Mediated Cross-Excitation in Rat Dorsal Root Ganglia. 1996 p.

[5] Amir R, Kocsis JD, Devor M. Multiple interacting sites of ectopic spike electrogenesis in primary sensory neurons. J Neurosci 2005;25:2576–2585. doi:10.1523/JNEUROSCI.4118-04.2005.

[6] Amir R, Liu CN, Kocsis JD, Devor M. Oscillatory mechanism in primary sensory neurones. Brain 2002;125:421–435.

[7] Amir R, Michaelis M, Devor M. Burst discharge in primary sensory neurons: Triggered by subthreshold oscillations, maintained by depolarizing afterpotentials. J Neurosci 2002;22:1187–1198. doi:10.1523/jneurosci.22-03-01187.2002.

[8] Amir R, Michaelis M, Devor M. Burst discharge in primary sensory neurons: Triggered by subthreshold oscillations, maintained by depolarizing afterpotentials. J Neurosci 2002;22:1187–1198. doi:10.1523/jneurosci.22-03-01187.2002.

[9] Amir R, Michaelis M, Devor M. Membrane potential oscillations in dorsal root ganglion neurons: Role in normal electrogenesis and neuropathic pain. J Neurosci 1999;19:8589–8596. doi:10.1523/jneurosci.19-19-08589.1999.

[10] Amir R, Michaelis M, Devor M. Membrane potential oscillations in dorsal root ganglion neurons: Role in normal electrogenesis and neuropathic pain. J Neurosci 1999;19:8589–8596. doi:10.1523/jneurosci.19-19-08589.1999.

[11] Bando Y, Grimm C, Cornejo VH, Yuste R. Genetic voltage indicators. BMC Biol 2019;17. doi:10.1186/s12915-019-0682-0.

[12] Bedi SS, Yang Q, Crook RJ, Du J, Wu Z, Fishman HM, Grill RJ, Carlton SM, Walters ET. Chronic spontaneous activity generated in the somata of primary nociceptors is associated with pain-related behavior after spinal cord injury. J Neurosci 2010;30:14870–14882. doi:10.1523/JNEUROSCI.2428-10.2010.

[13] Benarroch EE. HCN channels: Function and clinical implications. Neurology 2013;80:304–310. doi:10.1212/WNL.0b013e31827dec42.

[14] Bennett DL, Clark XAJ, Huang J, Waxman SG, Dib-Hajj SD. The role of voltage-gated sodium channels in pain signaling. Physiol Rev 2019;99:1079–1151. doi:10.1152/physrev.00052.2017.

[15] Bennett DL, Clark XAJ, Huang J, Waxman SG, Dib-Hajj SD. The role of voltage-gated sodium channels in pain signaling. Physiol Rev 2019;99:1079–1151. doi:10.1152/physrev.00052.2017.

[16] Berkey SC, Herrera JJ, Odem MA, Rahman S, Cheruvu SS, Cheng X, Walters ET, Dessauer CW, Bavencoffe AG. EPAC1 and EPAC2 promote nociceptor hyperactivity associated with chronic pain after spinal cord injury. Neurobiol Pain 2020;7:100040.

[17] Busserolles J, Tsantoulas C, Eschalier A, García JAL. Potassium channels in neuropathic pain: Advances, challenges, and emerging ideas. Pain. Lippincott Williams and Wilkins, 2016, Vol. 157. pp. S7–S14. doi:10.1097/j.pain.0000000000000368.

[18] Chorev E, Yarom Y, Lampl I. Rhythmic episodes of subthreshold membrane potential oscillations in the rat inferior olive nuclei in vivo. J Neurosci 2007;27:5043–5052. doi:10.1523/JNEUROSCI.5187-06.2007.

[19] Devor M. Unexplained peculiarities of the dorsal root ganglion. Pain 1999;82. doi:10.1016/S0304-3959(99)00135-9.

[20] Dib-Hajj SD, Waxman SG. Sodium Channels in Human Pain Disorders: Genetics and Pharmacogenomics. Annu Rev Neurosci 2019;42:87–106. doi:10.1146/annurev-neuro-070918-050144.

[21] Djouhri L, Smith T, Alotaibi M, Weng X. Membrane potential oscillations are not essential for spontaneous firing generation in L4 Aβ-afferent neurons after L5 spinal nerve axotomy and are not mediated by HCN channels. Exp Physiol 2018;103:1145–1156. doi:10.1113/EP087013.

[22] Dong H, Fan Y-H, Wang Y-Y, Wang W-T, Hu S-J. Lidocaine Suppresses Subthreshold Oscillations by Inhibiting Persistent Na + Current in Injured Dorsal Root Ganglion Neurons. 2008. Available: www.biomed.cas.cz/physiolresPhysiol.Res.57:639-645,2008. Accessed 22 Sep 2020.

[23] Du X, Hao H, Yang Y, Huang S, Wang C, Gigout S, Ramli R, Li X, Jaworska E, Edwards I, Deuchars J, Yanagawa Y, Qi J, Guan B, Jaffe DB, Zhang H, Gamper N. Local GABAergic signaling within sensory ganglia controls peripheral nociceptive transmission. J Clin Invest 2017;127:1741–1756. doi:10.1172/JCI86812.

[24] Estacion M, Dib-Hajj SD, Benke PJ, Te Morsche RHM, Eastman EM, Macala LJ, Drenth JPH, Waxman SG. NaV1.7 gain-of-function mutations as a continuum: A1632E displays physiological changes associated with erythromelalgia and paroxysmal extreme pain disorder mutations and produces symptoms of both disorders. J Neurosci 2008;28:11079–11088. doi:10.1523/JNEUROSCI.3443-08.2008.

[25] Goldstein RH, Barkai O, Íñigo-Portugués A, Katz B, Lev S, Binshtok AM. Location and Plasticity of the Sodium Spike Initiation Zone in Nociceptive Terminals In Vivo. Neuron 2019;102:801-812.e5. doi:10.1016/j.neuron.2019.03.005.

[26] González-González O, Bech F, Gallar J, Merayo-Lloves J, Belmonte C. Functional properties of sensory nerve terminals of the mouse cornea. Investig Ophthalmol Vis Sci 2017;58:404–415. doi:10.1167/iovs.16-20033.

[27] Hutcheon B, Yarom Y. Resonance, oscillation and the intrinsic frequency preferences of neurons. Trends Neurosci 2000;23:216–222. doi:10.1016/S0166-2236(00)01547-2.

[28] Johnston J, Forsythe ID, Kopp-Scheinpflug C. Going native: Voltage-gated potassium channels controlling neuronal excitability. Journal of Physiology. Wiley-Blackwell, 2010, Vol. 588. pp. 3187–3200. doi:10.1113/jphysiol.2010.191973.

[29] Kapoor R, Li YG, Smith KJ. Slow sodium-dependent potential oscillations contribute to ectopic firing in mammalian demyelinated axons. Brain 1997;120:647–652.

[30] Ke CB, He WS, Li CJ, Shi D, Gao F, Tian YK. Enhanced SCN7A/Nax expression contributes to bone cancer pain by increasing excitability of neurons in dorsal root ganglion. Neuroscience 2012;227:80–89. doi:10.1016/j.neuroscience.2012.09.046.

[31] Ke CB, He WS, Li CJ, Shi D, Gao F, Tian YK. Enhanced SCN7A/Nax expression contributes to bone cancer pain by increasing excitability of neurons in dorsal root ganglion. Neuroscience 2012;227:80–89. doi:10.1016/j.neuroscience.2012.09.046.

[32] Kovalsky Y, Amir R, Devor M. Simulation in Sensory Neurons Reveals a Key Role for Delayed Na^+ Current in Subthreshold Oscillations and Ectopic Discharge: Implications for Neuropathic Pain. J Neurophysiol 2009;102:1430–1442. doi:10.1152/jn.00005.2009.

[33] Kovalsky Y, Amir R, Devor M. Subthreshold oscillations facilitate neuropathic spike discharge by overcoming membrane accommodation. Exp Neurol 2008;210:194–206. doi:10.1016/j.expneurol.2007.10.018.

[34] Li CX, Jing YL, Xie YK. Glycosylation-induced depolarization facilitates subthreshold membrane oscillation in injured primary sensory neurons. Brain Res 2007;1139:201–209. doi:10.1016/j.brainres.2006.12.039.

[35] Lieberman A, Landon D. The peripheral nerve. 1976.

[36] Liu CN, Devor M, Waxman SG, Kocsis JD. Subthreshold oscillations induced by spinal nerve injury in dissociated muscle and cutaneous afferents of mouse DRG. J Neurophysiol 2002;87:2009–2017. doi:10.1152/jn.00705.2001.

[37] Liu CN, Devor M, Waxman SG, Kocsis JD. Subthreshold oscillations induced by spinal nerve injury in dissociated muscle and cutaneous afferents of mouse DRG. J Neurophysiol 2002;87:2009–2017. doi:10.1152/jn.00705.2001.

[38] Liu CN, Michaelis M, Amir R, Devor M. Spinal nerve injury enhances subthreshold membrane potential oscillations in DRG neurons: Relation to neuropathic pain. J Neurophysiol 2000;84:205–215. doi:10.1152/jn.2000.84.1.205.

[39] Lopez ER, Carbajal AG, Tian J Bin, Bavencoffe A, Zhu MX, Dessauer CW, Walters ET. Serotonin enhances depolarizing spontaneous fluctuations, excitability, and ongoing activity in isolated rat DRG neurons via 5-HT4 receptors and cAMP-dependent mechanisms. Neuropharmacology 2021;184. doi:10.1016/j.neuropharm.2020.108408.

[40] Madrid R, Donovan-Rodríguez T, Meseguer V, Acosta MC, Belmonte C, Viana F. Contribution of TRPM8 channels to cold transduction in primary sensory neurons and peripheral nerve terminals. J Neurosci 2006;26:12512–12525. doi:10.1523/JNEUROSCI.3752-06.2006.

[41] Mathers DA, Barker JL. Spontaneous voltage and current fluctuations in tissue cultured mouse dorsal root ganglion cells. Brain Res 1984;293:35–47. doi:10.1016/0006-8993(84)91450-1.

[42] Matzner O, Devor M. Method for distinguishing between drug action on impulse propagation versus impulse generation. J Neurosci Methods 1993;49:23–31. doi:10.1016/0165-0270(93)90106-2.

[43] Michels T, Ahmadi S, Graf N. Treatment of peripheral pain with low-dose local anesthetics by epidermal, epithelial and periosteal application. Local Reg Anesth 2018;11:129–136. doi:10.2147/LRA.S151316.

[44] Mordillo-Mateos L, Sánchez-Ramos A, Coperchini F, Bustos-Guadamillas I, Alonso-Bonilla C, Vargas-Baquero E, Rodriguez-Carrión I, Rotondi M, Oliviero A. Development of chronic pain in males with traumatic spinal cord injury: role of circulating levels of the chemokines CCL2 and CXCL10 in subacute stage. Spinal Cord 2019;57:953–959. doi:10.1038/s41393-019-0311-3.

[45] Noda M, Hiyama TY. The Nax channel: What it is and what it does. Neuroscientist 2015;21:399–412. doi:10.1177/1073858414541009.

[46] North RY, Li Y, Ray P, Rhines LD, Tatsui CE, Rao G, Johansson CA, Zhang H, Kim YH, Zhang B, Dussor G, Kim TH, Price TJ, Dougherty PM. Electrophysiological and transcriptomic correlates of neuropathic pain in human dorsal root ganglion neurons. Brain 2019;142:1215–1226. doi:10.1093/brain/awz063.

[47] Odem MA, Bavencoffe AG, Cassidy RM, Lopez ER, Tian J, Dessauer CW, Walters ET. Isolated nociceptors reveal multiple specializations for generating irregular ongoing activity associated with ongoing pain. Pain 2018;159:2347–2362. doi:10.1097/j.pain.0000000000001341.

[48] Olivares E, Salgado S, Maidana JP, Herrera G, Campos M, Madrid R, Orio P. TRPM8-

dependent dynamic response in a mathematical model of cold thermoreceptor. PLoS One 2015;10. doi:10.1371/journal.pone.0139314.

[49] Pedroarena CM, Pose IE, Yamuy J, Chase MH, Morales FR. Oscillatory membrane potential activity in the soma of a primary afferent neuron. J Neurophysiol 1999;82:1465–1476. doi:10.1152/jn.1999.82.3.1465.

[50] Pelkey KA, Marshall KC. Actions of excitatory amino acids on mesencephalic trigeminal neurons. Can J Physiol Pharmacol 1998;76:900–908. doi:10.1139/cjpp-76-9-900.

[51] Pleger B, Villringer A. The human somatosensory system: From perception to decision making. Prog Neurobiol 2013;103:76–97. doi:10.1016/j.pneurobio.2012.10.002.

[52] Puil E, Gimbarzevsky B, Spigelman I. Primary involvement of K+ conductance in membrane resonance of trigeminal root ganglion neurons. J Neurophysiol 1988;59:77–89. doi:10.1152/jn.1988.59.1.77.

[53] Puil E, Miura RM, Spigelman I. Consequences of 4-aminopyridine applications to trigeminal root ganglion neurons. J Neurophysiol 1989;62:810–820. doi:10.1152/jn.1989.62.3.810.

[54] Puil E, Spigelman I. Electrophysiological responses of trigeminal root ganglion neurons in vitro. Neuroscience 1988;24:635–646. doi:10.1016/0306-4522(88)90357-0.

[55] Puil E, Spigelman I. Electrophysiological responses of trigeminal root ganglion neurons in vitro. Neuroscience 1988;24:635–646. doi:10.1016/0306-4522(88)90357-0.

[56] Renganathan M, Cummins TR, Waxman SG. Contribution of Nav 1.8 sodium channels to action potential electrogenesis in DRG neurons. J Neurophysiol 2001;86:629–640. doi:10.1152/jn.2001.86.2.629.

[57] Rho YA, Prescott SA. Identification of molecular pathologies sufficient to cause neuropathic excitability in primary somatosensory afferents using dynamical systems theory. PLoS Comput Biol 2012;8. doi:10.1371/journal.pcbi.1002524.

[58] Sanhueza M, Bacigalupo J. Intrinsic subthreshold oscillations of the membrane potential in pyramidal neurons of the olfactory amygdala. Eur J Neurosci 2005;22:1618–1626. doi:10.1111/j.1460-9568.2005.04341.x.

[59] Schmitz D, Gloveli T, Behr J, Dugladze T, Heinemann U. Subthreshold membrane potential oscillations in neurons of deep layers of the entorhinal cortex. Neuroscience 1998;85:999–1004. doi:10.1016/S0306-4522(98)00113-4.

[60] Study RE, Kral MG. Spontaneous action potential activity in isolated dorsal root ganglion neurons from rats with a painful neuropathy. Pain 1996;65:235–242. doi:10.1016/0304-3959(95)00216-2.

[61] V-Ghaffari B, Kouhnavard M, Kitajima T. Biophysical properties of subthreshold resonance oscillations and subthreshold membrane oscillations in neurons. J Biol Syst 2016;24:561–575. doi:10.1142/S0218339016500285.

[62] Verdier D, Lund JP, Kolta A. Synaptic Inputs to Trigeminal Primary Afferent Neurons Cause Firing and Modulate Intrinsic Oscillatory Activity. J Neurophysiol 2004;92:2444–2455. doi:10.1152/jn.00279.2004.

[63] Wall PD, Devor M. Sensory afferent impulses originate from dorsal root ganglia as well as from the periphery in normal and nerve injured rats. Pain 1983;17:321–339. doi:10.1016/0304-3959(83)90164-1.

[64] Wang YY, Wen ZH, Duan JH, Zhu JL, Wang WT, Dong H, Li HM, Gao GD, Xing JL, Hu SJ. Noise enhances subthreshold oscillations in injured primary sensory neurons. NeuroSignals 2011;19:54–62. doi:10.1159/000324519.

[65] Woolf CJ. Central sensitization: Implications for the diagnosis and treatment of pain. Pain 2011;152. doi:10.1016/j.pain.2010.09.030.

[66] Wu N, Hsiao CF, Chandler SH. Membrane resonance and subthreshold membrane oscillations in mesencephalic V neurons: Participants in burst generation. J Neurosci 2001;21:3729–3739. doi:10.1523/jneurosci.21-11-03729.2001.

[67] Xie RG, Zheng DW, Xing JL, Zhang XJ, Song Y, Xie Y Bin, Kuang F, Dong H, You SW, Xu H, Hu SJ. Blockade of persistent sodium currents contributes to the riluzole-induced inhibition of spontaneous activity and oscillations in injured DRG neurons. PLoS One 2011;6:18681. doi:10.1371/journal.pone.0018681.

[68] Xing JL, Hu SJ, Jian Z, Duan JH. Subthreshold membrane potential oscillation mediates the excitatory effect of norepinephrine in chronically compressed dorsal root ganglion neurons in the rat. Pain 2003;105:177–183. doi:10.1016/S0304-3959(03)00200-8.

[69] Xing JL, Hu SJ, Xu H, Han S, Wan YH. Subthreshold membrane oscillations underlying integer multiples firing from injured sensory neurons. Neuroreport 2001;12:1311–1313. doi:10.1097/00001756-200105080-00051.

[70] Yang Q, Wu Z, Hadden JK, Odem MA, Zuo Y, Crook RJ, Frost JA, Walters ET. Persistent pain after spinal cord injury is maintained by primary afferent activity. J Neurosci 2014;34:10765–10769. doi:10.1523/JNEUROSCI.5316-13.2014.

[71] Yang RH, Wang WT, Chen JY, Xie RG, Hu SJ. Gabapentin selectively reduces persistent sodium current in injured type-A dorsal root ganglion neurons. Pain 2009;143:48–55. doi:10.1016/j.pain.2009.01.020.

Figure legends:

Figure 1. SMPOs recorded at different membrane voltages and their associated power spectral density. *A) DRG A-type neuron. B) DRG C-type neuron. Modified from Amir et al., 1999 and reproduced with permission of the copyright holder.*

Figure 2. Comparison of DSF and SMPOs recorded in the same cell type. *Note their differences in continuity of the oscillation, and the prominence towards depolarization (red arrows vs blue arrows) in A, compared to the even oscillation in B. Furthermore, both of them are tightly related with action potentials. A is from Odem et al., 2018, and B from Amir et al., 1999, reproduced with permission of the copyright holders.*

Figure 3. Generation of membrane resonance and subthreshold oscillations. *1) Resonant behaviour of the cell membrane could be modelled at its simplest molecular level by adding a generating and an amplifier current (I_K and I_{NaP} respectively, in the example) to the membrane capacitor. 2) Diagram showing how a resonant model like the one described above could be converted into a constantly oscillating system by fine tuning of the specific conductances composing it, mimicking a neuron displaying spontaneous SMPOs. Modified from* Hutcheon & Yarom, 2000 *and reproduced with permission of the copyright holder (Elsevier).*

Figure 4. *Recording of an A-type DRG neuron illustrating how the generation of repetitive firing is associated to the production of SMPOs (top panel). SMPOs are abolished by the burst-induced hyperpolarizations but then reappear as the membrane slowly depolarizes (best appreciated in the bottom panel). From Amir & Devor, 1997 and reproduced with permission of the copyright holder (John Wiley and Sons).*

Figure 5. Possible sites of SMPO generation in sensory neurons. *Top, in healthy neurons SMPOs could be present in the soma, generating ectopic firing additionally to the one transduced in the periphery. Bottom, after an axonal injury, SMPOs in the soma become upregulated, increasing the quantity of ectopic action potentials generated. Furthermore, in the site of the injury, local SMPOs arise, producing axonal ectopic firing. If the peripheral or central processes of primary sensory neurons display SMPOs is unknown in both cases.*

Table 1. Summary of the principal experimental findings regarding SMPOs characteristics and molecular players implying in SMPO generation.

Figures:

1:

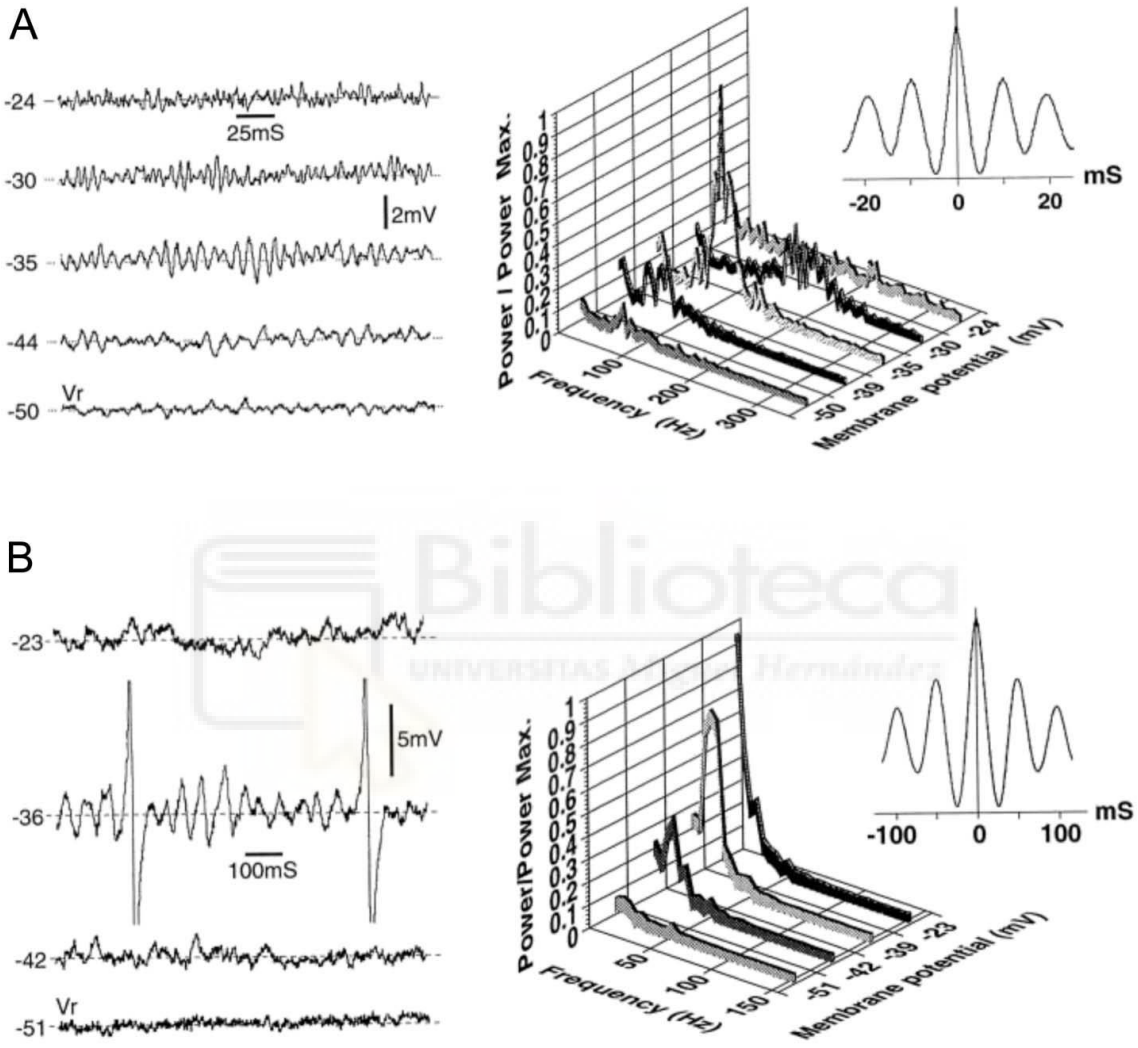

2:

A

Depolarizing spontaneous fluctuations (DSFs)

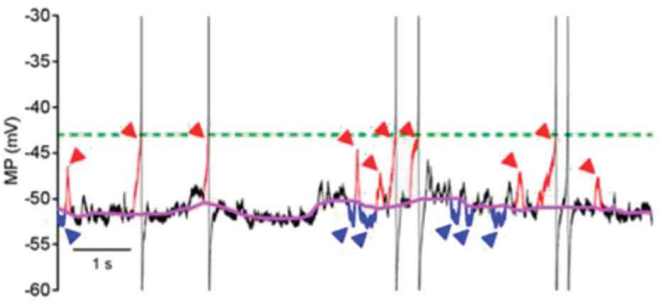

B Subthreshold membrane potential oscillations (SMPOs)

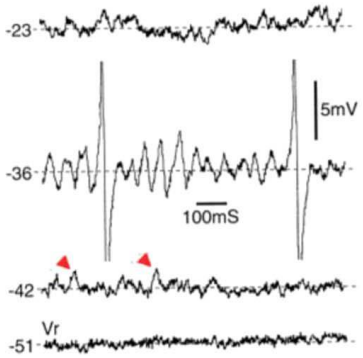

3:

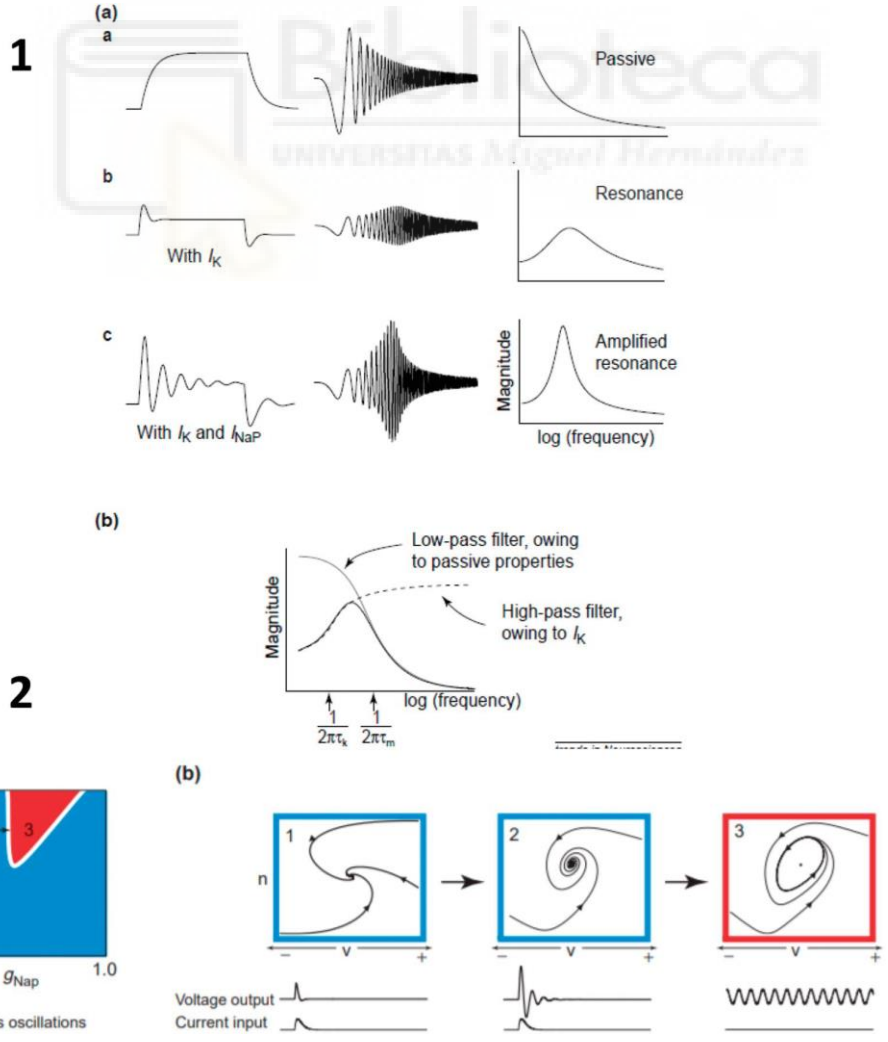

4:

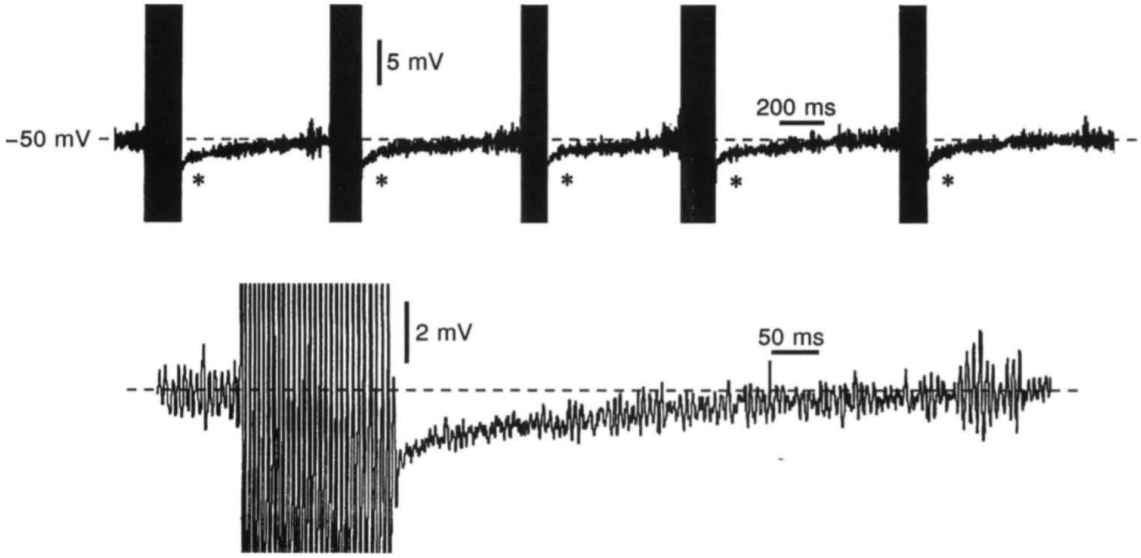

5:

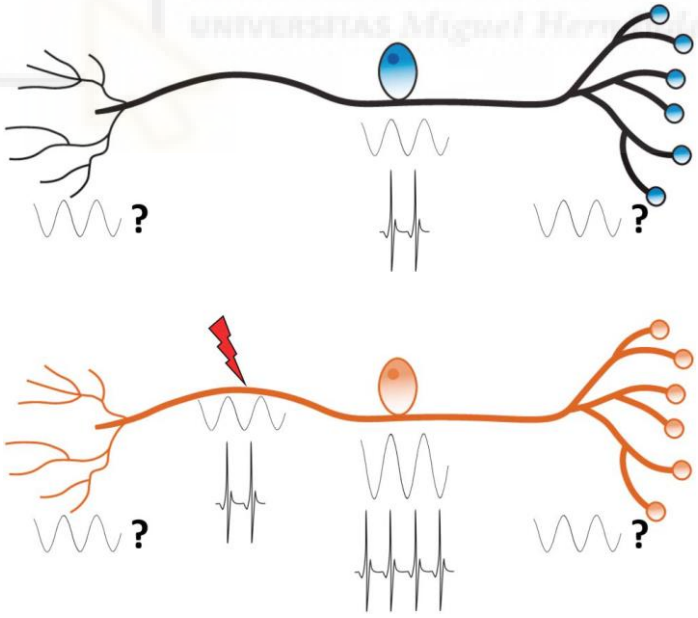

Table 1:

	Ganglia:	TG	DRG	Mes-V
General characteristics	Innervation	Face and mouth	Body	Jaw and periodontal tissues
	% of neurons spontaneously oscillating	Not documented	A-Neurons:12% C-Neurons: None	Not documented
	% of neurons capable of producing SMPOs	"Most neurons" in vitro	A-Neurons: 10-27% *in vitro* 1-14% *in vivo* C-Neurons: 25% *in vitro*	36% in vitro
	SMPOs Frequency	100Hz (unknown cell type)	A-Neurons: 80-200 Hz C-Neurons: 11-15 Hz	83.3 –142.8 Hz
	Experimental preparations	In vitro slice preparation	In vivo, cultured cells, full mounted ganglion	In vitro slice preparation
Extracellular ionic concentration	Na+ Depletion Ca2+ Depletion K+ Increase	Abolition No effect Not performed	Abolition No effect Abolition	Abolition No effect Not performed
Pharmacology	TTX (<0.1µM) TEA 4-AP	No effect Abolition Facilitation and frequency reduction	Abolition Facilitation and frequency reduction Facilitation and frequency reduction	Abolition Mild frequency reduction Strong frequency reduction
Representative references		(Puil et al., 1988, 1989; Puil & Spigelman, 1988)	(Amir et al., 1999; Amir, Liu, et al., 2002; Amir & Devor, 1997; Kapoor et al., 1997)	(Pedroarena et al., 1999; Wu et al., 2001)

Acknowledgements

El orden de estos agradecimientos ha sido aleatorizado mediante un script, porque no me veo capaz de ordenarlos yo:

A Karel y a Juan, por el ejemplo, por cuidar de mi pasión y regarla. Por hacer que nunca me sintiera inferior mientras aprendía y por abrirme la puerta de sus respectivos mundos, así como de su gente y de sus casas. Por darme algo en lo que seguir creyendo en los tiempos más duros.

A Sergio, por abrirme la puerta a lo que hoy es mi profesión y acompañarme de la mano en los primeros pasos.

A Laura, por el viaje que emprendimos juntos.

A V, Rei, Álex, D, S, el Sal y Ort, por una vida mano a mano, por recordarme que soy un imbécil.

A Fer, Almu, Omar y Fede, por las risas, los dolores, las comidas y las charlas compartidas. Por una ciencia increíble.

A Ine, y a Ana, y a Javi y a Juan. No todo el mundo puede decir que nunca ha dudado del amor de sus hermanos. No todo el mundo puede decir que lo han acompañado en cada cambio drástico en la vida, dándome algo que perseguir.

A Roca 2.0, por reencontrarme con el rendimiento en el deporte de una forma más amigable. En especial a Vicente por compartir conmigo su mundo: el interior y las montañas. Y a Álex, por dar amor sin condiciones, por ver más allá de las caretas que me pongo.

A Paula, por todo su cariño y por hacerme plantearme quién quiero ser, una vez más.

A Juana, que me enseñó (me enseña) y apostó por mí cuando nadie lo haría, y cuando estaba desencantado me dio una pasión por la que levantarme por las mañanas.

A Ari, por enseñarme su brujería, y por nunca, nunca, perder la fe en mí. Tampoco cuando yo la he perdido.

A Deli, porque la mitad de mi trabajo es tuyo, y la mitad de mi vida estos años también.

A Raquel, por acercarse al monstruo.

A mi madre, y a mi padre, que, humanos y asustados, como Héctor a las puertas de Troya, han luchado contra monstruos mitológicos por sus seres queridos. Hoy no estaría aquí, en ningún aspecto, sin vuestras noches en vela.

A la Cabezamelón, que en tantas cruzadas me ha acompañado. Seguimos plantando batalla ante el mundo.

A Nuria, por ser un trébol de cinco hojas y acompañarme en gran parte de este camino y hacerlo aún hoy.

A la gente del máster y otros amigos del INA, por acogerme en sus grupos y divertirse con este espantapájaros.

A Mari Carmen, Susana, David, Carol por haber sido parte de esta familia que me ha dejado huella.

A Patri, porque escuchar y cambiar es más difícil que ahogarse en el conflicto.

A Julio, por ponerme en contacto con los que nos precedieron, por la moral, la ideología, la amabilidad, las risas y el tiempo juntos. Por mirarme a los ojos como un igual, y sentar un precedente de cómo quiero tratar a los míos.

A mis profesores en Neurociencia, que han hecho de un extraño en el campo un neurocientífico a base de paciencia y compartir conocimientos.

A los científicos, fisioterapeutas y apasionados que quedan por venir. Por darme un motivo para mantener viva la curiosidad de contemplar sus logros y descubrimientos de mañana.

A Víctor y a Fito, por tantas lecciones, y por esforzarse en conocerme más allá del trabajo.

A le Messie, por ser para mí un referente, por ser un ejemplo de amistad.

A Fran Ortega y Vi100 Alepuz, que, confiando en nosotros, han hecho posible lo imposible y que siguen manteniendo viva la inocencia de un niño con la cabeza lúcida de los genios.